

Loss of E-cadherin Activates a Targetable IGF1R Pathway in Invasive Lobular Breast Carcinoma

by

Ashuvinee Elangovan

Bachelor of Arts, University of Colorado Boulder, 2017

Submitted to the Graduate Faculty of the
School of Medicine in partial fulfillment
of the requirements for the degree of
Doctor of Philosophy

University of Pittsburgh

2022

UNIVERSITY OF PITTSBURGH

SCHOOL OF MEDICINE

This dissertation was presented

by

Ashuvinee Elangovan

It was defended on

March 24, 2022

and approved by

Ferruccio Galbiati, PhD, Professor, Pharmacology & Chemical Biology

Jeffrey L. Brodsky, PhD, Professor, Biological Sciences

Thomas E. Smithgall, PhD, Professor, Microbiology & Molecular Genetics

Laura A. Stabile, PhD, Research Associate Professor, Pharmacology & Chemical Biology

Steffi Oesterreich, PhD, Professor, Pharmacology & Chemical Biology

Dissertation Advisor: Adrian V. Lee, PhD, Professor, Pharmacology & Chemical Biology

Copyright © by Ashuvinee Elangovan

2022

Loss of E-cadherin Activates a Targetable IGF1R Pathway in Invasive Lobular Breast Carcinoma

Ashuvinee Elangovan, PhD

University of Pittsburgh, 2022

Invasive Ductal Carcinoma (IDC) and Invasive Lobular Carcinoma (ILC) are two major subtypes of breast cancer with significant differences in their histological and molecular underpinnings. ILC has a unique hallmark of loss of E-cadherin (*CDHI*) in 90% of the cases, which we have previously demonstrated as a negative regulator of Insulin-like Growth Factor 1 (IGF1) receptor, IGF1R through a comprehensive analysis of cell line models and tumor samples on TCGA. We propose that the loss of E-cadherin in ILC sensitizes cells to growth factor signaling and thus alters their susceptibility to growth factor signaling inhibition. We generated *CDHI* knockout (KO) IDC cell lines to investigate the mechanism by which E-cadherin loss activates IGF pathway and its subsequent effectors while also assessing its targetability in patients. *CDHI* KO cells exhibited anchorage independent growth in suspension culture and altered p120 catenin localization as seen in ILC cells. Through *in vitro* studies, we observed increased signaling sensitivity to IGF/ insulin ligands where the high activation levels are sustained for an extended duration in the KO cells. In addition, there was higher migratory potential in the *CDHI* KO cells, which was further enhanced as a chemotactic response to IGF1 or serum and as a haptotactic response to Collagen I. This phenotype was reversed with an IGF1R inhibitor to exhibit phenotype specificity. Despite no consistent differences in membranous IGF1R levels, higher ligand-receptor interaction was observed with E-cadherin loss. Our results currently demonstrate IGF1R's increased availability for ligand binding which in turn allows for an enhanced signaling activation. As an extension to the pathway activation,

increased susceptibility to IGF1R, PI3K, AKT and MEK inhibitors was also observed in T47D *CDHI* KO cells. With about 90% of ILC cases being ER+, we investigated and showed the additive effect of Fulvestrant with Akt inhibitors in KO cells. Although a clear susceptibility to Akt inhibitor was not seen in ILC patient-derived organoids (PDO), a favorable trend was observed when compared to IDC PDOs. Our findings elucidated IGF1 signaling repression by E-cadherin in ILC, thus supporting the use of E-cadherin loss as a stratification method for improved targeted therapy approaches.

Table of Contents

Preface.....	xvi
1.0 Introduction.....	1
1.1 Breast Cancers	1
1.1.1 Overview of breast cancer	1
1.1.2 Molecular subtypes of breast cancer	2
1.1.3 Histological subtypes of breast cancer	5
1.2 Insulin-Like Growth Factor Pathway	7
1.2.1 IGF signaling in mammary development	9
1.2.2 Role of IGF signaling in breast cancer	11
1.2.3 Targeting IGF signaling in breast cancer	12
1.2.4 Biomarker selection for targeted IGF therapies	15
1.3 E-cadherin and breast cancer.....	16
1.4 Hypothesis	19
2.0 Elevated IGF and Akt Pathway Activation is Observed in ILC Tumors and Cell Lines	20
2.1 Introduction	20
2.2 Materials and methods.....	21
2.2.1 In silico analysis.....	21
2.2.2 Cell culture.....	22
2.2.3 Immunoblotting.....	23
2.3 Results.....	24

2.3.1 IGF pathway activity is enhanced in ILC	24
2.3.2 IGF pathway activity is enhanced in ILC cell lines <i>in vitro</i>	27
2.4 Discussion	29
3.0 <i>CDH1</i> Knockout (KO) IDC Isogenic Cell Lines as a Model to Study The Role of	
E-Cadherin in Regulating IGF Signaling	32
3.1 Introduction	32
3.2 Materials and methods.....	34
3.2.1 Cell culture.....	34
3.2.2 <i>CDH1</i> knockout cell line generation	34
3.2.3 Immunoblotting.....	35
3.2.4 qRT-PCR for <i>CDH1</i>	36
3.2.5 Immunofluorescence	36
3.2.6 2D and ULA cell growth assay.....	37
3.2.7 FACS for anoikis resistance	37
3.2.8 Bulk RNA sequencing sample preparation	37
3.2.9 Bulk RNA sequencing analysis MCF7 and T47D parental and <i>CDH1</i> KO cell lines	38
3.3 Results.....	39
3.3.1 <i>CDH1</i> KO IDC cell lines demonstrated altered morphology and re-localized p120 catenin	39
3.3.2 β -catenin expression is reduced following <i>CDH1</i> knockout.....	42
3.3.3 <i>CDH1</i> KO cells exhibit enhanced growth in ULA and are anoikis resistant	43

3.3.4 RNA sequencing reveals variations between WT and KO cells, with related pathway differences	45
3.4 Discussion	49
4.0 <i>CDHI</i> KO Renders Cells More Sensitive to IGF Signaling	53
4.1 Introduction	53
4.2 Materials and methods.....	55
4.2.1 Cell culture.....	55
4.2.2 IGF, EGF and FGF signaling assays.....	55
4.2.3 Immunoblotting.....	56
4.2.4 Colony formation assay	57
4.2.5 Haptotaxis, migration and invasion assays.....	58
4.3 Results.....	58
4.3.1 <i>CDHI</i> KO cells are hypersensitive to IGF1, IGF2 and Insulin stimulation .58	
4.3.2 <i>CDHI</i> KO cells do not exhibit increased sensitivity to EGF and FGF stimulations.....	62
4.3.3 IGF1 stimulation of <i>CDHI</i> KO cells results in robust signaling elevation over time	65
4.3.4 <i>CDHI</i> KO cells displayed enhanced colony formation in low density assays	66
4.3.5 <i>CDHI</i> KO cells exhibit migration towards IGF1 and serum.....	68
4.3.6 <i>CDHI</i> KO cells migrate towards collagen and exhibit collagen invasion	70
4.4 Discussion	71

5.0 Loss of <i>CDH1</i> Renders IGF1R More Available for Ligand Binding And Hyperactivates Downstream Signaling	75
5.1 Introduction	75
5.2 Materials and methods.....	77
5.2.1 Cell culture.....	77
5.2.2 Cell fractionation assay to compare receptor expression levels.....	77
5.2.3 Immunoblotting.....	78
5.2.4 qRT-PCR for IGF1R	78
5.2.5 Receptor availability assay	79
5.2.6 Co-Immunoprecipitation.....	79
5.2.7 Immunofluorescence to assess E-cadherin and IGF1R localization	80
5.2.8 Surface biotinylation assay.....	80
5.3 Results.....	81
5.3.1 T47D <i>CDH1</i> KO cells express higher IGF1R levels compared to WT cells .	81
5.3.2 <i>CDH1</i> KO cells exhibit higher IGF1 receptor availability for ligand binding	82
5.3.3 <i>CDH1</i> KO did not lead to changes in IGF1R re-localization on the membrane	84
5.3.4 IGF1R recycling is unchanged between WT and <i>CDH1</i> KO cells	86
5.4 Discussion	88
6.0 Targeting IGF Pathway Hyperactivity in <i>CDH1</i> Knockout Cells.....	91
6.1 Introduction	91
6.2 Materials and methods.....	93

6.2.1 Cell culture.....	93
6.2.2 Dose Response assays.....	93
6.2.3 Immunoblotting.....	94
6.2.4 Patient derived breast organoid culture and dose response assays.....	94
6.3 Results.....	95
6.3.1 T47D <i>CDH1</i> KO cells are sensitive to IGF1R, PI3K and Akt inhibitors.....	95
6.3.2 MCF7 and T47D <i>CDH1</i> KO cells exhibit sensitivity to a combination of MEK and IGF1R inhibitors.....	99
6.3.3 T47D <i>CDH1</i> KO cells exhibit sensitivity to a combination of Akt inhibitor and Fulvestrant.....	100
6.3.4 ILC patient derived organoids exhibit patterns of higher susceptibility to the Akt inhibitor, MK2206.....	103
6.4 Discussion.....	105
7.0 Assessing E-Cadherin Regulation of IGF Signaling in Murine Model with Mammary Gland-Specific <i>CDH1</i> Deletion.....	110
7.1 Introduction.....	110
7.2 Materials and methods.....	112
7.2.1 Mouse colony.....	112
7.2.2 PCR for genotyping.....	113
7.2.3 LR3-IGF1 tail vein injections.....	113
7.2.4 Immunohistochemistry for E-cadherin and H&E.....	114
7.2.5 Mammary gland whole mounts.....	114
7.2.6 Immunoblotting.....	115

7.3 Results.....	116
7.3.1 Generation of <i>WAP</i>⁺; <i>Cdh1</i>^{fl/fl} mouse cohort.....	116
7.3.2 <i>WAP</i>Cre⁺; <i>Cdh1</i>^{wt/wt} and <i>WAP</i>Cre⁺; <i>Cdh1</i>^{fl/fl} mice mammary glands appeared similar by H&E	118
7.3.3 E-cadherin expression was observed in <i>WAP</i>Cre⁺; <i>Cdh1</i>^{fl/fl} animals.....	121
7.3.4 Tail vein LR3-IGF1 injection activated IGF pathway in the mammary gland	123
7.3.5 Cre Reporter assay in mammary glands showed efficient RFP to GFP switch after pregnancy.....	125
7.4 Discussion	127
8.0 Conclusions.....	129
Appendix A.....	135
Appendix B.....	136
Appendix C.....	137
Appendix D.....	138
Bibliography	139

List of Tables

Table 1: Antibodies Used in IB, IF and IHC Experiments	138
---	------------

List of Figures

Figure 1: H&E staining of ILC and IDC reveal their distinct histologies	6
Figure 2: Simplified overview of the IGF signaling pathway	9
Figure 3: IGF pathway activity is enhanced in ILC tumors compared to IDC tumors.....	26
Figure 4: IGF pathway activity is enhanced in ILC cell lines <i>in vitro</i>	28
Figure 5: <i>CDH1</i> KO IDC cell lines demonstrate altered morphology and re-localization of p120 catenin.....	41
Figure 6: β -catenin signaling is not affected by <i>CDH1</i> knockout.....	43
Figure 7: <i>CDH1</i> KO cells exhibit enhanced growth in ULA and display anoikis resistance	45
Figure 8: RNA sequencing uncovers large variance between WT and KO cells, with related pathway differences	47
Figure 9: <i>CDH1</i> KO cells are hypersensitive to IGF1, IGF2 and Insulin stimulation	60
Figure 10: ILC <i>CDH1</i> overexpressing cells exhibit reduced IGF1 sensitivity	62
Figure 11: Pan growth factor sensitivity was not observed with EGF and FGF stimulations	64
Figure 12: <i>CDH1</i> KO cells show high activity of IGF signaling over a time course assay...	66
Figure 13: Altered cell survival phenotypes are observed in <i>CDH1</i> KO cells.....	67
Figure 14: <i>CDH1</i> KO cells migrate towards IGF1 and serum	69
Figure 15: <i>CDH1</i> KO cells migrate towards collagen and exhibit collagen invasion	71
Figure 16: T47D <i>CDH1</i> KO cells express higher IGF1R levels	82
Figure 17: <i>CDH1</i> KO cells exhibit higher IGF1 receptor availability for ligand binding ...	83

Figure 18: Co-localization of E-cadherin and IGF1R was observed although no interaction was detected via co-IP.....	85
Figure 19: No re-localization of IGF1R observed following <i>CDH1</i> knockout	86
Figure 20: No clear differences in IGF1R recycling are observed between WT and <i>CDH1</i> KO cells	87
Figure 21: T47D <i>CDH1</i> KO cells express susceptibility to IGF1R Akt inhibitors.....	97
Figure 22: T47D <i>CDH1</i> KO cells express susceptibility to PI3K and Akt inhibitors.....	98
Figure 23: MCF7 and T47D <i>CDH1</i> KO cells exhibit sensitivity to a combination of MEK and IGF1R inhibitors.....	100
Figure 24: T47D <i>CDH1</i> KO cells exhibit sensitivity to a combination of Akt inhibitor and Fulvestrant.....	102
Figure 25: IDC and ILC Patient Derived Organoids exhibit altered morphology.....	104
Figure 26: ILC organoids exhibit patterns of higher susceptibility to Akt inhibitor MK2206	105
Figure 27: <i>WAP</i>Cre and <i>Cdh1</i> flox breeding strategy	117
Figure 28: No significant differences observed between <i>WAP</i>Cre⁺; <i>Cdh1</i>^{wt/wt} and <i>WAP</i>Cre⁺; <i>Cdh1</i>^{fl/fl} mice mammary glands	120
Figure 29: E-cadherin expression is present in <i>WAP</i>Cre⁺; <i>Cdh1</i>^{fl/fl} animals	122
Figure 30: Tail vein IGF1 injection elicits IGF activation in the mammary gland	124
Figure 31: Cre Reporter assay in mammary glands shows efficient RFP to GFP switch with pregnancy.....	126
Figure 32: MCF7 and ZR75.1 WT and KO cells do not invade Collagen I	135

Figure 33: ILC *CDH1* OE cells demonstrate higher IGF1 receptor availability for ligand binding 136

Figure 34: IDC and ILC breast PDOs exhibit variability in response to Akt inhibitor MK2206 137

Preface

This journey would not have been possible without a strong support from the many people involved in the process. First, I would like to thank Adrian and Steffi for their continued trust in me while pursuing this project. They have been strong mentors both scientifically and personally by always advocating for self-growth in addition to scientific progress. Thank you both, for creating a wonderful lab environment with highly motivated members who support each other to do our best. Next, I would like to express my sincere gratitude to Dr Jennifer Xavier for being a wonderful mentor in lab. Your day-to-day conversations with me on science and personal development have been extremely helpful over the past 4 years. You have always been there when I needed your guidance. Thank you so much for believing in me and for always having my back – I could never thank you enough.

To my thesis committee, Dr Ferruccio Galbiati, Dr Laura Stabile, Dr Jeffrey Brodsky and Dr Tom Smithgall, you have all been immensely helpful in developing this project to where it is now and for guiding me through this path. I highly appreciate your mentorship and guidance throughout the past 3 years. I would like to also thank the Molecular Genetics and Developmental Biology Graduate Program - Dr Kara Bernstein, Dr Michael Tsang, Dr Arjumand Ghazi and Kristin DiGiacomo for always guiding me and making me feel supported in this journey. To the amazing past and present Lee/ Oesterreich lab team (in no particular order) - Megan, Kai, Laura, Neil, Beth, Jagmohan, Daniel, Geoff, Olivia, Jay, Jade, Lori, Jian, Samantha Liu, Yang Wu, Anokhi, Sushie, Lauren, Sayali, Osama, Renee, Nadine, Nilgun, Jackie, Kevin, Vaciry, Lyuqin, Ye Qin and Dorothy – thank you for creating a positive environment in the lab.

You are all amazing people who continue to inspire me to be the best version of myself and have been extremely supportive throughout my years in the lab. I wish the best for all of you and am excited to see what the future holds for us all. To my 4RS family, you allowed me to experience a whole new world that I am excited to learn more about. Thank you for welcoming me into the team and supporting me these past two years.

Finally, I would like to thank my family; my parents - Elangovan, Paruvathy, my uncle and aunt - Gunasekaran, Mathiarasi and my siblings - Mugilen, Revathy and Thamayanthy. Thank you for being my biggest support throughout this journey. You supported me in pursuing my dreams and have been my strength since I left to the US in 2013. Thank you for believing in me!

None of this would have been possible without all of you and I will be forever grateful to you.

1.0 Introduction

1.1 Breast Cancers

1.1.1 Overview of breast cancer

The latest cancer statistics estimates 290,560 new cases and 43,780 deaths in United States in 2022 due to breast cancer (1). In 2022, breast cancer is expected to be the most frequent cancer type in females for estimated new cases (31% of all cancers) and is estimated to be the second leading cause of cancer deaths in women (1). Due to its prevalence, breast cancer continues to be a well-studied cancer with significant advancements in therapeutic options. Female breast cancer rates have increased slightly by 0.5%/ year since the mid-2000s where obesity and declines in fertility rates are thought to play major roles (1, 2). The 5-year relative survival rate for all stages of breast cancer combined is at 90% for breast cancers in women, with mortality rate dropping by 42% since its peak in 1989 though the annual decline has reduced from 2-3% during the 1990-2000s to 1% from 2013 to 2019 potentially due to the continued increase in cases and a stagnant mammography awareness (1).

Breast cancer arises from an uncontrolled growth of cells in the breast. This can be caused by multiple factors including genetics, lifestyle, and environment. A cancer is called *in situ* when tumor growth is limited to a region without spreading to nearby tissues. This is also typically called a Stage 0 breast cancer due to its noninvasive nature and is often considered to be precancerous (3). Patients detected with breast cancer at this stage have a survival rate of

around 98% after 10 years of follow-up care and a normal life expectancy (4). This highlights the importance of routine mammograms to allow early detection of breast cancer. An invasive or infiltrating carcinoma refers to cancers that have infiltrated into the surrounding breast tissue. This type of breast cancer can be further divided into the Non-Special Type (NST) or commonly known as invasive ductal carcinoma (IDC) and the invasive lobular carcinoma (ILC). Breast cancers vary largely based upon their molecular and histological subtypes that can affect the prognosis, disease progression and treatment options. Understanding each unique subtype of breast cancer is critical to allow for a comprehensive understanding of the tumor and better treatment of the disease.

1.1.2 Molecular subtypes of breast cancer

Breast cancer is a heterogeneous disease, with the four major intrinsic molecular subtypes being luminal A, luminal B, HER2-enriched (human epidermal growth factor receptor 2) and basal-like (5). Luminal tumors are the most common, representing about 60-70% of all tumors, with HER2-enriched at 12-20% and basal-like at approximately 15% of all breast cancers (6). Luminal tumors are so called due to the similarity of gene expression between these tumors and those of luminal epithelial cells in the breast (7). The majority of luminal tumors express the estrogen receptor (ER) and the progesterone receptor (PR), which makes this their distinguishing characteristic (6). The luminal subgroup can be further divided into Luminal A and Luminal B, where the groups differ in several characteristics (7-10). Luminal A tumors are more common with a 40% incidence rates and luminal B at 20% of all breast cancers. Compared to luminal A tumors, luminal B tumors tend to have higher PR and HER2 expression, and higher Ki67 staining, higher p53 mutation frequency and a higher histologic grade which results in a worse

prognosis (8, 11, 12). Luminal A tumors also tend to be well-differentiated while luminal B tumors are typically less well differentiated (13). Due to these differences, luminal B tumors have a shorter overall survival (OS) and disease-free survival (DFS) compared to luminal A, likely due to the higher proliferative index and aggressiveness (8, 9, 14). The different tumor subtypes can be profiled using gene expression profiling methods such as Oncotype Dx, Mammaprint, Endopredict and PAM50 to allow for a quick and accurate clinical decision (6, 15). Given the ER+ nature of these luminal tumors, patients with luminal A and B breast cancer receive hormone therapy that inhibits ER activity in the form of Selective Estrogen Receptor Degraders (SERDs), Selective Estrogen Receptor Modulators (SERMs) or Aromatase Inhibitors (AI). SERDs such as fulvestrant cause degradation of ER while SERMs such as tamoxifen bind and block the activity of ER, both to inhibit ER activity (16). Meanwhile, aromatase inhibitors such as letrozole and anastrozole block the aromatase enzyme to reduce estrogen production in peripheral tissues for a suppressed ER activity (16). Patients with luminal breast cancers are at risk of relapse between 5-15 years (17) with common distant metastatic sites including bone, brain, liver, and lung (17, 18).

The HER2-enriched (HER2+) subtype of breast cancer refers to tumors with overexpression of HER2 (*ERBB2*). This subtype often leads to an aggressive cancer and poorer OS and DFS (8, 12, 19). HER2+ tumors exhibit an overexpression of gene sets related to HER2 signaling and thus is driven by HER2, which reduces the effectiveness of anti-estrogen therapy (7). However, therapies targeting HER2 have been very successful in patients with HER2 positive tumors. Inhibitors such as lapatinib and neratinib and monoclonal antibodies such as trastuzumab and pertuzumab which target HER2 often lead to durable responses in these patients

(20-23). Unlike the luminal tumors, relapse in the HER2+ tumors tend to occur within the first five years (17, 24) with the most common distant metastatic sites being liver and brain (17, 18).

Basal-like breast cancers are reported to have basal characteristics and thus express keratin 5, keratin 17, integrin-14, and laminin with an upregulation of proliferation related genes and a high frequency of p53 mutations (6, 7). Basal-like breast cancers do not express ER and tend to be large at the time of detection, high grade and aggressive (6-9, 12, 19). A predominant subtype within the basal-like subtype is triple negative breast cancer (TNBC), characterized by its ER-, PR-, HER2- nature (11, 12, 25-27). Histologically, TNBC is mostly a ductal carcinoma, with several other subtypes such as secretory and metaplastic carcinoma also present (13). There is a lack of targeted therapies for TNBC with the currently available best options being chemotherapy and, recently, immunotherapy. The aggressive nature of TNBCs with a high proliferative index does render them susceptible to chemotherapy although the prognosis for this subtype still remains poor (28). Risk of distant recurrence for basal-like breast cancer is 3 years after diagnosis with the common sites being brain, central nervous system, lung, and liver (6).

Characterization of breast cancers based on their gene expression profiles has allowed a shift towards more accurate diagnosis and treatment while avoiding cytotoxic and aggressive treatments where possible which in turn improves both prognosis and quality of life for patients.

1.1.3 Histological subtypes of breast cancer

The histological subtypes of breast cancer can be divided into 2 main groups – IDC and ILC as described previously. IDC accounts for about 80% of all breast cancers while ILC accounts for approximately 5-15% of cases (29, 30). These subtypes not only differ in terms of how the tumors look but also in terms of the molecular alterations, prognosis, and the clinicopathological aspects (30, 31). ILC tumors are largely characterized by their small cell morphology growing in a single file discohesive manner with stromal infiltration (30, 32-35) (Figure 1). This phenotype is primarily attributed to their loss of E-cadherin and can be observed through their deregulated cell-cell adhesion properties. Approximately 90% of ILC cases present with loss of E-cadherin due to genomic alteration, mostly seen as loss of heterozygosity and truncating frameshift mutations (30, 36-38). While loss of E-cadherin is a hallmark of ILC, it is important to appreciate that it is not the only difference between IDC and ILC. ILC tumors typically have good prognosis, with low to intermediate grade tumor, low Ki-67 expression and about 90% of cases are estrogen receptor positive (30) compared to 60-70% in IDC (31, 32, 39), which leads to this tumor type typically falling in the luminal A or B subtype (39). Although patients with ILC tend to have favorable outcomes in the early stages, these early benefits are often hampered by a higher risk for late recurrences with several longitudinal studies delineating poorer disease-free survival for ILC patients (30, 40-44).

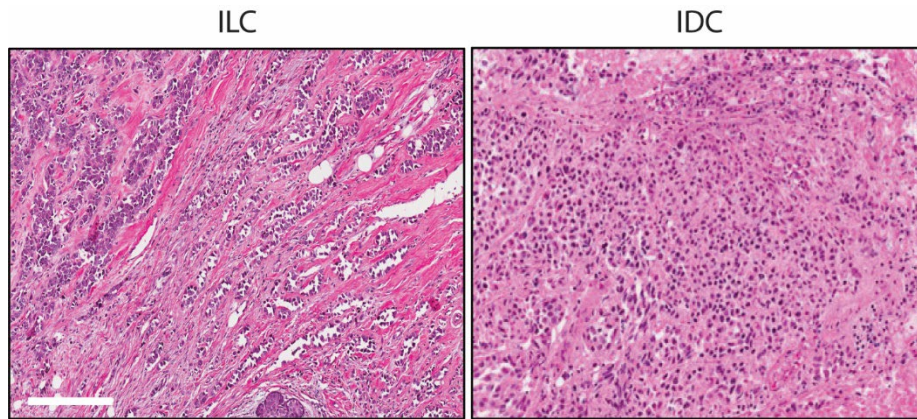


Figure 1: H&E staining of ILC and IDC reveal their distinct histologies

Single file cell growth of ILC versus bulky tumor growth of IDC is distinguishable via H&E staining of these tumors. Staining and imaging performed by Geoffrey Pecar, Lee/ Oesterreich laboratory, 2021. Magnification: 20X, scale bar: 200 μ m.

ILC tumors are more prone to spread to unique sites such as the gastrointestinal tract, peritoneum and ovaries, compared to IDC (30, 31). The single file growth pattern of ILC with stromal infiltration makes tumor detection on a mammogram more challenging and as such it is usually detected at a later stage than IDC (34). In addition to *CDH1* mutations and differences in immune signatures (34), multiple other molecular alterations such as Akt activation, *PTEN* loss, and mutations in *TBX3*, *FOXA1* and *ERBB2* have been detected at higher levels in ILC than in IDC (31, 43, 45-48). Despite these documented differences, both ILC and IDC are currently treated similarly in the clinic. Given the high ER positivity in ILC, hormone therapy is the first line treatment option, with the BIG 1-98 trial (49) comparing efficacy of letrozole and tamoxifen, reporting that patients with ILC had an overall greater benefit with letrozole. As such, aromatase inhibitors are now recommended for patients with ILC (49), although it does not eradicate the possibilities of endocrine resistance which continues to be a therapeutic challenge.

Complementary work from our group in ILC cell lines showed that tamoxifen had the potential

for driving proliferation in them with an agonistic effect, supporting the consideration of AIs or fulvestrant in ILC (50). Further efforts are needed to comprehensively characterize ILC as a unique subtype of breast cancer to identify targetable drivers of ILC as well as treatment biomarkers.

1.2 Insulin-Like Growth Factor Pathway

The insulin-like growth factor (IGF) signaling pathway plays a critical role in regulating cellular process such as proliferation, differentiation, apoptosis, survival, metabolism, and migration. These functions provide a critical system that regulates many other processes such as bone, muscle, and brain development in addition to overall organism growth. Primarily the IGF and insulin system comprises of three major ligands, IGF1, IGF2 and insulin as well as their cognate receptors, IGF1R, IGF2R and insulin receptor (IR) which they primarily bind to. Although at a lower affinity, ligands can bind to receptors other than their cognate receptors (51). These receptors are tetrameric proteins made of two ligand-binding extracellular α -subunits and two intracellular β -subunits which contain the tyrosine kinase signaling domains (52-54). Aside from the ligands and receptors, there are six ligand binding proteins, namely, IGFBP1 to 6 which also make up the pathway. About 99% of the IGF ligands in bloodstream and tissues are bound by one of these 6 IGFBPs, with equal or higher binding affinity compared to their receptors – thus they are a key mechanism of regulating signaling activity, often acting to attenuate signaling activation by ligands (55). Each binding protein is unique in its features and roles where some have been found to execute IGF-independent functions while others stay as a storage of IGFs (55).

Binding of IGF1 or insulin to its receptor on the cell membrane elicits intracellular tyrosine kinase activation. The activated receptor then phosphorylates specific substrates such as insulin receptor substrate 1 (IRS1), IRS2 and Shc (51). The phosphorylated residues of IRS1, IRS2 and Shc can be recognized by adaptors that contain a Src homology 2 (SH2) domain, which includes Grb2 and the p85 subunit of phosphatidylinositol 3-kinase (PI3K). Associations with these regulatory substrates have been shown to stimulate two main downstream pathways, the MAPK cascade or the PI3K cascade (Figure 2). These pathways play major roles in many processes by regulating the downstream signaling events of several growth factor receptors (56). While there are clear similarities in the pathways elicited by IGF and insulin, the major role of each pathway varies. The IGF pathway is primarily critical for proliferation, development and survival functions while the insulin pathway is critical for metabolism related roles (51). While IGF1R can elicit a signaling response upon ligand stimulation, IGF2R is a non-signaling receptor known to act as a storage of IGF2 ligands to attenuate signaling (57, 58). IGF2R regulates the amount of circulating IGF2 by transporting the ligand into the cell and degrading it through the lysosomal degradation pathway (58, 59). IGF2, however, can bind to IGF1R and insulin receptors, albeit at much lower affinity, to elicit a response (57). Interestingly, the insulin receptor isoform A (IR-A) which is typically critical in prenatal growth and is upregulated in cancers, has a high affinity for IGF2 (60) and could also activate signaling, thus complicating the efforts of targeting this pathway for therapeutic purposes.

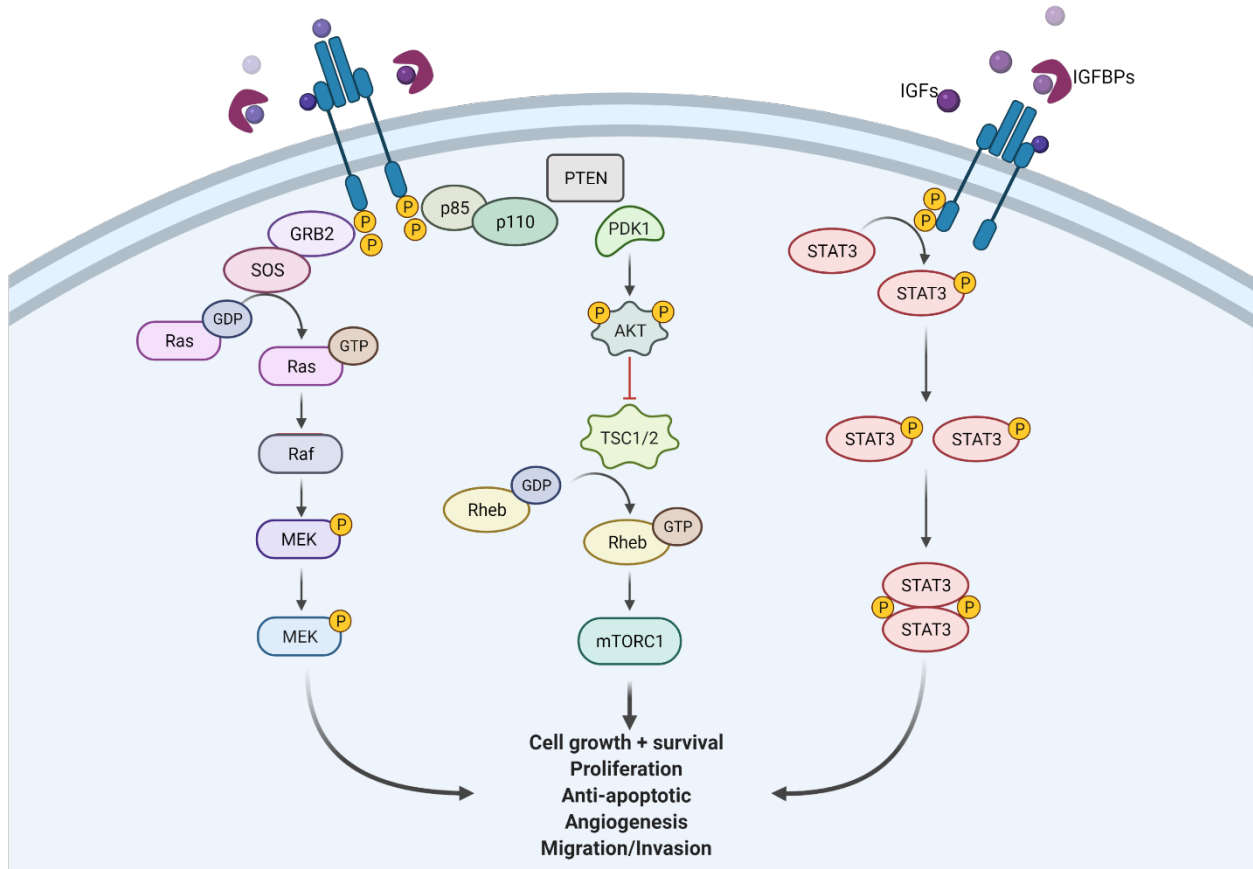


Figure 2: Simplified overview of the IGF signaling pathway

Figure shows a simplified image of the various signaling cascades such as PI3K, MAPK and JAK/STAT that are activated following IGF or insulin binding to its cognate receptor. Figure was generated and modified from a template available on BioRender.

1.2.1 IGF signaling in mammary development

Activation of the IGF pathway through ligand stimulation is critical in normal mammary gland development and physiology (61). Pituitary gland secreted growth hormone (GH) induces IGF1 production by the liver and the subsequent endocrine IGF1 regulation of growth during puberty is well established (62). Additionally, there is also an abundance of local expression of IGF1 in tissues postnatally, prompting the comparison between serum and local IGF1 roles on

the peripheral tissues (63-66), where both autocrine and paracrine actions of IGF1 on surrounding tissues have been shown (63, 64, 66-70). The majority of epithelial cell growth in mammary gland development occurs postnatally in both rodents and humans (66), where ductal elongation and outgrowth of mammary glands are initiated at early puberty when there are high levels of ovarian hormones and GH. This development process can be seen through the appearance of terminal endbuds (TEBs) (66). The necessity of IGF1 for this development was further exhibited by IGF1 knockout mice which had reduced viability and an overall absence of TEB formation and ductal outgrowth in the mammary glands (71, 72).

Complementary to IGF1 expression, IGF1R expression is also necessary for normal growth and mammary gland development, where a nonsense mutation of IGF1R results in perinatal lethality in mice (72, 73). A successful rescue experiment with IGF1R null epithelium transplanted into cleared WT mammary fat pads showed that IGF1R is also required for normal ductal outgrowth and TEB proliferation (74). In addition, overexpression of IGF1R was able to promote the development and cause hyperplasia and mammary tumors (75, 76). However, the endocrine versus autocrine/paracrine IGF1/ IGF1R signaling activation remains controversial. One study showed the presence of high IGF1 levels in the stromal compartment and strong IGF1R presence in the epithelium of rodent and human mammary glands, and thus concluded that the role of paracrine/autocrine signaling was necessary for mammary epithelial cell growth (66, 73). Critically, a separate study from 2010 showed that both local and endocrine IGF1 have roles in the mammary gland development, and that enhanced circulating IGF1 level is able to accelerate mammary epithelial proliferation (77), which led to this being the currently accepted notion.

1.2.2 Role of IGF signaling in breast cancer

A correlation between high plasma, circulating and serum IGF1 levels and breast cancer risk has been reported by several studies (78-81). In addition, high circulating IGF levels have also been correlated with poor prognosis in patients undergoing hormone therapy (82), where others have also cited high serum IGF1 correlation with increased mortality in patients with breast cancer (83). Owing to the many known downstream effects of the IGF pathway such as cell proliferation, migration, invasion and growth, countless pre-clinical studies have been conducted with cell line and mouse models to delineate the role of IGF1 in breast cancer. Studies using cell lines such as ER+ MCF7 and TNBC MDA-MB-231 depicted clear increases in cell growth, migration, and survival in response to IGF1 (84, 85) via Akt and MAPK pathways. Critically, a co-culture assay of MCF7 cells with differentiated or precursor adipocytes from obese volunteers showed two-fold higher release of IGF1 than that from lean individuals, which subsequently also led to higher proliferation of the MCF7 cells (85). This highlights the role of local IGF1 production that could increase breast cancer risk, with elevated risk for overweight individuals. In an *in vivo* model, constitutive IGF1 overexpressing MCF7 cells exhibited significantly higher tumor volumes compared to WT cells (86). The role of IGF1 and obesity in terms of breast cancer risk is well studied, where caloric restriction (CR) was shown to prevent mammary tumorigenesis in mice via a diminished IGF1/AKT/mTOR pathway (87, 88) and has also been shown to reduce metastatic burden (89, 90), with CR being suggested as a method to lower cancer risks (91).

Given the organismal function of the IGF pathway, the pathway has also been studied for a potential function in breast cancer metastasis. Bone is among the common distant metastatic sites

in breast cancer and the role of IGF1 in osteoblast proliferation and differentiation is well described (92). The high IGF1 environment in the bone has been shown to potentially prime breast cancer cells to metastasize to bone (93). Indeed, an *in vivo* study showed that bone derived IGF1 is necessary for proliferation and bone localization of breast cancer cells through Akt activation and recruitment of NF-kB (94). Finally, a discussion on breast cancer and IGF1 would not be complete without the consideration of its crosstalk with the ER signaling. Breast cancer cells may exhibit varied responses to IGF1 depending on their ER status, where cells expressing both IGF1R and ER can exhibit additive growth effects from stimulation with both IGF1 and estradiol (E2) (95, 96). The ER is a transcription factor and numerous IGF signaling components are regulated by this pathway. Interestingly, a bidirectional regulation of ER by IGF1 has also been reported (88), driving the importance of combination therapies targeting both pathways. Aside from ER and IGF1 synergistic effects, upregulation of the IGF pathway has been reported in tumors exhibiting HER2 treatment resistance (97). The association between IGF signaling and HER2/ EGFR signaling is a topic of critical importance and has been well documented, indicating a potential crosstalk between IGF1 and HER2 via autocrine/ paracrine signaling (98, 99) which also proposes therapeutics that target both downstream activators for maximal signaling inhibition.

1.2.3 Targeting IGF signaling in breast cancer

Various therapeutic strategies targeting the IGF pathway have been developed and tested both pre-clinically and clinically, with early clinical trial data reported in 2006 (100). These therapies can be divided into three main categories: monoclonal anti-IGF1R antibodies, small molecule tyrosine kinase inhibitors (TKIs), and anti-IGF ligand antibodies. These categories of

therapies vary in their selectivity, toxicity, and efficacy (101-105). IGF1R targeted antibodies act by blocking ligand binding, inducing receptor internalization and its subsequent degradation (106-108). These antibodies can bind both IGF1R and insulin receptors, which unfortunately led to toxicities in patients due to insulin signaling inhibition. Therefore, new generations of antibodies such as MEDI-573 from AstraZeneca and Xentuzumab (BI836845) from Boehringer Ingelheim have been developed to bind and inhibit IGF ligands with the goal of avoiding effects on insulin signaling. These antibodies bind to IGF1 and IGF2, preventing them from binding to their receptor, thus inhibiting signaling via IGF1R and IR-A without affecting glucose metabolism (103, 105, 109). Despite encouraging preclinical data, a phase 2 randomized study for MEDI-573 in combination with an Aromatase Inhibitor (AI) versus AI alone in women with hormone sensitive, HER2-, metastatic breast cancer was discontinued upon completion due to lack of clinical response. Similarly, Xentuzumab showed preclinical antitumor efficacy in breast and prostate cancer (110-112) but this failed to translate to the clinic when tested in combination with everolimus or exemestane in a phase Ib/II study for metastatic breast cancer and failed to improve PFS in the overall population (113). However, upon subgroup analysis, a PFS benefit was observed specifically in patients without visceral metastases when treated with xentuzumab/everolimus/exemestane and it is now in a phase II XENERA™-1 trial (NCT03659136) (103). This is a welcoming result for ILC researchers as bone metastasis is more common in ILC than in IDC (35), potentially suggesting a role for this combination in patients with ILC.

Small molecule TKI of IGF1R work by binding to and inhibiting the kinase domains of the targeted receptor. Examples of this class of compounds include Linsitinib (OSI-906),

BMS754807 and KW-2450. This class of inhibitors lack selectivity as the kinase domains of IGF1R and IR share 84% identity (103), and can thus inhibit both IGF1R and IR. Multiple studies demonstrated the successful inhibition of IGF1R/IR phosphorylation and AKT activation by these compounds which resulted in apoptosis, decreased cell proliferation, and tumor suppression in cell line and xenografts models (103, 114, 115). While there might have some benefits in targeting both pathways, glucose metabolism and toxicity was noticed in patients likely owing to the inhibitor activity on the IR (103, 116). As of now, these compounds have all been terminated from breast cancer trials (104, 105). Given that almost 80% of breast cancers are ER+, the crosstalk between IGF and ER has been evaluated as a combination strategy (117). Unfortunately, the majority of clinical trials addressing the combination of IGF1R and ER therapies have also not led to any improvement in clinical outcome (118).

Therapies targeting downstream activators in the IGF1 pathway such as PI3K/Akt/MAPK have been developed as these are the major signaling effectors (119). PI3K inhibitors such as LY294002 and Alpelisib, MAPK inhibitors such as U0126, AKT inhibitors such as MK2206 and AZD5363 and dual PI3K/mTOR inhibitors such as NVP-BEZ235 have been studied in pre-clinical settings where the results have been favorable (120-127). However, clinical trials with these agents have shown little activity, apart from the use of PI3K inhibitors in patients with PI3K/Akt pathway mutations which led to the 2019 approval of Piqray (Alpelisib) in combination with Fulvestrant for breast cancer with *PIK3CA* mutation.

1.2.4 Biomarker selection for targeted IGF therapies

Following the need for better selection of patients for IGF targeted therapies, our lab performed a Reverse Phase Protein Array (RPPA) in 21 breast cancer cell lines of varying subtypes to identify possible biomarkers affecting IGF1 response (128). These cell lines were stimulated with 10nM of IGF1 or insulin for varying durations and were then subjected to RPPA analysis for 134 target proteins (MD Anderson Cancer Center RPPA Core Facility). All cell lines tested were responsive to IGF1 treatment and showed IGF1R/IR phosphorylation. Critically, only a few cell lines showed activated downstream Akt phosphorylation, in addition to the extent of activation being variable between these lines. Through lasso regression modeling of this data, E-cadherin was identified as a negative regulator of IGF1 and insulin signaling, with stronger effects observed for IGF1. These findings were additionally validated by E-cadherin knockdown *in vitro*, where the knockdown enhanced IGF1 signaling and sensitized *CDH1* knockdown cells to IGF1R inhibition (128, 129). With the known regulation of IGF signaling by E-cadherin, and our interest in ILC, we compared IGF signaling levels between IDC and ILC tumor samples in The Cancer Genome Atlas (TCGA, GEO: GSE96058). We observed higher IGF1 mRNA and phospho-IGF1R/IR (pIGF1R/IR) levels in estrogen receptor positive (ER+) ILC compared to ER+ IDC (129). This finding was also replicated in a 2018 report from Patrick Derksen's group with ILC cells identified as having an elevated growth factor signaling, presenting with high Akt activation (130). From a separate study, mesenchymal TNBC cell lines with E-cadherin loss were also shown to be more IGF1 responsive than E-cadherin expressing TNBC, and thus highly sensitive to dual IGF1R/IR TKI, BMS-754807 (131). Taken together, we have a strong basis for hypothesizing high IGF pathway activation in the absence of E-cadherin in patient samples and

cell line models, thus proposing the use of E-cadherin loss as a functional biomarker for IGF targeted therapies.

Other groups have also searched for therapeutic vulnerabilities in E-cadherin null cells. A study by Bajrami et. al uncovered synthetic lethal phenotypes with inhibition of the ROS1 tyrosine kinase in E-cadherin deficient cells (132) while another group showed that MCF10A *CDHI* null cells showed increased susceptibility to RNAi mediated inhibition of several pathways, including the PI3K/AKT pathway, GPCRs, ion channels and proteasomal subunit proteins. These cells were also more sensitive to compounds that can disrupt the plasma membrane composition and trafficking, consistent with the role of E-cadherin in the adherens junction (133). Finally, a high throughput screen of almost 114,000 compounds was performed to identify targets causing synthetic lethality in E-cadherin null MCF10A cells, identifying 12 novel compounds that preferentially harmed cells lacking E-cadherin (134). These recent studies highlight the increasing attention given to identify pathways that may be selectively targetable in E-cadherin deficient cells such as in ILC, thus accentuating the need for a comprehensive study on the efficacy of using loss of E-cadherin as a potential functional biomarker for targeted therapies.

1.3 E-cadherin and breast cancer

E-cadherin is a calcium-dependent cell-cell adhesion molecule known to have roles in epithelial cell behavior and the structural formation of adherens junction (135-137). It consists of an intracellular domain, a transmembrane domain and five cadherin repeats in the extracellular

domain. The extracellular domain interacts with that of another E-cadherin molecule on an adjacent cell to establish cell-cell adhesion while the intracellular carboxy-terminal domain binds to p120 and β -catenin for subsequent association with α -catenin. This intracellular complex interacts with actin filaments to maintain cell integrity. E-cadherin expression is typically observed in breast epithelial cells with temporary downregulation only observed in budding lobules invading the breast stroma (138). Intercellular interactions are important to allow for differentiation necessary during the development processes of the breast and for maintaining the integrity of the tissues following development. Mutation and loss of E-cadherin expression has been reported in ILC as discussed previously and in hereditary diffuse gastric carcinoma. Interestingly, germline *CDH1* mutations in a single family have so far been associated with the development of metachronous diffuse gastric cancer and invasive lobular breast cancer (138, 139).

Due to its function in maintaining cell-cell adhesion, E-cadherin loss through epithelial-mesenchymal transition (EMT), genetic deletion, loss of heterozygosity or epigenetic silencing is correlated with increased tumor invasion, increased tumor grade, metastasis, and a poor prognosis overall (137, 140-148). It is thought that by losing the adherens junction, tumor cells are free to migrate and metastasize to distant locations. Along those lines, exogenous expression of E-cadherin has also been shown to decrease growth of several breast cancer cell lines (142, 149), further highlighting the importance of losing E-cadherin to promote tumor progression in some settings. Although historically the loss of E-cadherin expression in these special subtypes of cancers or other cancers as part of EMT has been noticed as a step in metastatic progression, recent reports have showed the importance of E-cadherin for metastasis (150, 151). Studies in

immortalized human breast epithelial cells showed that E-cadherin loss alone was sufficient to drive metastasis in an otherwise non-metastatic model by inducing EMT, rendering them anoikis resistant and increasing cellular motility and invasiveness (152). This role of E-cadherin was well agreed upon until a recent study with mouse mammary tumor organoids and xenografts showed the requirement for E-cadherin for metastasis (150) while another elucidated that it's the functional state of E-cadherin that truly determines a tumor's metastatic potential by using E-cadherin activating monoclonal antibodies (151).

Following the loss of E-cadherin, a re-localization of p120 to the cytoplasm is observed, with the release of β -catenin and α -catenin also to the cytoplasm. One might hypothesize that the release of β -catenin would stimulate Wnt signaling activation in E-cadherin null cells, however a decrease in both α and β -catenin have been reported in ILC (153, 154). In addition, several studies have reported that only non-canonical Wnt signaling activity is detectable in ILC cells, suggesting that effects of E-cadherin loss are largely independent of changes in canonical Wnt signaling (155, 156). Given the array of signaling differences between IDC and ILC (31, 34), it is critical to understand which mechanisms might be regulated specifically by the loss of E-cadherin in ILC. Our lab as well as other groups have reported on the downregulation of E-cadherin by growth factors to promote EMT (157). Although less extensive, there have been studies showing growth factor signaling regulation by E-cadherin (130, 140, 158-160) where multiple groups have shown that E-cadherin inhibits ligand-dependent activation of EGFR signaling.

1.4 Hypothesis

Given the evidence of interaction between growth factor receptors and E-cadherin in the literature as well as our preliminary data, we hypothesize that E-cadherin is a negative regulator of IGF1R. Our work investigates the negative regulation of IGF1R by E-cadherin and tests whether loss of E-cadherin is a functional biomarker for patient selection in IGF1 signaling-targeted therapy. The mechanism by which E-cadherin negatively regulates IGF1R is unknown and the effect of genetic loss of E-cadherin towards development and progression of ILC is also understudied. An understanding of how IGF1R is negatively regulated by E-cadherin is important to fully comprehend the mechanism and uncover additional potential therapeutic targets. In addition to breast cancers, there are other types of cancers such as hereditary diffuse gastric cancer (HDGC) that also presents with loss of E-cadherin. Our studies will benefit not only lobular breast cancer patients, but potentially also patients with HDGC. Our work will incorporate cell line models, patient derived organoids and mouse modeling to comprehensively address the questions proposed with a strong intent for translational relevance.

2.0 Elevated IGF and Akt Pathway Activation is Observed in ILC Tumors and Cell Lines

2.1 Introduction

Our lab previously performed a Reverse Phase Protein Array (RPPA) study to identify biomarkers for IGF1 response by comparing 21 breast cancer cell lines of varying subtypes (128). Cell lines were stimulated with 10nM IGF1 or insulin for varying durations and were then subjected to RPPA analysis for 134 target proteins. All cell lines were responsive to IGF1 treatment as seen through phosphorylation of IGF1R/IR. However, only a few cell lines showed activated downstream Akt phosphorylation. Lasso regression modeling identified E-cadherin among the negative regulators of IGF1 and Insulin signaling. This study was validated with *in vitro* knockdown of E-cadherin and a western blot analysis for signaling activation.

With the relationship between E-cadherin and IGF signaling discovered, our lab probed the TCGA dataset to learn more about how the loss of E-cadherin in ILC affects IGF signaling in ILC compared to IDC that retains E-cadherin expression. Higher IGF1 mRNA and phospho-IGF1R/IR (pIGF1R/IR) levels were observed in estrogen receptor positive (ER+) ILC compared to ER+ IDC (129). Consistent with the increased IGF1 mRNA seen in ILC, a stronger positive correlation was observed between IGF1 mRNA and pIGF1R levels in ILC than in IDC, suggesting increased IGF1 signaling in the absence of E-cadherin. IGF1 mRNA levels that do not necessarily lead to IGF1R phosphorylation and pathway activation in IDC suggests the presence of a putative negative regulation mechanism in IDC that is potentially lost in ILC. In a separate study, mesenchymal TNBC cell lines with E-cadherin loss were shown to be more IGF1

responsive than E-cadherin expressing TNBC, and thus highly sensitive to dual IGF1R/IR TKI, BMS-754807 (131). In addition, Dr Patrick Derksen's group also identified ILC cells as having elevated growth factor signaling where they showed high Akt activation in ILC models (130). Taken together, our findings and related reports in the literature provide a strong basis for pursuing E-cadherin as a potential biomarker to stratify patients for anti-IGF1 therapies for a tailored targeted therapeutic intervention.

In this chapter, we sought to validate our findings of elevated IGF signaling in ILC compared to IDC in The Sweden Cancerome Analysis Network - Breast (SCAN-B) comparing Luminal A IDC and ILC tumors (161). This dataset was curated from a consortium that was started in 2010 in a multicenter manner with an aim to analyze breast cancer tumors with NGS technologies to allow for better translational research. We also performed *in vitro* studies comparing IGF and EGF signaling activation in classic IDC and ILC cell lines which provided additional support for our hypothesis.

2.2 Materials and methods

2.2.1 In silico analysis

Gene expression data from the Sweden Cancerome Analysis Network–Breast (SCAN-B) study and The Cancer Genome Atlas (TCGA) were downloaded from Gene Expression Omnibus, accession GSE96058 (161) and GSE62944 (162) respectively. Differential gene expression between luminal A lobular (N = 157) and ductal (N = 307) breast cancer samples in

TCGA was performed using DESeq2 as described in (34). The differential expression analysis was corrected for tumor purity using a Consensus measurement of Tumor Purity as detailed in (34). For SCAN-B samples, differential gene expression between luminal A lobular (N = 265) and ductal (N = 1165) breast cancer samples was assessed using DESeq2. Tumor purity for SCAN-B samples was estimated using the R package ESTIMATE (163). FDR cut off of 0.05 was used to identify significantly differentially expressed genes. Heatmap for genes of interest was created using the R package ComplexHeatmap. Gene set variation analysis (GSVA) was performed on log transformed gene FPKM matrices using the R package GSVA (164) with default settings including “Gaussian” for kernel selection. Gene sets of interest were obtained from MSigDB version 7.4. The GSVA enrichment scores were compared between luminal A lobular and ductal breast cancer samples using Mann-Whitney U test. Gene set enrichment analysis (GSEA version 4.1.0. Broad Institute) (165) was also conducted on normalized raw counts with default settings and gene sets of interest obtained from MSigDB.

2.2.2 Cell culture

Cell lines utilized in this study were obtained from ATCC: MCF7 (RRID: CVCL_0031), T47D (RRID: CVCL_0553), ZR75.1 (RRID: CVCL_0588), MDA-MB-134-VI (RRID: CVCL_0617), MDA-MB-231 (RRID: CVCL_0062) and Asterand for SUM44PE (RRID: CVCL_3424). Cell lines were maintained in 10% fetal bovine serum (FBS; Life Technologies) supplemented media (Thermo Fisher Scientific): MDA-MB-134 in 1:1 DMEM: L-15; MCF7 and MDA-MB-231 in DMEM; and T47D and ZR75.1 in RPMI. SUM44PE was maintained in DMEM/F12 with 2% charcoal stripped serum (CSS; Life Technologies) with additional supplements as previously described (34). Cell lines were cultured for less than 6 months at a

time, routinely tested to be Mycoplasma free and authenticated by the University of Arizona Genetics Core (Tucson, Arizona) by short tandem repeat DNA profiling.

2.2.3 Immunoblotting

Protein for immunoblotting experiments were harvested using RIPA buffer (50mM Tris pH 7.4, 150mM NaCl, 1mM EDTA, 0.5% Nonidet P-40, 0.5% NaDeoxycholate, 0.1% SDS) supplemented with 1x HALT protease and phosphatase cocktail (Thermo Fisher #78442), probe sonicated for 15 seconds (20% amplitude) and centrifuged at 14,000rpm at 4°C for 15 minutes. Protein concentration was assessed using BCA assay (Thermo Fisher #23225) and 50ug of protein per sample was run on 10% SDS-PAGE gel, then transferred to PVDF membrane. Membrane blocking was performed with Intercept PBS blocking buffer (LiCOor #927-40000) for one hour at room temperature and probed with primary antibodies overnight at 4°C: pIGF1R/IR (Cell Signaling Technology #3024; RRID:AB_331253), IGF1R (Cell Signaling Technology #3027; RRID:AB_2122378), pAkt S473 (Cell Signaling Technology #4060; RRID:AB_2315049), Akt (Cell Signaling Technology #9272; RRID:AB_329827), InsR (Cell Signaling Technology #3025; RRID:AB_2280448), E-cadherin (BD Biosciences #610182; RRID:AB_397581), pEGFR Y1068 (Cell Signaling Technology #2234; RRID:AB_331701), EGFR (Cell Signaling Technology #4267; RRID:AB_2246311) and β -actin (Millipore Sigma #A5441, RRID:AB_476744). This was followed by 1 hour room temperature incubation with secondary antibodies (1:10,000; anti-mouse 680LT: LiCor #925-68020; anti-rabbit 800CW: LiCor #925-32211). Membranes were subsequently imaged on the LiCOor Odyssey CLx Imaging system, with band quantifications performed with built in software.

2.3 Results

2.3.1 IGF pathway activity is enhanced in ILC

To comprehensively understand differences in the IGF pathway between ILC and IDC, we analyzed the publicly available Sweden Cancerome Analysis Network–Breast (SCAN-B) study. SCAN-B has three times as many breast cancer cases as TCGA. This analysis was performed in collaboration with a lab colleague, Dr Susrutha Puthanmadhomnarayan. The SCAN-B dataset allowed a direct comparison of growth factor signaling differences between luminal A IDC (n=1165) and luminal A ILC (n=265) tumors. Significantly higher IGF1 and IGF2 expression were observed in ILC tumors in addition to several other growth factor signaling related genes (Figure 3A). Downregulation of several IGF binding proteins which typically suppress the IGF pathway was also observed in ILC. We also analyzed luminal A lobular (N = 157) and ductal (N = 307) breast cancer samples in the TCGA dataset (GSE62944) where we observed upregulation of IGF1 in ILC compared to IDC however, IGF2 expression was lower in ILC. Interesting findings with several other growth factor receptors such as EGFR, FGFR4 and NGFR was also observed where they were all significantly upregulated in ILC tumors (Figure 3B).

Analyzing the SCAN-B dataset further by gene set variation analysis (GSVA), we observed that IGF1/2 signaling activation was higher in ILC ($p=0.005$) (Figure 3C). To assess downstream activation, we probed the PI3K/Akt signaling pathway and observed that it was significantly higher in ILC by gene set enrichment analysis (GSEA) (Figure 3D, $p=0.04$) and by GSVA for signaling activation overall (Figure 3E, $p=3.144^{-6}$) and specifically in cancer (Figure

3F, $p=0.0002$). Overall, analysis of the SCAN-B dataset here and TCGA dataset from our previous work supports our hypothesis of the IGF pathway being more highly activated in ILC relative to IDC tumors.

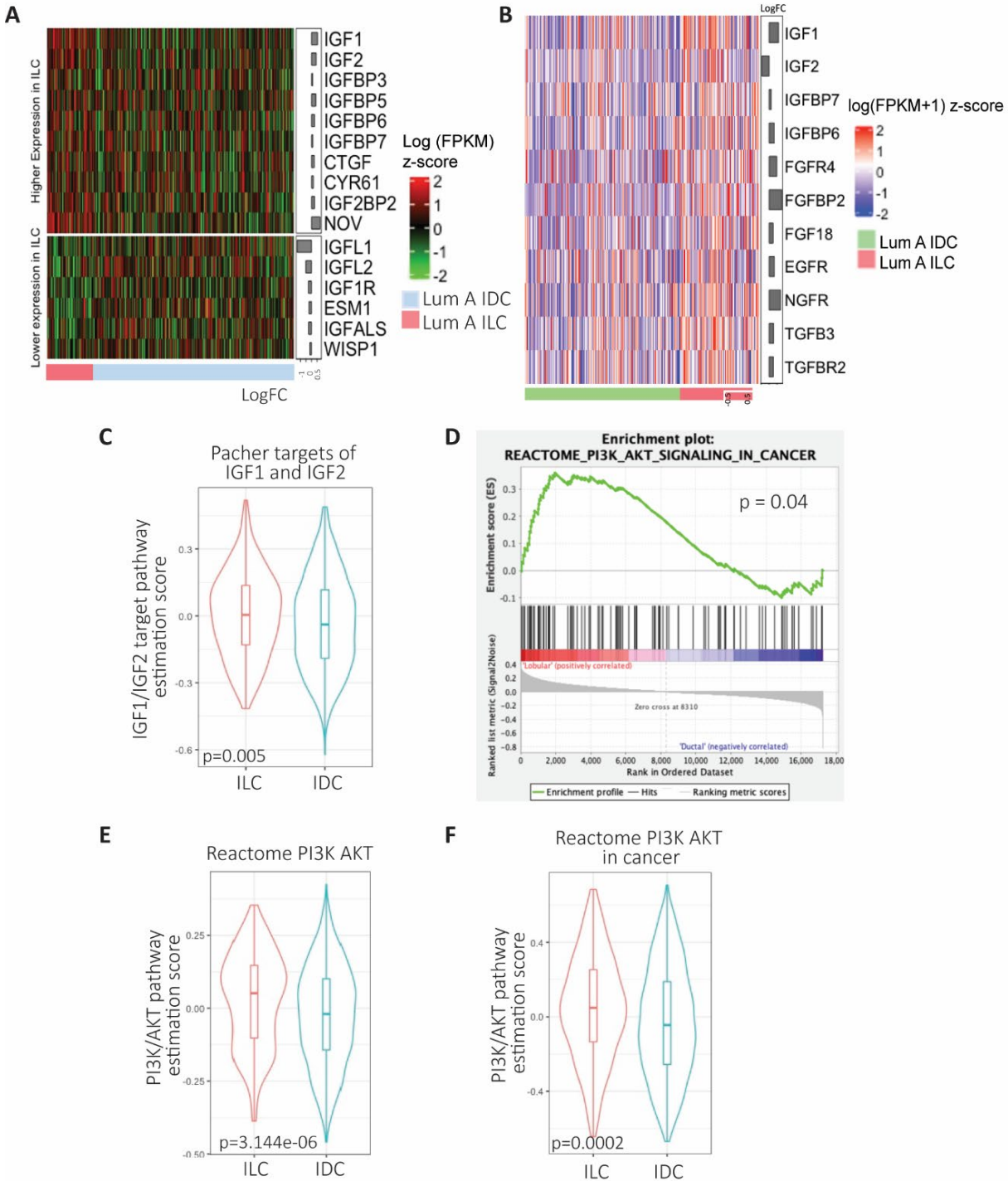


Figure 3: IGF pathway activity is enhanced in ILC tumors compared to IDC tumors

Gene expression analysis of growth factor signaling related genes comparing Luminal A IDC and ILC with significantly different expression values displayed from the (A) SCAN-B dataset and (B) TCGA dataset. (C) GSVA analysis of Luminal A IDC and ILC samples for targets of IGF1 and IGF2 using respective signature sets from MSigDB with significantly higher pathway activation in ILC. (D) GSEA analysis for PI3K/Akt showing significantly higher pathway activation in ILC samples obtained from the SCAN-B dataset. (E, F) GSVA analysis of Luminal A

IDC and ILC samples using respective signature sets from MSigDB with significantly higher pathway activation in ILC. This analysis was performed by a lab colleague, Dr Susrutha Puthanmadhomnarayan.

2.3.2 IGF pathway activity is enhanced in ILC cell lines *in vitro*

We investigated the differences in IGF pathway activity in IDC (MCF7, T47D, ZR75.1) and ILC (MDA-MB-134-VI, SUM44PE) cell lines. ILC cell lines showed higher pIGF1R/IR expression after IGF1 stimulation compared to the IDC cell lines, though the expression of total IGF1R/IR varied across cell models (Figure 4A). pAkt (S473) levels, as a measure of downstream pathway activation, did not always correlate with pIGF1R/IR levels. We observed Akt activation in the absence of ligands in T47D and ZR75.1 cells, while MCF7 cells demonstrated robust pAkt induction despite modest pIGF1R/IR levels. The presence of *PIK3CA* activating mutations in MCF7 and T47D (166-168), and *PTEN* loss in ZR75.1 cells (168) may be the potential reasoning as to why a baseline level activation is higher in these cell lines. To assess the effects of growth factors other than IGF1 and IGF2, we stimulated these cells with insulin and again observed that ILC cell lines demonstrated enhanced activation of pIGF1R/IR, although with this ligand ZR75.1 also showed robust activation (Figure 4B). To test whether there was a difference between ILC and IDC cell lines in response to ligands targeting other cell surface receptors that may be regulated by E-cadherin (158, 159, 169, 170), we assessed the effects of EGF stimulation in our panel of cell lines (Figure 4C). Very minimal EGFR activation could be detected in ILC cell lines suggesting cellular context specific changes in growth factor signaling activation. Overall, these data support an increased IGF pathway activity in ILC compared to IDC in our cell line models and support the patient tumor results presented in Chapter 2.3.1.

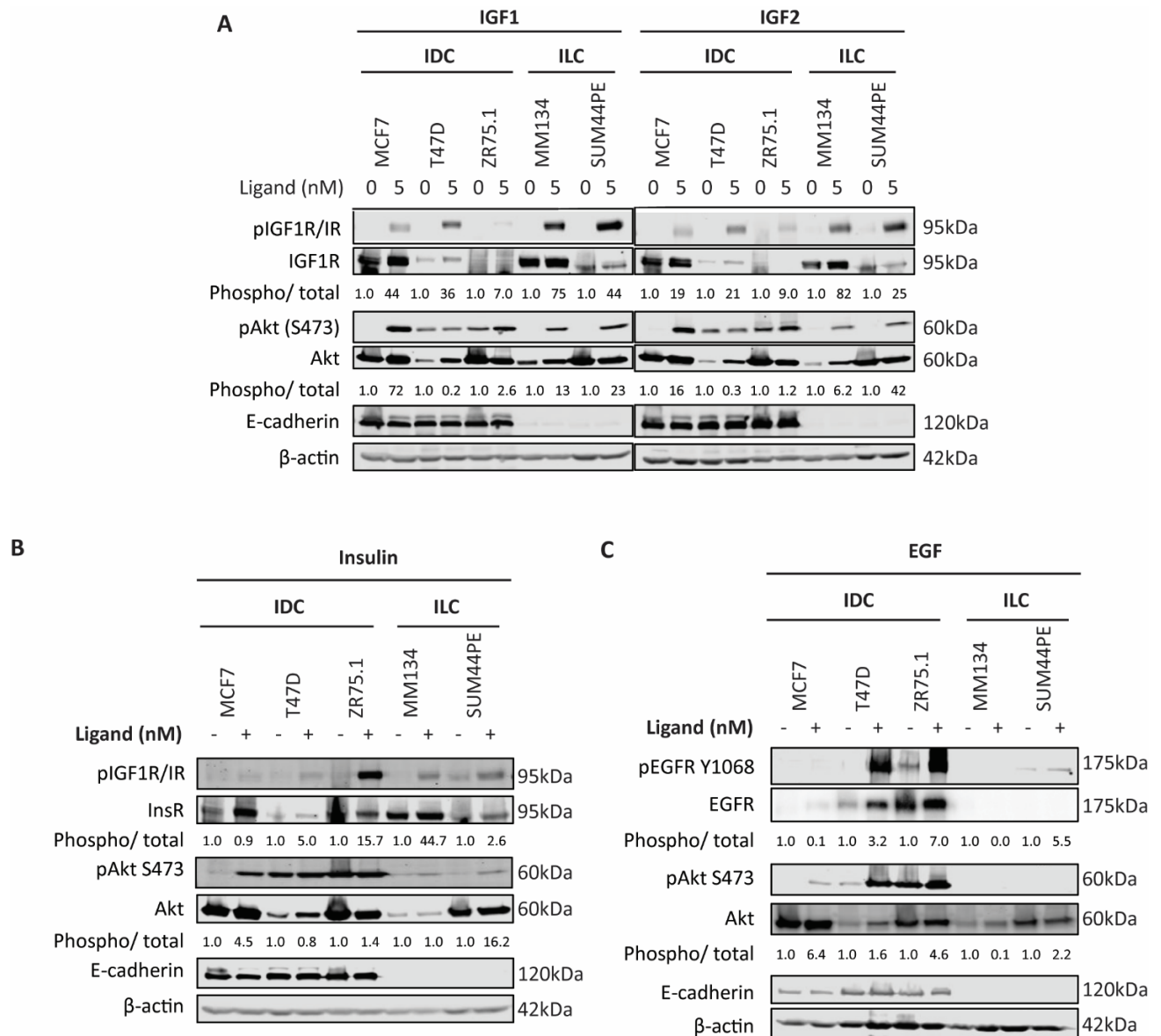


Figure 4: IGF pathway activity is enhanced in ILC cell lines *in vitro*

MCF7, T47D, ZR75.1, MM134 and SUM44PE cells were serum starved overnight and stimulated with (A) IGF1 and IGF2 (B) Insulin (C) EGF (0-10nM) for 15 minutes at 37°C. Cells were harvested for Western blot to assess IGF1R/IR, EGFR and Akt signaling. For quantification, phosphorylated protein levels were normalized to corresponding total protein levels and loading controls, and then normalized to their respective vehicle controls. Ligand treated sample values were further normalized to respective cell line vehicle treated samples. Representative experiment shown for all, n=2 for each experiment.

2.4 Discussion

In this chapter, we investigated the differences in IGF and Akt pathways between IDC and ILC patient tumor samples within the SCAN-B dataset. We report that both pathways assessed were indeed higher in ILC tumors, with higher expression of IGF1 and IGF2 ligands also evident in ILC compared to IDC. Aside from the ligands being expressed at a higher level, a signature of their target genes was also upregulated in ILC, further supporting pathway activation. In addition, the GSEA enrichment for PI3K and Akt signaling pathways strongly supports our future work to understand the role of E-cadherin in regulating the IGF/Akt axis and the potential of utilizing E-cadherin as a functional biomarker to support pathway targeting.

In addition to these findings, we were also able to validate our SCAN-B results with the TCGA cohort (129) and published literature (31, 130), providing a strong foundation for our hypothesis. Comparison between IDC and ILC tumors with and without E-cadherin showed that the IGF/Akt axis is upregulated in the absence of E-cadherin. Further *in vitro* validation with a panel of cell line models demonstrated a pattern of higher IGF/Akt signaling in the ILC cell lines tested, albeit with cell specific differences. This aligns well with results obtained from *Cdh1*^{-/-}; *p53*^{-/-} derived mouse ILC cell lines from Dr Patrick Derksen's group (130). Our effort to explore if this is a pan-growth factor effect by testing EGF signaling showed minimal activation in the ILC cell lines, suggesting that this phenotype may most robustly apply to IGF signaling. Although our findings from these experiments are not definitive, there certainly is a clear trend supporting our hypothesis. A major difference between the patient data and our *in vitro* results is the nature of the samples themselves. Our *in vitro* experiments were performed in a controlled manner with one concentration of each ligand tested, whereas the results from patient data such

as in the SCAN-B dataset is more representative of the tumor microenvironment. Our ability to obtain promising results with these models suggests the importance of this study.

A wealth of literature supports growth factor signaling in breast cancer an attractive target for therapeutics. Many growth factor signaling pathways are continuously being probed (171, 172) in response to the vast numbers of inhibitors being developed (173). However, it has become evident that not all tumors are sensitive to the same treatments despite being similar in their subtypes, highlighting the need for personalized medicine approaches (174, 175). An example of this is the approval of Alpelisib (Piqray) in combination with Fulvestrant for patients with hormone receptor positive (HR+), HER2-, *PIK3CA*-mutated metastatic breast cancer (176). Breast cancers with a *PIK3CA* activation can be successfully treated with a targeted therapy if the activation is driven by a mutation (177), which significantly benefits patient prognosis. Our research suggests that tumors with loss of E-cadherin may respond favorably to IGF-targeted therapies and that E-cadherin loss may provide a biomarker with which to stratify patients for treatment with agents targeting this pathway. As discussed previously, clinical trials with IGF-targeted therapies in an unstratified breast cancer patient population did not show clinical benefit. However, a small subset of patients did show benefit (178-180) although their specific disease characteristics were unfortunately not analyzed retrospectively. A recent study with an IGF ligand blocking antibody Xentuzumab (BI836845) reported clinical benefits in patients with non-visceral metastasis (113) which could potentially allude to patients with ILC (35, 130), thus further supporting the need to treat the right patients with the right treatments.

Overall, in this chapter, we present evidence of comparatively higher IGF/Akt signaling in ILC compared to IDC tumor samples using SCAN-B data and sensitivity of cell lines *in vitro*. Given that the loss of E-cadherin is routinely assessed for ILC diagnosis, the growing evidence that we have on loss of E-cadherin correlating with activated growth factor signaling (31, 129, 130) is extremely valuable towards utilizing it as a functional biomarker of response.

3.0 *CDH1* Knockout (KO) IDC Isogenic Cell Lines as a Model to Study The Role of E-Cadherin in Regulating IGF Signaling

3.1 Introduction

Cell lines are a simple yet valuable model for studying protein interactions and their effects on tumorigenesis. A good example of this is the distinct differences in sensitivity to IGF, insulin and EGF stimulation observed between IDC and ILC cell lines investigated in Chapter 2. While making direct comparisons between IDC and ILC cell lines may provide crucial information on the role of E-cadherin, it is imperative to consider the genomic, epigenomic and proteomic differences between these cell lines. While IDC has been studied in detail, fewer investigations on ILC has led to very few models being available for research. For example, only three ILC cell lines are in the Cancer Cell Line Encyclopedia (CCLE) database while over 30 breast ductal carcinoma cell lines are available (181). Each cell line is derived from patients and tumors with very different backgrounds, varying therapeutic interventions, and disease progression. The presence of wide heterogeneity between cell lines despite being from the same subtype, in addition to the small number of cell lines available, may lead to challenges with data consistency. Furthermore, it is also important to note that while loss of E-cadherin is one of the major differences between IDC and ILC, it is not the only point of differentiation between them. Therefore, making direct comparisons between ILC and IDC cell lines and concluding that the effects are due solely to E-cadherin would be implausible, thus, requiring more and better models to investigate our hypothesis that E-cadherin regulates the IGF pathway in ILC.

To establish models to study where phenotypes can be directly ascribed to the role of E-cadherin, we generated isogenic *CDHI* knockout IDC cell lines. These models allow us to specifically study the role of E-cadherin in regulating the IGF pathway without cell line backgrounds and other potential genetic alterations compromising our interpretation of the data. The CRISPR/Cas9 system has opened a wide array of new approaches for molecular studies (182, 183). Using the CRISPR/ Cas9 system, we performed *CDHI* knockout in three commonly studied ER+ IDC cell lines. Previously, several groups including Dr Patrick Derksen's and Dr Christopher Lord's have also generated MCF7 *CDHI* KO cell lines, by utilizing the CRISPR/Cas9 system to unravel an autocrine activation of growth factor signaling (130) and a synthetic lethality of *CDHI* KO with ROS1 inhibition (132). To orthogonally study the role of E-cadherin, Laura Savariau, a graduate student, and colleague in the Lee/Oesterreich lab generated ILC cell lines overexpressing a Doxycycline inducible E-cadherin, and I have used these additional models to perform crucial validation experiments.

This chapter explores the process of generating *CDHI* knockout cell line models and characterizes their morphology, growth, and culture phenotypes.

3.2 Materials and methods

3.2.1 Cell culture

Cell lines utilized in this chapter were obtained from ATCC: MCF7 (RRID: CVCL_0031), T47D (RRID: CVCL_0553) and ZR75.1 (RRID: CVCL_0588). Cell lines were maintained in 10% fetal bovine serum (FBS; Life Technologies) supplemented media (Thermo Fisher Scientific): MCF7 in DMEM; and T47D and ZR75.1 in RPMI. Cell lines were cultured for less than 6 months at a time, routinely tested to be Mycoplasma free and authenticated by the University of Arizona Genetics Core (Tucson, Arizona) by short tandem repeat DNA profiling.

3.2.2 *CDH1* knockout cell line generation

CRISPR mediated knockout of *CDH1* in MCF7 and T47D cells was performed by utilizing the Gene Knockout Kit (V1) from Synthego (Redwood City, California) as previously described (184, 185). Single cell clones generated were continually cultured in 50% of 0.4µm filtered conditioned media to support viability. The parental cell line was used a comparator for MCF7 and T47D, referred as wildtype (WT). Sanger sequencing for *CDH1* (F: AGGAGACTGAAAGGGAACGGTG, R: GTGCCCTCAACCTCCTCTTCTT) was performed to confirm the presence of an indel. For ZR75.1, a lentiviral doxycycline inducible Cas9 was utilized (pLV[Exp]-Bsd-TRE3G>hCas9). In addition, an adenoviral vector harboring either short guide RNA (sgRNA) for *CDH1* (pAV[2gRNA]-EGFP:P2A:Puro-U6>gRNA *CDH1* exon11-U6>gRNA *CDH1* exon5) or a non-targeting control (NTC) sequence (pAV[2gRNA]-EGFP:P2A:Puro-U6>NTCguide1-U6>NTCguide2) was utilized. All three plasmids were

generated by VectorBuilder. A total of 3 rounds of infection and Puromycin selection was performed before single cell sorting of the ZR75.1 cells. The ZR75.1 *CDHI* KO and NTC cells were generated by Dr Jagmohan Hooda, a senior research scientist in our group. 8 clones from each KO and NTC cells were isolated by single cell cloning and combined to generate a pool for subsequent experiments.

3.2.3 Immunoblotting

Protein for immunoblotting experiments were harvested using RIPA buffer (50mM Tris pH 7.4, 150mM NaCl, 1mM EDTA, 0.5% Nonidet P-40, 0.5% NaDeoxycholate, 0.1% SDS) supplemented with 1x HALT protease and phosphatase cocktail (Thermo Fisher #78442), probe sonicated for 15 seconds (20% amplitude) and centrifuged at 14,000rpm at 4°C for 15 minutes. Protein concentration was assessed using BCA assay (Thermo Fisher #23225) and 50ug of protein per sample was run on 10% SDS-PAGE gel, then transferred to PVDF membrane. Membrane blocking was performed with Intercept PBS blocking buffer (LiCoR #927-40000) for one hour at room temperature and probed with primary antibodies overnight at 4°C: E-cadherin (BD Biosciences #610182; RRID:AB_397581), β -catenin (BD Biosciences #610154; RRID:AB_397555), p120 catenin (BD Biosciences; #610134; RRID:AB_397537), non-phospho β -catenin (Cell Signaling Technology #1980; RRID:AB_2650576) and β -actin (Millipore Sigma #A5441, RRID:AB_476744). This was followed by 1 hour room temperature incubation with secondary antibodies (1:10,000; anti-mouse 680LT: LiCoR #925-68020; anti-rabbit 800CW: LiCoR #925-32211). Membranes were subsequently imaged on the LiCoR Odyssey CLx Imaging system, with band quantifications performed with the built-in software.

3.2.4 qRT-PCR for *CDHI*

RNA extraction was performed using RNeasy mini kit (Qiagen #74106) and the RNA quality and amount quantified on NanoDrop. Reverse transcription to cDNA was performed with PrimeScript™ RT Master Mix (Takara Bio #RR036B). RT-PCR was then performed with SsoAdvanced Universal SYBR (Bio-Rad #1726275) with *CDHI* primers (F: GAACAGCACGTACACAGCCCT, R: GCAGAAGTGTCCCTGTTCCAG). Results were normalized to reads from housekeeping gene RPLPO. Statistical differences evaluated using a paired t-test.

3.2.5 Immunofluorescence

Cells were plated at a density of 100,000-200,000 cells/well on glass coverslips (Fisher #12-545-80P) in 24-well plates, fixed on ice in ice cold methanol for 30 minutes and blocked with buffer (0.3% Triton X-100, 5% BSA, 1X DPBS) for 1 hour at room temperature. Primary antibody incubation was performed overnight at 4°C: E-cadherin (Cell Signaling Technology; #3195; RRID: AB_2291471; 1:100) and p120 catenin (BD Biosciences; #610134; RRID: AB_397537; 1:100). Secondary antibody incubation was done for 1 hour at room temperature followed by Hoechst 33342 (Thermo Scientific #62249; 1:10000) staining. Coverslips were mounted with Aqua-Poly/Mount (Polysciences #18606-20) and images were taken on a Nikon A1 confocal microscope with a 60X objective.

3.2.6 2D and ULA cell growth assay

Cells were plated in 100 μ L of respective media with 10% FBS at 5,000 cells/well in 2D and ULA (Corning #3474) 96-well plates. Plates were collected at days 0, 2, 4, 6 and 8 and measured by CellTiter-Glo (Promega #PR-G7573) following the manufacturer's protocol. Cell viability values were analyzed following blank cell deductions and normalization to vehicle readings. Statistical differences were evaluated using 2way-ANOVA ($p < 0.05$).

3.2.7 FACS for anoikis resistance

Cells were stained with APC-Annexin V (BD Biosciences #550474) and Propidium Iodide (BD Biosciences #556463) in 1X Annexin binding buffer (BD Biosciences #556454) for 15 minutes at room temperature. Samples were analyzed on an LSR II Flow cytometer (BD Biosciences) and processed using BD FACSDiva and FlowJo software (BD Biosciences) as previously described (184). Live cell percentages in 2D conditions for each cell line was used to normalize the live cell percentages in ULA conditions. Statistical differences were tested using a two-way ANOVA.

3.2.8 Bulk RNA sequencing sample preparation

MCF7 and T47D, parental and *CDHI* KO cells were plated at 500,000 cells/ well in a full 6-well plate each in their respective full serum media. RNA extraction was performed with Qiagen RNeasy (#75162) by combining 2 wells into one sample, thus obtaining 3 biological replicates/ cell line. All samples were subjected to a qRT-PCR for *CDHI* as a quality control

measure. Upon confirmation, all samples were sent to the UPMC Genome Center to conduct a paired end sequencing with a sequencing depth of 25-33 million reads.

3.2.9 Bulk RNA sequencing analysis MCF7 and T47D parental and *CDH1* KO cell lines

RNA expression quantification and gene-level summarization were performed using Salmon v1.1.0 (186) with index generated from GRCh38 Ensemble and tximport v1.16.1 (187), respectively. Resulting expression estimates were summarized to gene-level by tximport. Principal component analysis was generated using the rlog function from the R package DESeq2 v1.30.0 (188) and the first 2 PCs were plotted using ggplots. DESeq2 was used for differential expression analysis of E-cadherin KO vs Parent cells. Significantly expressed genes (DEGs) were defined as those with absolute log₂ fold change ≥ 1 and adjusted p-value of < 0.05 for MCF7 (515 genes) and absolute log₂ fold change ≥ 1.5 and adjusted p-value of < 0.05 for T47D (787 genes). Top 20 genes were plotted using Complex Heatmap v2.7.8.1000. Using the significant DEGs, Genes Set Enrichment Analysis (GSEA) was performed using gseGO function from the clusterProfiler package v3.16.1. GSEA results were plotted with dotplot on R.

3.3 Results

3.3.1 *CDHI* KO IDC cell lines demonstrated altered morphology and re-localized p120 catenin

To generate *CDHI* knockout (KO) cell lines, we utilized the Synthego Gene Knockout Kit (V1) as detailed in the Materials and Method section and as previously described (184, 185). Single clones were plated in 96-well plates via flow sorting to ensure selection of individual cell clones with complete gene knockout. Upon clonal outgrowth, and confirmation of KO by immunoblots and Sanger sequencing for *CDHI*, 8 clones from each cell line (MCF7 and T47D) were combined at equal frequency. A few passages of cell culture were performed before a final round of confirmation with immunoblotting and Sanger sequencing was performed. Parental MCF7 and T47D cell lines of the same passage numbers were utilized as the comparators and were annotated MCF7 WT and T47D WT. For ZR75.1, Jagmohan Hooda, PhD in the lab used a separate method with a Doxycycline inducible Cas9 and an adenoviral delivery of sgRNA was performed to obtain the *CDHI* KO cells. A lentiviral plasmid system was used to express Dox-inducible Cas9. This model was first tested for efficiency of Cas9 expression with Dox treatment before 3 rounds of adenoviral *CDHI* targeting sgRNA or a non-targeting control (NTC) sgRNA were infected. Following clone outgrowth, cells were selected as before, and 8 clones pooled for further experimentation. The NTC sgRNA infected cells were also selected in the same way and were annotated ZR75.1 WT. ZR75.1 *CDHI* KO and NTC cells.

Both MCF7 and T47D *CDHI* KO cells exhibited complete loss of E-cadherin expression (Figure 5A, B) as ascertained via immunoblotting and qRT-PCR. ZR75.1 *CDHI* KO cells,

however, did not exhibit complete gene deletion with about 40% of the protein expression remaining. We hypothesize that the *CDHI* amplification in ZR75.1 is a potential reason for this challenge in obtaining a complete gene knockout model (189). Despite the incomplete deletion, ZR75.1 *CDHI* KO cells are still a valuable model for understanding the role of E-cadherin in regulating the IGF axis and were utilized for critical experiments in this project.

Following the generation of these cell line models, I assessed the similarity of *CDHI* KO IDC cell lines to ILC cell lines. In 2D culture, MCF7 and T47D KO cells demonstrate varied morphology compared to their WT cells (Figure 5C). KO cells were more distant from their neighboring cells, with less cell-cell interaction and less cell-plate attachment. In ultra-low attachment (ULA) where cells grow in suspension, both KO cells formed more loose structures with individual cell perimeters still being visible while the WT cells formed tight clusters. Meanwhile, in the ZR75.1 cell pair, no major differences were observed between the WT and KO cells in either growth conditions. This might be due to the incomplete *CDHI* deletion, thus masking any potential changes that may occur with a *CDHI* KO.

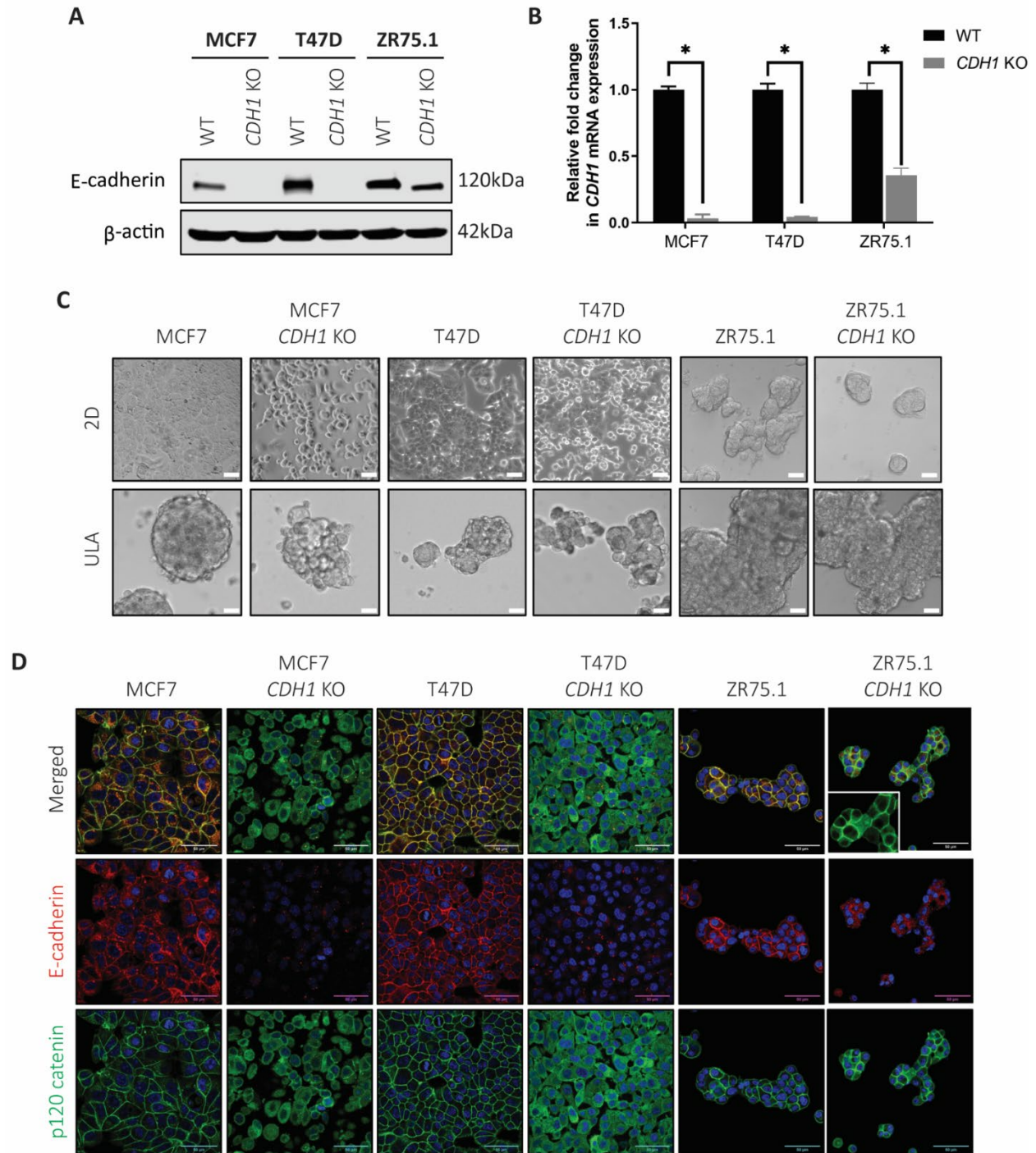


Figure 5: *CDH1* KO IDC cell lines demonstrate altered morphology and re-localization of p120 catenin

(A) Western blotting and (B) qRT-PCR confirms reduction of E-cadherin in *CDH1* KO MCF7, T47D and ZR75.1 CRISPR cell lines compared to wildtype (WT) parental cells. Statistical differences evaluated using paired t-test ($*p < 0.05$). Representative experiment shown, $n=2$ (each with two biological and 3 technical replicates). (C) Representative brightfield images (10X magnification) of WT and *CDH1* KO cell line models plated in 2D and ULA plates. (D) E-cadherin (red) and p120 catenin (green) staining of WT and *CDH1* KO cells confirms *CDH1* loss and

p120 re-localization in *CDHI* KO cell models by confocal microscopy (60X objective). Inset in the ZR75.1 *CDHI* KO panel shows a zoomed in image. Scale bar: 50 μ m. Representative experiment shown for all, n=2-3 for each experiment. ZR75.1 *CDHI* KO and NTC cells were generated by Dr Jagmohan Hooda.

We next assessed *CDHI* deletion via immunofluorescence to observe if there was any remaining expression and to also evaluate the potential changes to the cells' adherens junction. While no membranous E-cadherin staining was observed in MCF7 and T47D KO cells, some puncta staining was observed (Figure 5D). This is similar to the puncta-like E-cadherin staining in ILC cells we have seen previously (129, 154). Membranous E-cadherin staining was observed in ZR75.1 KO, although at lower intensity than the WT cells. To visualize the adherens junction formation, we stained for p120 catenin and observed its re-localization to the cytoplasm following *CDHI* deletion, where p120 catenin is retained on the membrane by E-cadherin, and its loss leads to p120 re-localization and the loss of an intact adherens junction.

3.3.2 β -catenin expression is reduced following *CDHI* knockout

In addition to retaining p120 catenin on the membrane, E-cadherin is also known to retain β -catenin on the membrane. The release of β -catenin from the cell membrane could result in its free availability in the cytoplasm, which could in turn lead to either its proteasomal degradation or its accumulation resulting in subsequent activation of Wnt signaling (190). As our goal to delete *CDHI* was to assess its effects specifically on IGF signaling and not to have this phenotype be affected by potential changes to β -catenin signaling, we sought to investigate if the β -catenin expression is affected. As seen in ILC cells, E-cadherin knockout in MCF7 and T47D led to reduced β -catenin expression (Figure 6). Using a GSK inhibitor, CHIR-99021

(Selleckchem #S2924), we confirmed that β -catenin in *CDH1* KO cells is indeed targeted for proteasomal degradation (Figure 6), thus ruling out increased β -catenin activity in the absence of E-cadherin in our KO models.

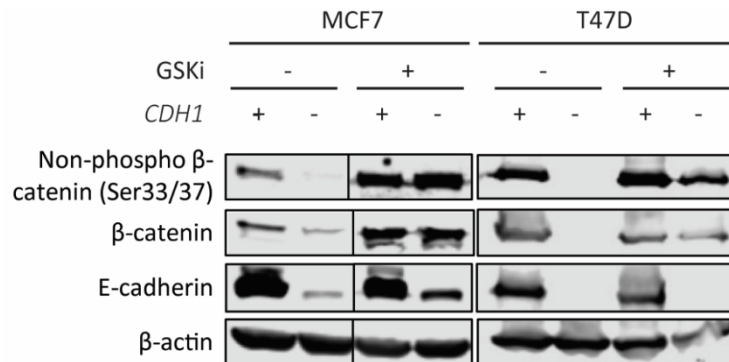


Figure 6: β -catenin signaling is not affected by *CDH1* knockout

MCF7 and T47D, WT and *CDH1* KO cells were treated with GSK-3 inhibitor, CHIR 99021 for 24 hours and harvested for Western blotting. Total and active β -catenin protein levels were assessed. Representative experiment shown, n=2.

3.3.3 *CDH1* KO cells exhibit enhanced growth in ULA and are anoikis resistant

To assess if the changes in the KO cell morphology bring about any changes to their growth in 2D and ULA settings, I set up a 6 to 8-day growth assay in which cells were grown in their respective media in 96-well plates. As shown in Figure 7A, there were no significant changes in 2D growth between WT and KO cells of all three cell lines. However, there was significantly increased growth in MCF7 and T47D KO cells in the ULA plates (MCF7 $p < 0.05$; T47D $p < 0.001$), suggesting that cells without E-cadherin grow better in a suspension setting or vice versa where cells expressing E-cadherin are not able to grow as well in suspension. Our group has previously investigated this in transient models (184), with these KO models

confirming our previous findings. The ZR75.1 models did not show any differences in ULA growth, again potentially due to the incomplete gene deletion masking any effects.

With the difference between WT and KO cells growth in ULA now known, we further assessed differences in anoikis resistance in the KO cells and/or anchorage independent growth in the KO cells. WT and KO cells were grown in 2D or ULA plates for 3 days and subjected to an apoptosis assay via flow cytometry (Figure 7B). Cell growth in the 2D setting was similar between WT and KO cells and this percentage of live cells was used to normalize their ULA growth. A higher percentage of Annexin V-stained apoptotic cells were observed in the T47D WT cells, suggesting an anoikis resistance phenotype of the T47D KO cells ($p < 0.05$) in suspension. However, no significant differences were observed between the MCF7 WT and KO cells despite exhibiting differences in ULA growth. It is important to note that MCF7 cells are deficient in caspase 3 (191, 192) and thus additional steps are needed to comprehensively address the apoptosis in this cell line.

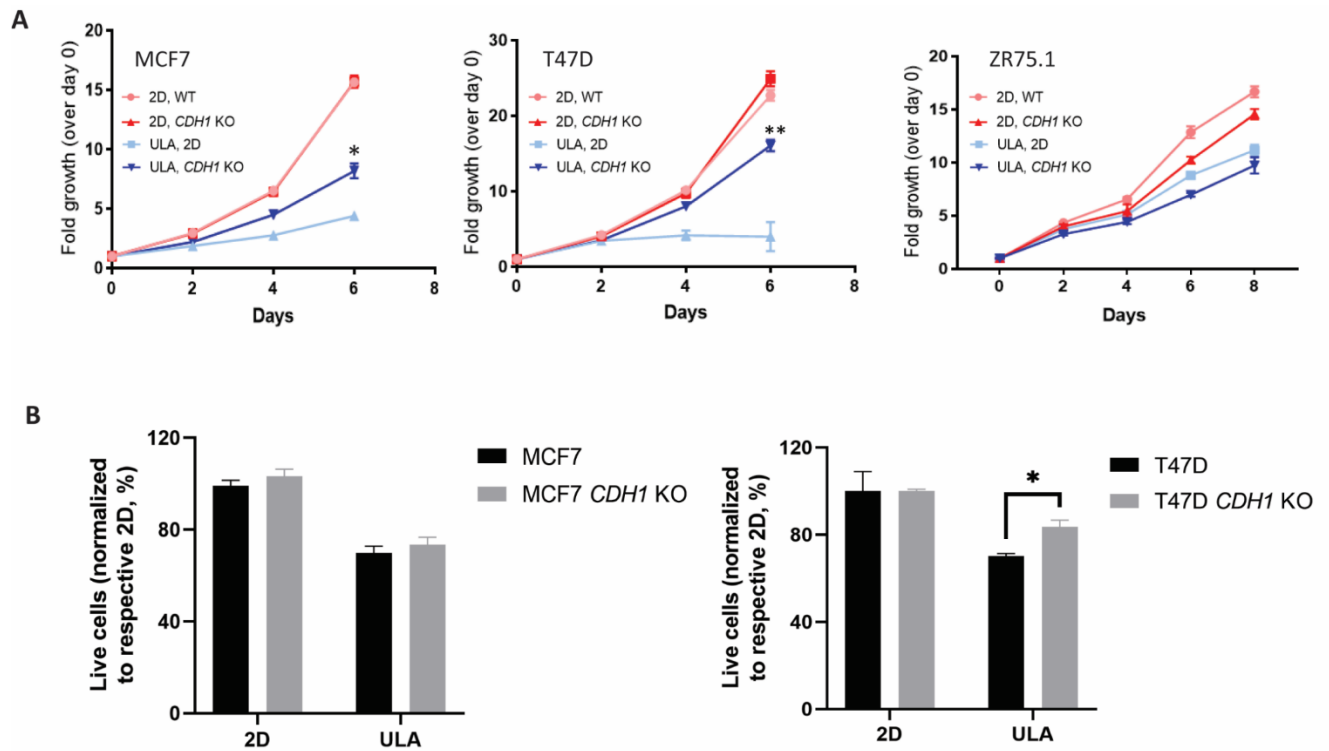


Figure 7: *CDH1* KO cells exhibit enhanced growth in ULA and display anoikis resistance

(A) MCF7, T47D, ZR75.1 WT and *CDH1* KO cells were plated at 5000 cells/ well in 2D and ULA 96-well plates in their respective full serum media. Cell viability was quantified on days 0-8 with CellTiter-Glo assay and data was normalized to day 0 quantification. Statistical differences were evaluated using two-way ANOVA (* $p < 0.05$, ** $p < 0.01$, representative experiment shown, $n = 3$ (each with six biological replicates)). (B) MCF7 and T47D WT and *CDH1* KO cells were grown in 2D and ULA plates for 3 days and stained with Annexin V and propidium iodide to measure live and apoptotic cells, respectively. Live cell percentage in 2D for each cell line was used to normalize the live cell percentages in ULA plates. Representative experiment shown; $n = 3$ (each with three biological replicates). Statistical differences were evaluated using two-way ANOVA (* $p < 0.05$).

3.3.4 RNA sequencing reveals variations between WT and KO cells, with related pathway differences

To assess differences between our WT and KO cell lines we performed bulk RNA sequencing on the MCF7 and T47D cell line pairs. The analysis of RNA sequencing was performed by a lab colleague, Laura Savariau. Principal Component Analysis (PCA) of the WT

cell line compared to its *CDHI* KO cell line showed a 70% variance between the MCF7 cells and an 85% variance between the T47D cell pairs (Figure 8A), highlighting the major changes to the cell lines following *CDHI* deletion. To understand the gene expression changes between the cell lines, DESeq2 analysis was performed to identify significantly differentially expressed genes between MCF7 cells (absolute log₂ fold change ≥ 1 and adjusted p-value of < 0.05) and T47D cells (absolute log₂ fold change ≥ 1.5 and adjusted p-value of < 0.05 for). A total of 515 genes and 787 genes were uncovered for MCF7 and T47D respectively. Figures 8C and D list the top 20 most significant differentially expressed genes for each cell line pair.

As expected, *CDHI* was listed in the top 20 DEGs for both cell lines (Figure 8C, D). Interesting genes from the MCF7 cells include upregulation of *IGFBP5* and *BAMBI*, and downregulation of *PKIB* and *KRT81* in the KO cells. Insulin-like growth factor-binding protein 5 (IGFBP5) is known to have antiproliferative effects (193) due to its role as an IGF binding protein. BMP And Activin Membrane Bound Inhibitor (*BAMBI*)'s involvement in breast cancer as a tumor suppressor is being considered (194), although it is not well studied. Downregulation of Keratin 81 (*KRT81*) and cAMP-dependent Protein Kinase Inhibitor Beta (*PKIB*) in the MCF7 KO cells was observed among other genes and there are studies in breast cancer showing the potential role of these genes in the disease via regulating Akt activity (195).

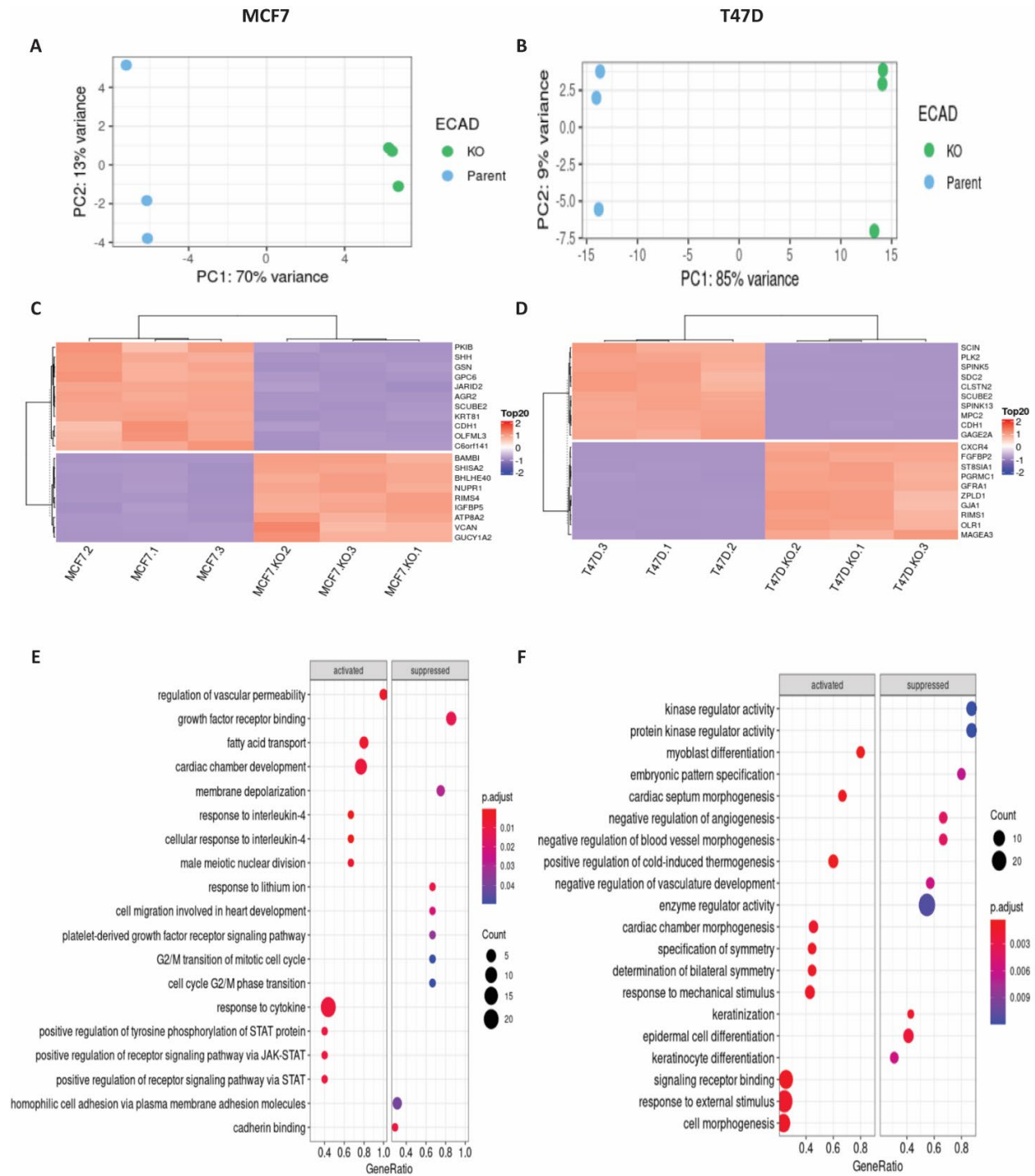


Figure 8: RNA sequencing uncovers large variance between WT and KO cells, with related pathway differences

PCA plot comparing (A) MCF7 WT and *CDH1* KO cells and (B) T47D WT and *CDH1* KO cells. Top 20 differentially expressed genes from DESeq2 analysis between (C) MCF7 cells (absolute log₂ fold change ≥ 1 and adjusted p-value of < 0.05) and (D) T47D cells (absolute log₂ fold change ≥ 1.5 and adjusted p-value of < 0.05 for). Gene Set Enrichment Analysis based on the differentially expressed genes between (E) MCF7 cells and (F) T47D cells. Analysis was performed by Laura Savariau.

In T47D cells, Polo-like Kinase 2 (*PLK2*) was among the downregulated genes following *CDH1* deletion. Discovery of *PLK2* downregulation in T47D KO cells is exciting and requires further investigation, especially given its tumor suppressor function towards mTOR signaling (196) which could go hand in hand with understanding the PI3K pathway activation in KO cells. Among upregulated genes in *CDH1* KO cells, the Gap Junction protein alpha 1 gene (*GJAI*) is present. As its name suggest, *GJAI* forms gap junction transmembrane channels for adjacent cell communications. Given the deletion of E-cadherin in the KO cells, this upregulation of a gap junction protein potentially suggests an increase in gap junctions in cells lacking adherens junctions. *GJAI* expression has been reported to be breast cancer subtype dependent (197) with a potential for its loss during metastasis (198).

Using the significant DEGs, a Genes Set Enrichment Analysis (GSEA) was performed. The topmost differentially regulated pathways in KO cells compared to WT cells were included in this analysis (Figure 8E, F). We identified several related pathways, such as growth factor receptor binding (suppressed in KO), PDGF signaling pathway (suppressed in KO), homophilic cell adhesion via plasma membrane adhesion molecules (suppressed in KO) and positive regulation of receptor signaling pathway via STAT (activated in KO) in the MCF7 cells. While these are interesting findings, some of the pathways that we expected to be activated were suppressed, requiring further analysis and experimentation to understand. In T47D cells, we identified kinase regulator activity (suppressed in KO), response to external stimulus (activated in KO) and signaling receptor binding (activated in KO). These results go hand in hand with the data to be discussed in the following chapter of this thesis. A suppression in the kinase regulator activity and an activated signaling receptor binding suggests a potential method for how deletion

of *CDHI* in the KO cells allows them to have a hyperactivated growth factor signaling as will be discussed later.

3.4 Discussion

In this chapter, we explored the generation and use of *CDHI* knockout cell line models to study the role of E-cadherin. Using the Synthego Gene Knockout Kit and the dox-inducible Cas9 with adenoviral delivery of sgRNA for *CDHI* proved successful with 60-95% gene knockout efficiency. Unfortunately, we did not obtain a complete gene knockout in the ZR75.1 cells, which may be due to its copy number amplification of *CDHI* (167, 199) which is not present in MCF7 and T47D cells. Regardless, the 60% reduction in E-cadherin expression led us to continue utilizing ZR75.1 *CDHI* KO cells as a model while keeping the remaining expression in consideration.

Genetic deletion of E-cadherin in IDC cells caused them to have a reduced cell-cell attachment and morphology transformation into looser cell clusters in suspension. This was evident in two of our three models and is a well characterized phenotype of ILC cell lines (154, 200-202). As the generation of *CDHI* KO cells was to replicate ILC cell lines but with isogenic models, the similarities found between IDC *CDHI* KO and ILC cell lines with respect to morphology and suspension growth were promising. In addition, re-localization of p120 catenin to the cell cytoplasm was also an encouraging result as it is a classic presentation of ILC (154, 203). Interestingly, E-cadherin loss was also associated with enhanced anchorage independence and anoikis resistance, all of which are features observed in ILC tumors and cell lines (154, 184,

204). The first step in metastasis is the detachment of cells from the ECM that previously supported the primary tumor. Following detachment, the tumor cells need to survive being unattached to a support system before being able to metastasize (205-207). This is when these cells are typically rounded up due to the absence of attachment and are exposed to a wide variety of chemical and mechanical stimuli that could lead to cell cycle arrest and anoikis (206). However, being able to survive after detachment is a major malignant characteristic which includes phenotypes such as anoikis resistance and anchorage independence (205-207). These phenotypes are often brought about by the upregulation of survival signaling such as mitogenic pathways and growth factor signaling or an adaptation to the new environment via EMT or by integrin switching (205). The presence of anchorage independence and anoikis resistance in our *CDHI* KO cells compared to their parental cell lines are certainly supportive of their increased similarity to that of ILC cell's tumorigenic properties. However, it is important to note that the survival changes were mainly observed in only one or two of the three cell lines, highlighting the cell line-dependent effects of E-cadherin loss potentially due to their background or adaptive mechanism differences.

Finally, our RNA sequencing analysis helped shed light on transcriptomic difference between the cell lines. Based on our previous single cell RNAseq study, we have observed significant differences between cell lines, where distinct cell lines were indeed more different to one another than the WT cells are to their KO cells (185). Knockout of *CDHI* also led to the WT and KO cells being distinctly different as seen here and in our recent study using single cell RNAseq (185). However, contrary to our expectations we did not discover new targets that were commonly significantly different between both MCF7 and T47D parental and KO cells. We did

identify several genes with interesting differences such as *PKIB*, *BAMBI* and *IGFBP5* in MCF7 cells although their expression profile did not necessarily correlate with the phenotypes observed. There have been contradicting reports on *IGFBP5*'s roles where it has been shown to have no effect on IGF-driven proliferation (208) and may influence extrinsic apoptotic pathways (209). Changes to the *IGFBP5* expression is interesting but does not correlate with the signaling hyperactivation to be discussed in Chapter 4. BMP And Activin Membrane Bound Inhibitor (*BAMBI*) is being studied, as a breast cancer suppressor gene (194) with high levels detected in colorectal cancer as an inhibitor of TGF- β signaling (210). Meanwhile, downregulation of Keratin 81 (*KRT81*) and cAMP-dependent Protein Kinase Inhibitor Beta (*PKIB*) in the MCF7 KO cells was observed among other genes. Studies in breast cancer have shown a strong positive correlation between *PKIB* and pAkt (195), with a strong correlation also seen with TNBC. This correlation, although exciting, does not relate to the pAkt activation to be discussed in Chapter 4 as we observe a downregulation of *PKIB* in the KO cells.

Discovery of *PLK2* downregulation in T47D KO cells requires further investigation, especially given its tumor suppressor function towards mTOR signaling (196). *PLK2* has been shown to promote chemoresistance in colorectal cancer (211), has a tumor suppressor function in regards to mTOR signaling (196) where its loss in Glioblastoma Multiforme (GBM) has been reported to activate Notch signaling (212). While we are unsure of the function of *PLK2* in the KO cells, this is certainly an interesting finding for future experimentations. Interestingly, the upregulation of *GJAI* in T47D *CDHI* KO cells potentially explains an alternative cell-cell communication mechanism that may be activated to compensate for the loss of adherens junction when *CDHI* is knocked out. *GJAI* has been shown to be upregulated by E2 and an increased

GJAI activity decreased breast cancer cell proliferation with increased sensitivity to tamoxifen, thus being correlated with favorable prognosis (213). The potential role of *GJAI* in T47D *CDHI* KO cells could be a very interesting avenue to explore although the caveat of this being present in only one of two KO cell lines exists. Another interesting finding of *CXCR4* (C-X-C Motif Chemokine Receptor 4) upregulation in T47D *CDHI* KO cells, where this chemokine has been reported to regulate cellular processes such as proliferation and migration in breast cancer (214). They are mostly expressed on the cell surface of most leukocytes, including B cells, monocytes and T lymphocytes (215), thus raising a strong need to further explore this, especially given the higher immune response pathway enrichment observed in ILC over IDC (34).

Overall, we have now generated and characterized three isogenic *CDHI* KO cell line models both phenotypically and transcriptionally. Referring back to our hypothesis of loss of E-cadherin activating the IGF pathway, we will next investigate the changes in the IGF pathway sensitivity in these cell lines.

4.0 *CDHI* KO Renders Cells More Sensitive to IGF Signaling

4.1 Introduction

The Insulin-like growth factor 1 (IGF1) pathway is known to have a critical role in breast cancer progression (117, 122, 216-218). IGF1 is imperative both in mammary gland development and in preventing apoptosis during post-lactation involution (219). Further to its role in mammary gland development, IGF1 can also promote cell proliferation and anti-apoptosis through several pathways including PI3K/Akt, MAPK and JAK/STAT (117, 216-218, 220). Binding of IGF1 to its receptor (IGF1R) or the insulin receptor (IR) triggers the receptors' autophosphorylation and activation of the PI3K/AKT and RAF/MAPK pathways, among others (117, 216-218, 220, 221). The activation of these two pathways is mediated by insulin receptor substrate 1 (IRS-1), which has been reported to be overexpressed in breast tumors (216). Due to high levels of circulating IGF1 reported in breast cancer patients with poor prognosis (222), it is critical to understand the dysregulation of this pathway in the disease and to develop a strategy to reduce pathway activity.

Our group recently reported E-cadherin as a modulator of IGF1 signaling and a potential biomarker of inhibitor response (128, 129). Treatment of IDC and ILC cell lines with IGF1 and insulin coupled with a lasso regression model uncovered negative regulation by E-cadherin on IGF1-induced Akt activation. Loss of E-cadherin being a pathognomonic feature of ILC led us to study how E-cadherin regulates growth factor signaling in IDC and how that regulation is affected when it is lost in ILC. Transient E-cadherin knockdown in IDC cell lines sensitized

them to IGF1 signaling and to IGF1R inhibition (128, 129). We further reported that ILC tumors have higher IGF1/2 expression and pIGF1R/IR activation compared to IDC tumors (129, 130).

In this chapter, we expand our earlier observations by experimenting on our *CDH1* knockout IDC cell lines to elucidate the effects of E-cadherin deletion on IGF pathway activation in an isogenic system. Given previous evidence for E-cadherin regulation of other growth factor pathways (130, 158), we also extended our studies to additional growth factor signaling pathways. IGF1 has also been implicated in promoting cell survival, migration, and invasion *in vitro* (88, 223, 224), thus piquing our interest to investigate how hypersensitivity of our *CDH1* KO cells to IGF1 pathway activation can affect additional tumorigenic phenotypes of IDC cells, and thus necessitate a rationale for IGF-targeted therapies in ILC. Our findings in this chapter provide insights into better understanding the effects of deleting E-cadherin in IDC cells and how in turn this affects downstream signaling and other tumorigenic properties of these cells.

4.2 Materials and methods

4.2.1 Cell culture

Cell lines utilized in this study were obtained from ATCC: MCF7 (RRID: CVCL_0031), T47D (RRID: CVCL_0553), ZR75.1 (RRID: CVCL_0588), MDA-MB-134-VI (RRID: CVCL_0617), MDA-MB-231 (RRID: CVCL_0062) and Asterand for SUM44PE (RRID: CVCL_3424). BCK4 cells were obtained as a gift from Dr Britta Jacobsen, developed as detailed (225). Cell lines were maintained in 10% fetal bovine serum (FBS; Life Technologies) supplemented media (Thermo Fisher Scientific): MDA-MB-134 in 1:1 DMEM: L-15; MCF7 and MDA-MB-231 in DMEM; T47D and ZR75.1 in RPMI and BCK4 in MEM with nonessential amino acids (Life Technologies) and insulin (Sigma-Aldrich). SUM44PE was maintained in DMEM/F12 with 2% charcoal stripped serum (CSS; Life Technologies) with additional supplements as previously described (34). For *CDHI* overexpression in ILC cell lines, Doxycycline inducible p20-EV (EV) and p20-*CDHI* (*CDHI*) plasmids were utilized. These cell lines were generated by Laura Savariau, a graduate student in the Lee/Oesterreich lab. Cell lines were cultured for less than 6 months at a time, routinely tested to be Mycoplasma free and authenticated by the University of Arizona Genetics Core (Tucson, Arizona) by short tandem repeat DNA profiling.

4.2.2 IGF, EGF and FGF signaling assays

Cells were plated in 6-well plates and serum starved overnight in 0.5% FBS media upon reaching 75% confluency. IGF1 (GroPep CU100) and EGF (Thermo Scientific #PHG0311)

stimulations at 0, 0.5, 1, 5 or 10nM and IGF2 (GroPep #FU100)/insulin (Sigma #I2643-250MG) stimulations were performed at 0, 5 or 10nM final concentrations. Meanwhile, FGF cocktail stimulations were performed with FGF19, 21, 23 at 50ng/mL and FGF1, 2, 4, 6, 8 and 17 at 20ng/mL with Heparin supplementation at 1µg/mL for high concentrations and the respective concentrations halved for low concentrations. All stimulations were performed for 15 minutes at 37°C before harvesting for immunoblotting.

4.2.3 Immunoblotting

Protein for immunoblotting experiments were harvested using RIPA buffer (50mM Tris pH 7.4, 150mM NaCl, 1mM EDTA, 0.5% Nonidet P-40, 0.5% NaDeoxycholate, 0.1% SDS) supplemented with 1x HALT protease and phosphatase cocktail (Thermo Fisher #78442), probe sonicated for 15 seconds (20% amplitude) and centrifuged at 14,000rpm at 4°C for 15 minutes. Protein concentration was assessed using BCA assay (Thermo Fisher #23225) and 50ug of protein per sample was run on 10% SDS-PAGE gel, then transferred to PVDF membrane. Membrane blocking was performed with Intercept PBS blocking buffer (LiCO#927-40000) for one hour at room temperature and probed with primary antibodies overnight at 4°C: pIGF1R/IR (Cell Signaling Technology #3024; RRID:AB_331253), IGF1R (Cell Signaling Technology #3027; RRID:AB_2122378), pAkt S473 (Cell Signaling Technology #4060; RRID:AB_2315049), Akt (Cell Signaling Technology #9272; RRID:AB_329827), InsR (Cell Signaling Technology #3025; RRID:AB_2280448), E-cadherin (BD Biosciences #610182; RRID:AB_397581), β-catenin (BD Biosciences #610154; RRID:AB_397555), p120 catenin (BD Biosciences; #610134; RRID:AB_397537), pEGFR Y1068 (Cell Signaling Technology #2234; RRID:AB_331701), EGFR (Cell Signaling Technology #4267; RRID:AB_2246311), α-Biotin

(Cell Signaling Technology #5597; RRID:AB_10828011), non-phospho β -catenin (Cell Signaling Technology #1980; RRID:AB_2650576), pFGFR4 Y642 (Signalway #11836), FGFR4 (Cell Signaling Technology #8562; RRID:AB_10891199), pFRS2 Y196 (Cell Signaling Technology #3864; RRID:AB_2106222), pSTAT3 Y705 (Cell Signaling Technology #9131; RRID:AB_331586), p-p44/42 MAPK (Cell Signaling Technology #4377; RRID:AB_331775) and β -actin (Millipore Sigma #A5441, RRID:AB_476744). This was followed by 1 hour room temperature incubation with secondary antibodies (1:10,000; anti-mouse 680LT: LiCor #925-68020; anti-rabbit 800CW: LiCor #925-32211). Membranes were subsequently imaged on the LiCor Odyssey CLx Imaging system, with band quantifications performed with built in software.

4.2.4 Colony formation assay

Cells were plated at a density of 2000 cells/well in 6-well plates (Fisher #08-772-1B) in either full serum (10% FBS) or low serum (0.5% FBS) with 5nM IGF1 (GroPep Bioreagents #AQU001) supplemented media. Cells were monitored every few days and media refreshed every 4 days. Cells plated in full serum media were fixed with 100% methanol on ice and stained with 0.5% Crystal Violet (Sigma-Aldrich #C0775) in 40% methanol after 14 days while cells grown in low serum + 5nM IGF1 were stained after 21-28 days. Wells were imaged on an Olympus SZX16 dissecting microscope and de-stained with 10% acetic acid in water and quantified by spectrophotometry at 560nm. Statistical differences were tested using two-way ANOVA.

4.2.5 Haptotaxis, migration and invasion assays

For haptotaxis experiments, the QCM Haptotaxis Cell Migration Assay Collagen I (EMD Millipore #ECM582) kit was used as previously described (154). Cells were plated at a density of 300,000 cells/well in 300 μ L serum free media in the top chamber; all bottom chambers were also filled with serum free media. For Transwell migration assays, transparent 24 well PET membranes of 8 μ m pore size (Fisher Scientific # 08-771-21) were used. For Collagen I invasion assays, QCM Collagen Cell Invasion Assay (EMD Millipore #ECM551) was used according to manufacturer's protocol. For both assays, cells were plated at a density of 300,000 cells/well in 300 μ L 0.5% FBS media in the top chamber; all bottom chambers were filled with 0.5% FBS media +/- 5nM IGF1 (GroPep Bioreagents # AQU100) or full serum (10%) media. In all three assays, cells were incubated at 37°C for 72 hours. Excess cells were removed from the top chambers using cotton swabs and inserts were stained with Crystal Violet (Sigma-Aldrich #C0775) before being imaged on an Olympus SZX16 dissecting microscope and quantified with ImageJ software. Quantifications were normalized to low serum WT samples and p-values calculated with one-way ANOVA.

4.3 Results

4.3.1 *CDHI* KO cells are hypersensitive to IGF1, IGF2 and Insulin stimulation

As per the findings from Chapter 2, we first assessed if our *CDHI* KO cells exhibited increased sensitivity towards IGF stimulation. MCF7, T47D and ZR75.1 WT and *CDHI* KO

cells were serum starved with serum free media overnight upon achieving 70-80% confluency. Cells were then stimulated with 0, 0.5, 1, 5 or 10nM of IGF1 for 15 minutes at 37°C before being harvested for Western blot. To assess IGF1R activation, I blotted for phospho-IGF1R/IR and a direct downstream activator pAkt S473. All three cell lines showed a hypersensitivity to IGF1 stimulation as shown by the pIGF1R bands and its normalization to their respective total IGF1R band levels (Figure 9A). Higher phospho/total IGR1R levels were observed in all cell lines. This enhanced signaling response was especially apparent at 5nM IGF1 where the largest differential of activation could be appreciated between WT and KO cells in all models (2.7-fold, 1.3-fold and 1.5-fold higher in MCF7, T47D and ZR75.1 KO cells respectively compared to their parental cells). Similar findings were also obtained from the pAkt levels for MCF7 and T47D cells while ZR75.1 cells showed high pAkt throughout all IGF1 doses, suggesting a high background activity, potentially due to its PTEN loss (1.08-fold, 1.6-fold and 0.9-fold higher in MCF7, T47D and ZR75.1 KO cells respectively at 5nM IGF1 compared to their parental cells). Since the IGF axis can also be activated by IGF2 and insulin, we tested these ligands and observed mixed results. MCF7 and ZR75.1 KO cells showed higher pIGF1R with both IGF2 and insulin while T47D KO cells showed no differences (Figure 9B, C). All three cell lines showed mixed results in terms of Akt activation with no clear higher activation observed in KO cells, overall suggesting an inconsistency in the models and their response to different ligands.

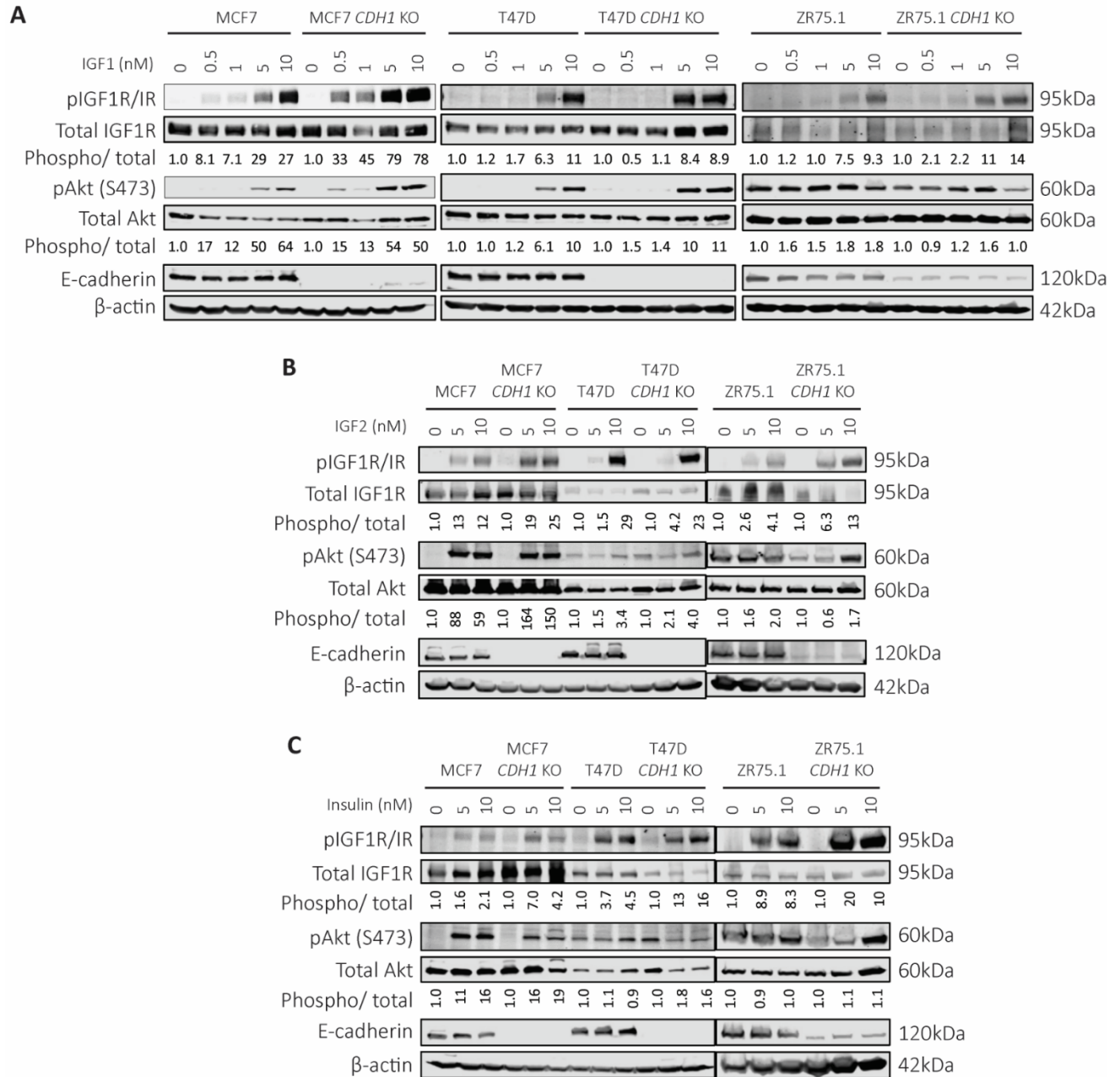


Figure 9: *CDH1* KO cells are hypersensitive to IGF1, IGF2 and Insulin stimulation

MCF7, T47D, ZR75.1 WT and *CDH1* KO cells were serum starved overnight and stimulated with (A) IGF1, (B) IGF2 or (C) Insulin (0-10nM) for 15 minutes at 37°C. Cells were harvested for Western blot to assess IGF1R/IR and Akt signaling. For quantification, phosphorylated protein levels were normalized to corresponding total protein levels and loading controls. Ligand treated sample values were further normalized to respective cell line vehicle treated samples. Representative experiment shown for all, n=2-3 for each experiment.

To better delineate the effects of *CDHI* loss on IGF pathway activation, we also examined ligand sensitivity on ILC cell lines with a dox-inducible *CDHI* overexpression, generated by Laura Savariau in our lab. Identical IGF1 stimulation signaling experiments were performed in BCK4, MM134 and SUM44 empty vector (EV) or *CDHI* overexpressing cells after a 24-hour 1 µg/mL Doxycycline treatment. We hypothesized we would observe a decrease in IGF sensitivity with *CDHI* overexpression (OE) and this was the case with pIGF1R in BCK4 at 5nM IGF1 and SUM44 at 1nM IGF1 (Figure 10). However, no changes were observed at 5nM IGF1 in SUM44 and MM134 cells (Figure 10). Surprisingly, 1nM IGF1 treatment in MM134 cells led to higher activation in *CDHI* OE cells, which was against our hypothesis. While we noted the consistency in pIGF1R results between IDC *CDHI* KO and ILC *CDHI* OE cells albeit not in all cell lines tested, this was not accompanied by a decrease in pAkt as per our expectations, potentially due to other activation by other signaling pathways. Given the sensitivity to growth factor signaling seen thus far, we were interested to see if this phenotype was limited to the IGF axis or was extensive to other growth factors as well.

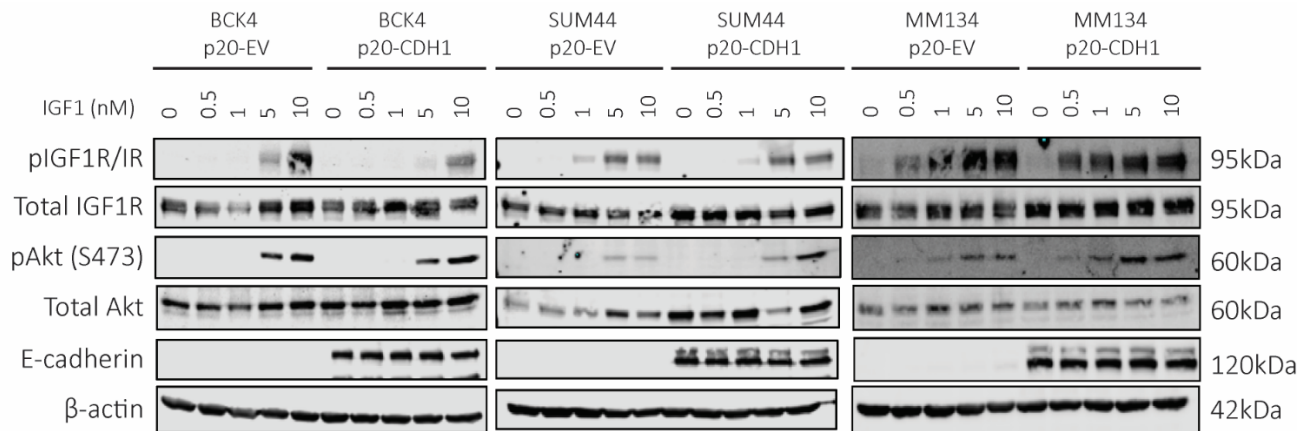


Figure 10: ILC *CDH1* overexpressing cells exhibit reduced IGF1 sensitivity

BCK4, SUM44PE and MM134 p20-EV and p20-*CDH1* cells were treated with 1 µg/mL doxycycline to induce *CDH1* expression for 24 hours and serum starved overnight. Cells were then stimulated with 0-10nM IGF1 for 15 minutes at 37°C. Cells were harvested for Western blot to assess IGF1R/IR and Akt signaling. Representative experiment shown for all, n=2-3 for each experiment. These cell lines were generated by Laura Savariau, a graduate student in the Lee/Oesterreich lab.

4.3.2 *CDH1* KO cells do not exhibit increased sensitivity to EGF and FGF stimulations

To assess loss of E-cadherin's potential effect on other growth factor receptors, we performed EGF and FGF stimulation experiments in the same manner as the IGF experiments. Treatments of EGF (0, 0.5, 1, 5 and 10nM) on MCF7 and T47D WT and KO cells did not show any significant differences in the response, suggesting that loss of *CDH1* may not have a broad effect of signaling via multiple growth factor receptors (Figure 11A). Next, we specifically examined the effects of E-cadherin deletion on FGFR activity given recent studies on the role of FGFR4 as a driver of endocrine resistance (226), particularly in ILC (227). Cells were stimulated with a cocktail of FGF ligands (FGF 1, 2, 4, 6, 8, 17, 19, 21 and 23) resulting in strong enhancement in both raw and normalized pFGFR4 levels in both MCF7 and T47D *CDH1* KO cells, despite decreased total FGFR4 levels in the *CDH1* KO cells (Figure 11B). Surprisingly,

while pFGFR4 was elevated in *CDHI* KO cells, downstream activators did not display a difference between WT and *CDHI* KO cells. While a pan-growth factor effect of *CDHI* loss is intriguing, these experiments have suggested a more focused effect on the IGF pathway and led us to focus most closely on this pathway in subsequent experiments.

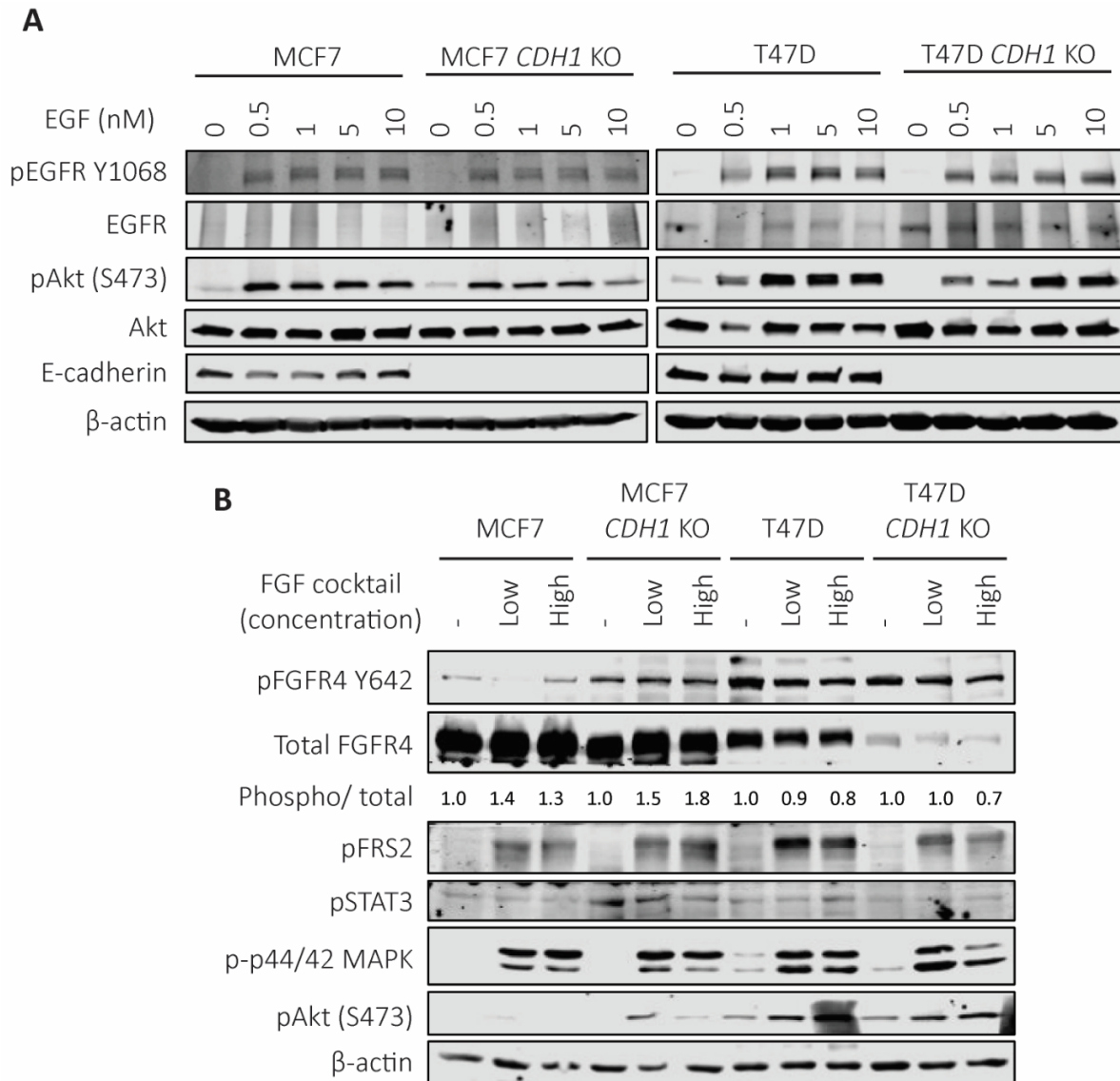


Figure 11: Pan growth factor sensitivity was not observed with EGF and FGF stimulations

MCF7 and T47D WT and *CDH1* KO cells were serum starved overnight and stimulated with (A) EGF or (B) cocktail of FGF ligands (10-50ng/mL, detailed in the Methods section) for 15 minutes at 37°C. Cells were harvested for Western blot to assess downstream signaling. For quantification, phosphorylated protein levels were normalized to corresponding total protein levels and loading controls. Ligand treated sample values were further normalized to respective cell line vehicle treated samples. Representative experiment shown for all, n=2-3 for each experiment. Representative experiment shown for all, n=2-3 for each experiment).

4.3.3 IGF1 stimulation of *CDHI* KO cells results in robust signaling elevation over time

Following the hypersensitivity towards IGF1 observed earlier, we assessed if *CDHI* KO cells also have sustained high levels of activation over a 6-hour time course. Cells were treated with 10nM IGF1 for varying durations: 0, 15, 30, 60, 120, 240 or 360 minutes and harvested to immunoblot for IGF1 pathway activation. As seen in Figure 12A, MCF7 and T47D KO cells not only showed hypersensitivity as seen previously, but also showed hyperactivation for the duration of pathway activity, which did not differ between the WT and KO cells in terms of both pIGF1R and pAkt. For example, a 60-minute stimulation with IGF1 led to a 2.2-fold and a 1.89-fold increase in pIGF1R in MCF7 and T47D *CDHI* KO respectively compared to their WT cells. This was strongly followed by pAkt as well. Evidently, T47D has shorter IGF pathway activity post stimulation (peaking around 120 minutes), while MCF7 remains high until around 240 minutes. ZR75.1 KO cells were challenging to blot, and it remains unclear as to whether they also have a hyperactive signaling axis following stimulation (Figure 12B). Given our strong findings for high IGF1 induced signaling in MCF7 and T47D KO cells, we next assessed if the pathway hyperactivation led to unique phenotypes in those cell lines.

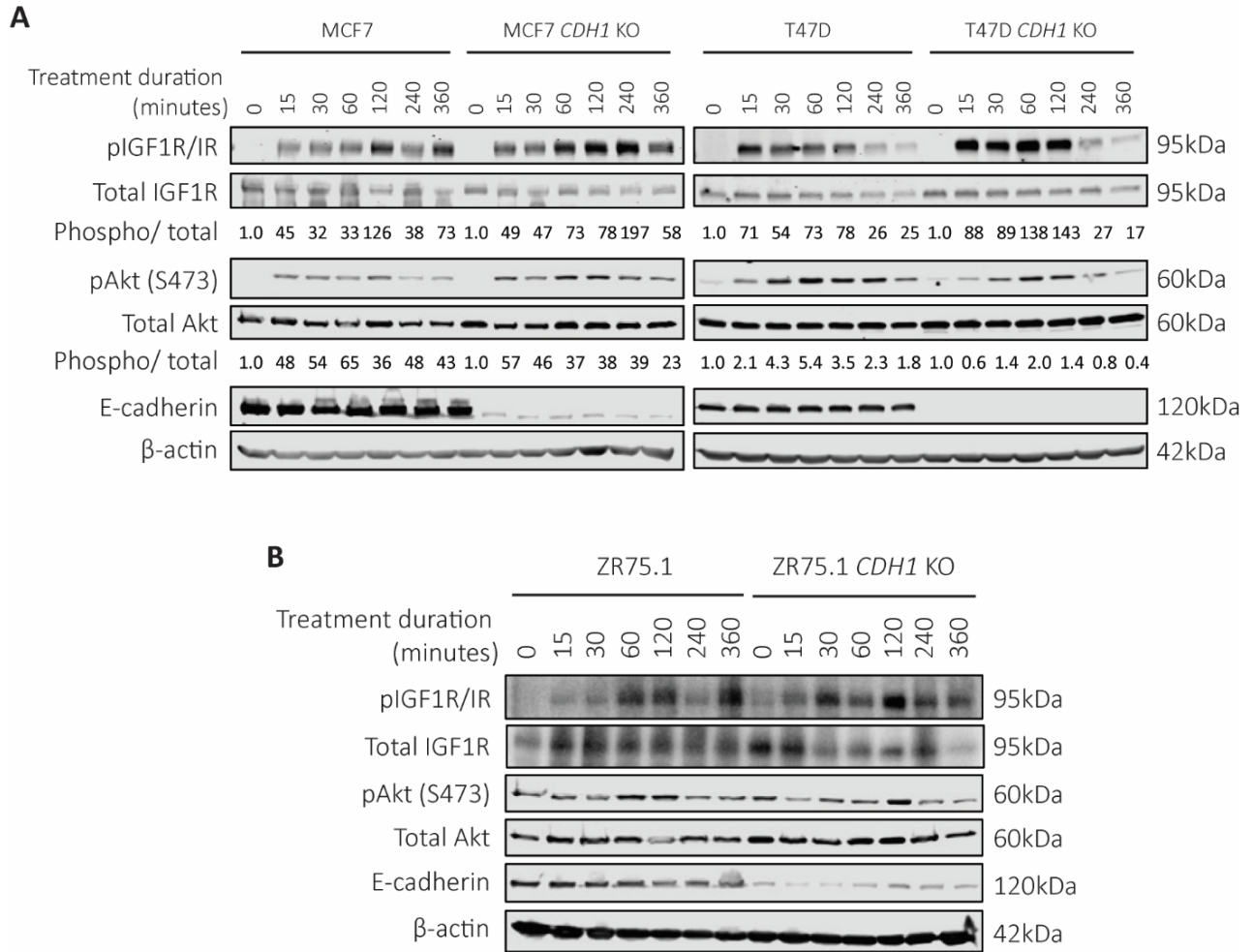


Figure 12: *CDH1* KO cells show high activity of IGF signaling over a time course assay

(A) MCF7, T47D (B) ZR75.1 WT and *CDH1* KO cells were serum starved overnight and stimulated with 10nM IGF1 for a time course from 0-6 hours to assess the duration of signaling activity between WT and *CDH1* KO cells. Cells were harvested for Western blot to assess IGF1R/IR and Akt signaling. For quantification, phosphorylated protein levels were normalized to corresponding total protein levels and loading controls. Ligand treated sample values were further normalized to respective cell line vehicle treated samples. Representative experiment shown for all, n=2-3 for each experiment.

4.3.4 *CDH1* KO cells displayed enhanced colony formation in low density assays

To explore changes in cell survival following *CDH1* deletion, we performed colony formation assays by plating cells at a low density in either full serum media (10% FBS) or low

serum (0.5% FBS) media containing 5nM IGF1 in 2D plates. Media was refreshed every 6 days until wells were ready to be stained after 2 weeks (full serum) and 3 weeks (low serum). T47D KO cells showed increased clonogenic survival in both conditions (Figure 13). ZR75.1 KO cells also demonstrated increased colonies in full serum compared to WT, but with no colonies observed in low serum conditions. MCF7 *CDH1* KO cells showed no clear differences in full serum quantifications, however, they formed a greater number of smaller colonies than the WT cells, which was also the case in low serum conditions. These results suggest that *CDH1* KO cells have an enhanced ability to form colonies under the conditions tested compared to WT cells.

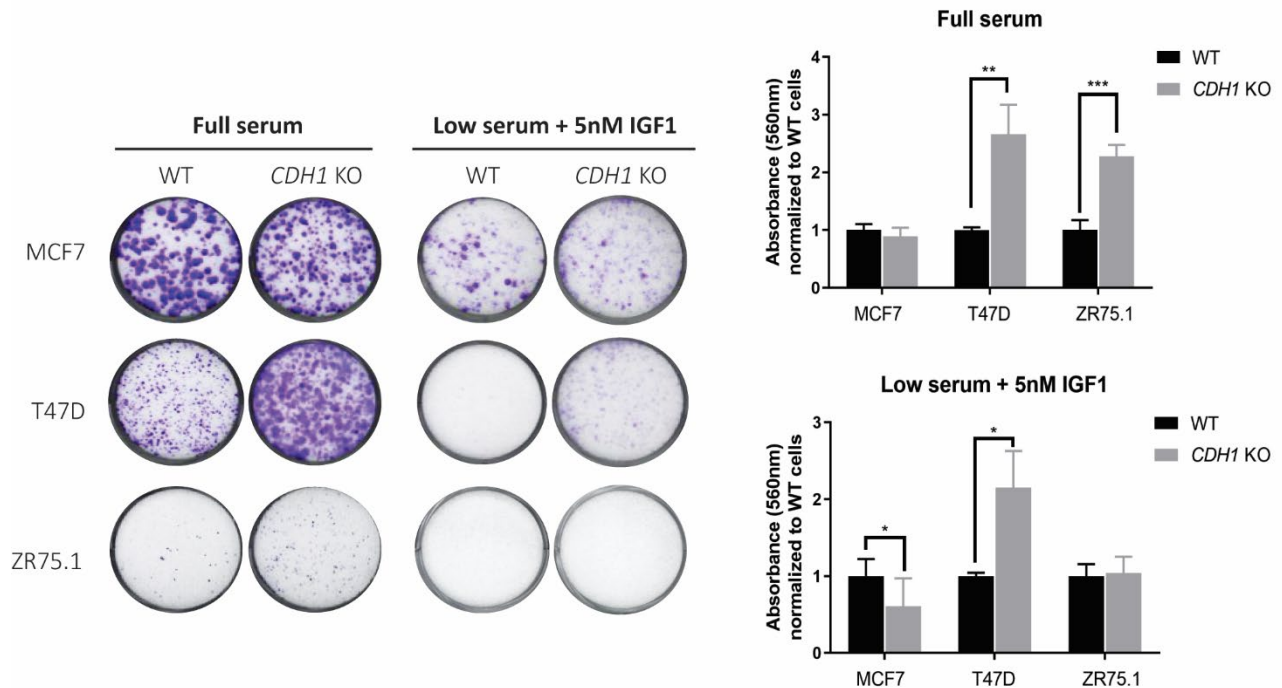


Figure 13: Altered cell survival phenotypes are observed in *CDH1* KO cells

MCF7, T47D and ZR75.1 WT and *CDH1* KO cells were plated at 2,000 cells/well in full serum and low serum supplemented with 5nM IGF1 media and stained with 0.5% Crystal Violet after two to three weeks. Representative images are shown. Plates were de-stained with 10% acetic acid, absorbance quantified and graphed after normalization to WT cells of corresponding conditions. Statistical differences were evaluated using two-way ANOVA (* $p < 0.05$, ** $p < 0.01$, *** $p < 0.001$, representative experiment shown, $n = 3$ (each with three biological replicates)).

4.3.5 *CDH1* KO cells exhibit migration towards IGF1 and serum

Given the hypersensitivity towards IGF stimulation, we next explored migration of these cells towards serum and IGF1. MCF7, T47D, ZR75.1 WT and *CDH1* KO cells were subjected to Transwell migration assays with chemotactic low serum (0.5% FBS) media +/- 5nM IGF1 or full serum (10% FBS) media. All cells were plated in inserts with low serum media containing no IGF1. Over 72 hours, all three *CDH1* KO cell models showed higher migration towards serum compared to WT cells (Fig 14A, B); $p < 0.05$, $p < 0.0001$ and $p < 0.05$ for MCF7 KO, T47D KO and ZR75.1 KO respectively. Interestingly, consistent with the IGF1-sensitive nature of these KO cell lines, MCF7 and T47D KO cells also showed significantly higher migration towards IGF1; $p < 0.05$ and $p < 0.0001$ for MCF7 KO and T47D KO respectively. In addition, higher migration of T47D KO cells without the presence of any chemotactic gradient ($p < 0.0001$) also highlights the migratory phenotype driven by the independent loss of E-cadherin in this model which were not observed in the remaining two models. To confirm the higher migration towards IGF1, we added an IGF1R inhibitor, BMS-754807 into the Transwell inserts with the cells in a dose response manner and observed a stepwise decrease in percentage of cells migrated towards IGF1 (Figure 14C-E) in both MCF7 and T47D *CDH1* KO cell lines; $p < 0.0001$ and $p < 0.001$ for MCF7 KO and T47D KO respectively compared to vehicle treated wells.

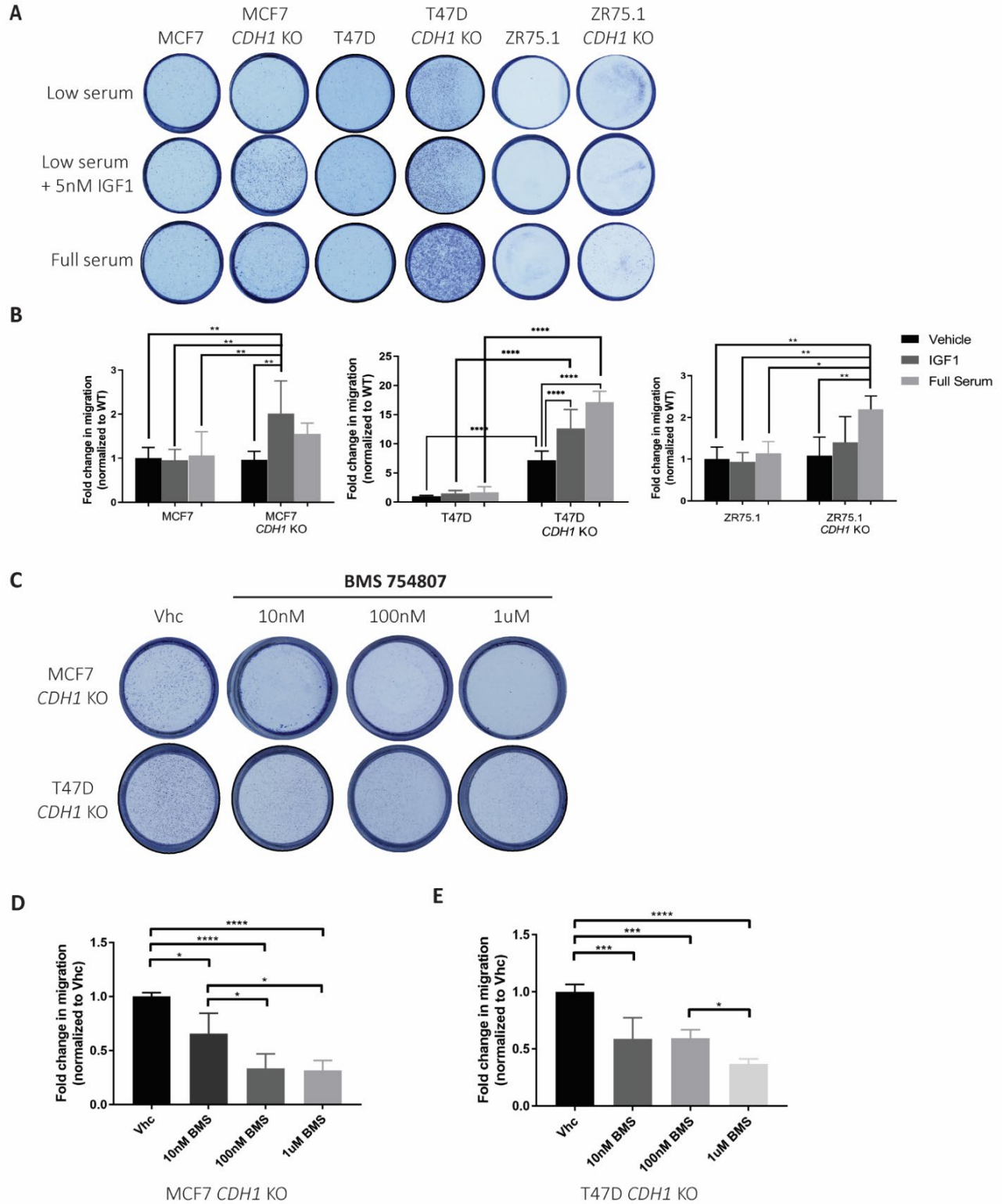


Figure 14: *CDH1* KO cells migrate towards IGF1 and serum

Respective cells were plated at 300,000 cells/ insert in 24-well Transwell inserts in low serum media. (A) Representative images and (B) quantification of Crystal Violet-stained Transwell inserts from migration assays

towards the indicated attractants after 72 hours are shown. (C) Representative images and (D, E) quantification of Crystal Violet-stained Transwell inserts from migration assays towards the indicated attractants after 72 hours with treatments of BMS-754807 shown. Graphs show representative data normalized to low serum WT cell samples from two to three independent experiments (n=2-3 biological replicates). p-values from one-way ANOVA statistical testing. * $p \leq 0.05$; ** $p \leq 0.01$; *** $p \leq 0.001$; **** $p \leq 0.0001$.

4.3.6 *CDH1* KO cells migrate towards collagen and exhibit collagen invasion

We next investigated if deletion of *CDH1* in IDC cell lines confers haptotactic migration towards the extracellular matrix (ECM), a phenotype that is observed in ILC cell lines (154). We noticed a significantly higher migration towards Collagen I in MCF7 KO ($p < 0.05$) and T47D KO cells ($p < 0.0001$) (Fig 15A) compared to their respective WT cells. Although multiple studies have reported on E-cadherin loss promoting cell migration and invasion (137, 152, 228); conflicting studies on the requirement of E-cadherin for metastasis have also been reported (150). Following our observation of haptotactic migration towards Collagen I and migration towards IGF1 and serum, we hypothesized that *CDH1* KO cells may also be able to invade through Collagen I (154) towards a gradient of IGF1 and serum. No Collagen I invasion was observed with the MCF7 and ZR75.1 cells (Appendix A, Figure 32). However, T47D KO cells showed a strong Collagen I invasion towards serum (Figure 15B); $p < 0.01$ compared to parental cells, which was not observed when low serum plus IGF1 was used as an attractant. It is important to note that neither of these three cell lines are invasive by nature and the invasive phenotypes observed in T47D KO cells is promising and requires greater investigation in the context of tumor invasion.

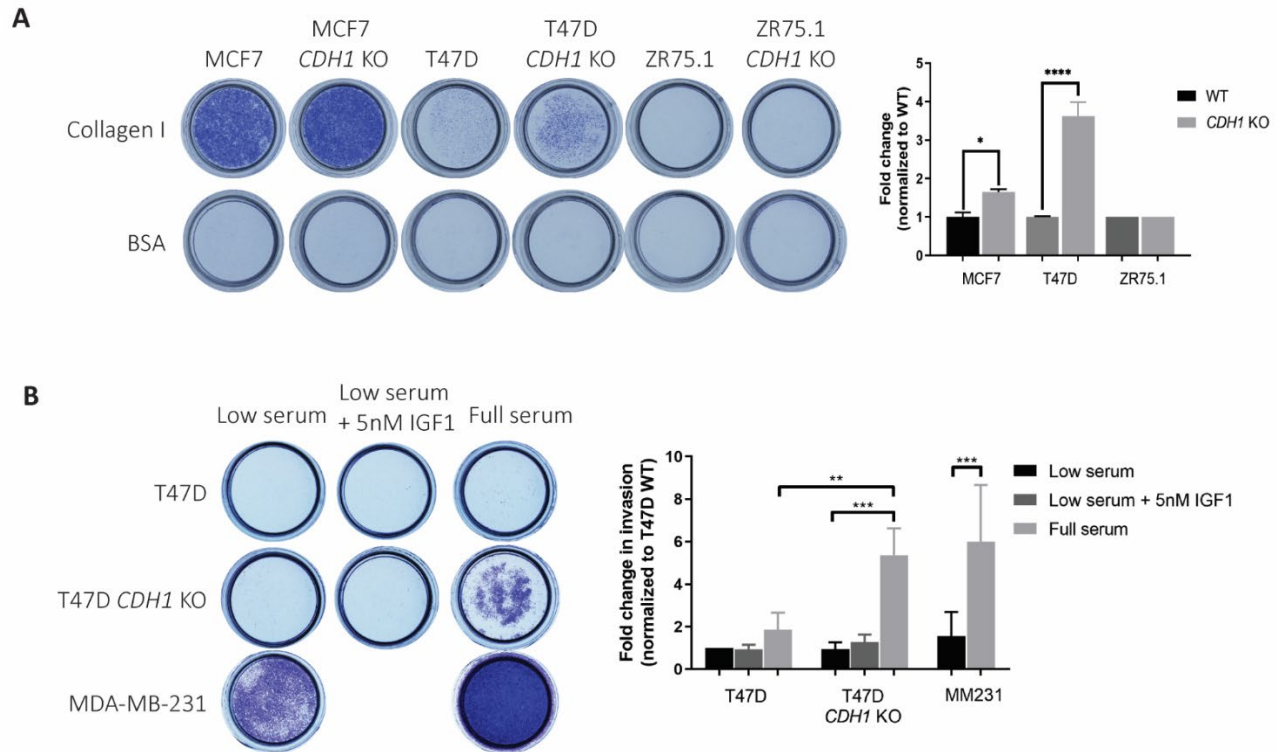


Figure 15: *CDH1* KO cells migrate towards collagen and exhibit collagen invasion

Respective cells lines were plated at 300,000 cells/ well in indicated inserts in serum free media. (A) Representative images and quantification of Crystal Violet-stained Collagen I coated inserts from haptotaxis assays after 72 hours. Migrated cell colonies were quantified with ImageJ and plotted. (B) Representative images and quantification of Crystal Violet-stained Collagen I inserts from invasion assays towards the indicated attractants after 72 hours. Graphs show representative data normalized to low serum WT cell samples from two to three independent experiments (N=2 biological replicates). p-values from one-way ANOVA statistical testing. * $p \leq 0.05$; ** $p \leq 0.01$; *** $p \leq 0.001$; **** $p \leq 0.0001$.

4.4 Discussion

In this chapter we delineated the signaling effects of *CDH1* knockout on MCF7, T47D and ZR75.1 cells. All three KO cell lines exhibited hypersensitivity to IGF stimulation, with some increased sensitivity also shown towards IGF2 and insulin. Interestingly, this does not appear to be a pan-growth factor phenotype, with no differences observed following EGF

stimulation. However, MCF7 and T47D KO cells lines were more sensitive to cocktail of FGF ligand stimulation although no variations in downstream effects were observed. While Akt activation has been seen previously with *CDHI* KO cells (130), the IGF and FGF sensitivity is a novel finding from our work. An effort to corroborate this with ILC *CDHI* overexpression cell lines showed that two out of the three cell lines moderately reduced their ligand sensitivity with *CDHI* restoration. Overall, we conclude that E-cadherin loss sensitizes cells to IGF stimulation.

Looking further into their stimulation effects, the signaling activation stayed at a high level for as long as the pathway remained active, thus suggesting that not only KO cells are sensitized to IGF, but the strong pathway activation is sustained. This discovery strongly supports our hypothesis and led to additional phenotypes being tested to better understand the effects of IGF pathway activation. The sustained activity of IGF/Akt axis is an interesting topic and has been investigated by multiple groups. A study by Teresa Wood and group using the central glial (CG)-4 cell line showed that internalization of IGF1R following IGF1 stimulation is necessary for sustained Akt signaling, where the inhibition of IGF1R endocytosis reduced Akt phosphorylation (229). They also reported that *de novo* synthesis of IGF1R is not required for sustained Akt phosphorylation, placing the sustained signaling role on IGF1R recycling. This strongly agrees with a 2005 statement by Renato Baserga: “An antibody against the IGF-IR, to be effective, has to inhibit the binding of both IGF1 and IGF-2, induce the downregulation of the receptor, and have little or no effect on the IR signaling” (230). Interestingly, a study by Shin-Ichiro Takahashi’s group showed that IGF1R internalization led to a transient Akt activation over a sustained activation when IGF1R is retained on the surface by IRS in HEK293-T cells (231). Their model presents IRS1 with an AP2 binding site to engage and act as an endocytic

regulator to prevent Clathrin and AP2 interaction and the subsequent IGF1R endocytosis. The depletion of IRS1 led to a short term IGF1R membrane retention and hence, a transient Akt activation. These conflicting studies were performed in different cell line backgrounds but nonetheless are interesting topics for future studies to understand how membrane receptors recycling affects sustained signaling, especially the IGF1R. There have been studies on receptors such as EGFR signaling from the endosomes, eliciting distinct responses which would be an interesting avenue to explore with IGF1R to completely understand the role of IGFR endocytosis on its downstream signaling activation in the context of breast cancer and to investigate if E-cadherin has a regulatory role in the process (232). Our time course IGF1 signaling assay with WT and KO cells was designed to assess whether there could be signaling duration differences them due to E-cadherin deletion. However, due to the large range of timepoints tested and the long durations between each time point, a clear result could not be made. A future experiment is to identify any potential differences between the cell lines and also assess the role of IRS1 in them as referenced above (231). Attempts at addressing the IGF1R internalization rate differences between WT and KO will be discussed in Chapter 5. Our survival clonogenic assays showed that overall, the *CDHI* KO cells had a better survival phenotype and coupled with the anoikis resistance phenotype discussed in Chapter 3 reinforces the tumorigenic phenotypes supported by loss of E-cadherin in IDC cells. This also highlights the role of growth factor signaling pathways being activated in the absence of E-cadherin that could lead to cell survival (133, 233), further supporting the critical need for our study.

Due to the role of E-cadherin in maintaining cell-cell adhesion, its loss through EMT or genetic deletion is often thought to correlate with increased tumor invasion and metastasis (234,

235). Studies have outlined the disruption of cell-cell contacts following E-cadherin loss during the induction of EMT to allow anoikis resistance and promote tumor invasiveness by activating multiple transcriptional changes to subsequently support metastasis (152). Other studies, however, have suggested a requirement for E-cadherin in metastasis (150), wherein many metastases still express E-cadherin and a complete EMT is not necessary for metastasis to occur (151). Here we show that *CDHI* KO cells demonstrated increased migration towards Collagen I (8). The *CDHI* KO cells also showed an enhanced migration towards serum and IGF1, with T47D *CDHI* KO cells showing increased migration even in the absence of a chemoattractant. T47D *CDHI* KO also showed invasion through Collagen I, providing additional *in vitro* evidence supporting that the loss of E-cadherin may enhance metastatic phenotypes. The *in vitro* nature of these findings, however, is a limitation and *in vivo* experimentation is needed to better understand the role of E-cadherin in metastasis and validate if this is mediated by IGF signaling.

5.0 Loss of *CDH1* Renders IGF1R More Available for Ligand Binding And Hyperactivates Downstream Signaling

5.1 Introduction

In previous chapters, we have delineated that the loss of E-cadherin in ILC gives rise to hyperactive IGF signaling as seen via patient tumor samples and cell lines *in vitro*. This is further supported by our previous works as referenced previously (128, 129). Using *CDH1* KO cells in Chapter 4, we showed that deletion of *CDH1* in IDC cell lines was sufficient to hypersensitize these cells to stimulation by IGF1 as well as IGF2 and insulin. Our findings are also supported by that of others including an increase in Akt activation in mouse cell line with E-cadherin loss (130). Interestingly, however, little is understood about the mechanism of how loss of E-cadherin allows for hyperactivity of IGF1R and its downstream activator, Akt. This chapter will address our efforts in investigating the interaction between E-cadherin and IGF1R at cell-cell contacts and how this could lead to regulation of IGF1 signaling.

In our previous work using IDC cells with *CDH1* knockdown (129), control cells exhibited co-localization of E-cadherin with IGF1R at cell-cell boundaries. Interestingly, we also noted that IGF1R localization in the presence of E-cadherin was limited to only cell-cell junctions and not present at the membrane where there was no adjacent cell (129). However, knockdown of E-cadherin resulted in IGF1R being re-localized around the entire cell membrane, including areas without cell-cell junctions, thus leading us to hypothesize that the loss of E-cadherin causes re-localization of IGF1R, likely altering downstream signaling. We hypothesized

that E-cadherin represses IGF1R at cell-cell junctions and limits its ability to bind IGF ligands and thus regulates the extent of signaling activation (158). In addition, another possibility underlying the altered IGF1R activity was related to the duration IGF1R spends on the membrane. While it is common for membrane proteins to be internalized following activation, it is also common for E-cadherin - being a dynamic cell-cell adhesion and actin cytoskeleton regulating protein - to be endocytosed and recycled (234, 236). Due to the co-localization of E-cadherin and IGF1R seen previously (237), we hypothesized that IGF1R might be endocytosed with E-cadherin in IDC cells, maintaining a lower number of receptors on the membrane compared to ILC cells, resulting in lower pathway activation. Given the well-known role of growth factors in tumor progression, multiple efforts have been taken to understand the method of IGF1R internalization (238-240). Conflicting literature is available on whether it is the membrane localized IGF1R or its endocytosed version that allows for sustained downstream signaling (229, 231).

In this chapter, I describe the use of our isogenic cell line models to delineate the mechanism by which the loss of E-cadherin affects IGF signaling, understand if IGF1R's presence of the membrane is affected by E-cadherin loss and finally, if trafficking of IGF1R has a role in this process. I also investigated the interaction between IGF1R and E-cadherin and if this could play a major role in the process.

5.2 Materials and methods

5.2.1 Cell culture

Cell lines utilized in this study were obtained from ATCC: MCF7 (RRID: CVCL_0031), T47D (RRID: CVCL_0553), ZR75.1 (RRID: CVCL_0588), MDA-MB-134-VI (RRID: CVCL_0617), MDA-MB-231 (RRID: CVCL_0062) and Asterand for SUM44PE (RRID: CVCL_3424). Cell lines were maintained in 10% fetal bovine serum (FBS; Life Technologies) supplemented media (Thermo Fisher Scientific): MDA-MB-134 in 1:1 DMEM: L-15; MCF7 and MDA-MB-231 in DMEM; and T47D and ZR75.1 in RPMI. SUM44PE was maintained in DMEM/F12 with 2% charcoal stripped serum (CSS; Life Technologies) with additional supplements as previously described (34). Cell lines were cultured for less than 6 months at a time, routinely tested to be Mycoplasma free and authenticated by the University of Arizona Genetics Core (Tucson, Arizona) by short tandem repeat DNA profiling.

5.2.2 Cell fractionation assay to compare receptor expression levels

Cell fractionation was performed using a kit (Cell Signaling Technology #9038) and following the manufacturers protocol. Respective controls for membrane, cytosolic and nuclear fractions were utilized as directed in the manufacturer's protocol. Fractions were compared via immunoblotting and quantified on the LiCOr Odyssey CLx Imaging system.

5.2.3 Immunoblotting

Protein for immunoblotting experiments were harvested using RIPA buffer (50mM Tris pH 7.4, 150mM NaCl, 1mM EDTA, 0.5% Nonidet P-40, 0.5% NaDeoxycholate, 0.1% SDS) supplemented with 1x HALT protease and phosphatase cocktail (Thermo Fisher #78442), probe sonicated for 15 seconds (20% amplitude) and centrifuged at 14,000rpm at 4°C for 15 minutes. Protein concentration was assessed using BCA assay (Thermo Fisher #23225) and 50ug of protein per sample was run on 10% SDS-PAGE gel, then transferred to PVDF membrane. Membrane blocking was performed with Intercept PBS blocking buffer (LiCoR #927-40000) for one hour at room temperature and probed with primary antibodies overnight at 4°C: IGF1R (Cell Signaling Technology #3027; RRID:AB_2122378), E-cadherin (BD Biosciences #610182; RRID:AB_397581), p120 catenin (BD Biosciences; #610134; RRID:AB_397537), α -Biotin (Cell Signaling Technology #5597; RRID:AB_10828011 and β -actin (Millipore Sigma #A5441, RRID:AB_476744). This was followed by 1 hour room temperature incubation with secondary antibodies (1:10,000; anti-mouse 680LT: LiCoR #925-68020; anti-rabbit 800CW: LiCoR #925-32211). Membranes were subsequently imaged on the LiCoR Odyssey CLx Imaging system, with band quantifications performed with built in software.

5.2.4 qRT-PCR for IGF1R

RNA extraction was performed using RNeasy mini kit (Qiagen #74106) and the RNA quality and amount quantified on NanoDrop. Reverse transcription to cDNA was performed with PrimeScript™ RT Master Mix (Takara Bio #RR036B). RT-PCR was then performed with SsoAdvanced Universal SYBR (Bio-Rad #1726275) with IGF1R primers (F:

AGTTATCTCCGGTCTCTGAGG, R: TCTGTGGACGAACTTATTGGC). Results were normalized to reads from housekeeping gene RPLPO. Statistical differences evaluated using a paired t-test.

5.2.5 Receptor availability assay

Cells were seeded in 6cm plates (Fisher #08-772-E), and serum starved overnight after achieving a 70-80% confluency. Cells were then stimulated with biotinylated IGF1 (GroPep #AQU100) for 15 minutes at 4°C to reduce receptor internalization. Following PBS washes on ice, cells were treated with 2mM BS3 crosslinker (Thermo Scientific #21580) reconstituted in PBS (pH 8.0) with 6mM KCl and 10mM EGTA for 1 hour at 4°C with occasional rocking. BS3 quenching was performed with 10mM Glycine for 15 minutes and cells were harvested for subsequent immunoblotting (158).

5.2.6 Co-Immunoprecipitation

Co-IP was performed with E-cadherin (BD Biosciences #610182; RRID: AB 397581) and IGF1R (Cell Signaling Technology #3027; RRID: AB_2122378) antibodies. Cells were lysed in 20 mM Tris-HCl pH 7.4 with 1% NP-40, 137 mM NaCl and 5 mM EDTA with fresh protease and phosphatase inhibitors (1:100) and quantified using Pierce BCA Protein Assay Kit (Thermo Scientific #23225). Additional optimization steps also included n-Octylglucoside (Cayman Chemical Company #14327). 1mg protein from each sample was pre-cleared in 20uL of Pierce™ Protein G Agarose beads (Thermo Fisher Scientific #20398) and incubated in either 3µg of E-cadherin, IGF1R or IgG antibodies (Normal mouse IgG; Millipore #12-371; RRID:

AB_145840 and Normal rabbit IgG; Millipore #12-370; RRID: AB_145841) overnight at 4°C with rotation. One 4-hour incubation was performed the next day with 45uL of Pierce™ Protein G Agarose beads at 4°C with rotation. Protein was eluted with Laemmli buffer and analyzed by immunoblotting.

5.2.7 Immunofluorescence to assess E-cadherin and IGF1R localization

Cells were plated at a density of 100,000-200,000 cells/well on glass coverslips (Fisher #12-545-80P) in 24-well plates, fixed on ice in ice cold methanol for 30 minutes and blocked in blocking buffer (0.3% Triton X-100, 5% BSA, 1X DPBS) for 1 hour at room temperature. Primary antibody incubation was performed overnight at 4°C: IGF1R β -subunit (Cell Signaling Technology #3027; RRID: AB_2122378; 1:100), EpCAM (Cell Signaling Technology; #2929; RRID: AB_2098657; 1:100) and E-cadherin (Cell Signaling Technology; #3195; RRID: AB_2291471;1:100). Secondary antibody incubation was done for 1 hour at room temperature followed by Hoechst 33342 (Thermo Scientific #62249; 1:10000) staining. Coverslips were mounted with Aqua-Poly/Mount (Polysciences #18606-20) and images were taken on a Nikon A1 confocal microscope with a 60X objective. To assess changes in IGF1R presence on the membrane following E-cadherin deletion, EpCAM was used as a membrane control, where the presence of IGF1R co-localization with EpCAM was quantified as membrane localization.

5.2.8 Surface biotinylation assay

Cells were seeded in 6cm plates (Fisher #08-772-E), and serum starved overnight after achieving a 70-80% confluency. Cells were then treated with 10nM IGF1 (GroPep #AQU100)

and incubated at 37°C for varying durations (0-240 minutes) to allow receptor internalization. At respective time points, cells were washed with cold PBS and labeled with 0.5mg/mL EZ-Link™ Sulfo-NHS-Biotin (ThermoFisher Scientific #21217) for 30 minutes at 4°C. Biotinylation was quenched with 15mM Glycine and cells lysed for protein harvest. Following BCA assay, 400ug of protein was used for overnight incubation with Pierce Streptavidin Agarose (ThermoFisher Scientific #20353). After elution, 25uL of protein for each sample was analyzed by immunoblotting for IGF1R and E-cadherin. Following PBS washes on ice, cells were treated with 2mM BS3 crosslinker (Thermo Scientific #21580) reconstituted in PBS (pH 8.0) with 6mM KCl and 10mM EGTA for 1 hour at 4°C with occasional rocking. BS3 quenching was performed with 10mM Glycine for 15 minutes and cells were harvested for subsequent immunoblotting (158).

5.3 Results

5.3.1 T47D *CDH1* KO cells express higher IGF1R levels compared to WT cells

To understand the mechanism(s) by which loss of E-cadherin leads to higher IGF1 sensitivity, we compared the levels of IGF1R following *CDH1* knockout. Using a cell fractionation assay kit, I noted minimal differences between the MCF7 and ZR75.1 WT and KO cells (Figure 16A). Higher IGF1R expression was observed in both whole cell and membrane fractions of the T47D KO cells compared to WT cells. The elevated total levels were orthogonally validated via a qRT-PCR for IGF1R where we observed similar results. As seen with the cell fractionation assay, no differences were observed between the MCF7 and ZR75.1

cells, although the difference between ZR75.1 WT and KO cells was statistically significant via qRT-PCR ($p=0.025$) (Figure 16B). While higher IGF1R expression could explain the ligand hypersensitivity we observed in Chapters 3 and 4 for T47D, it does not provide the whole story as IGF1R levels were unchanged in MCF7 and ZR75.1 KO cells.

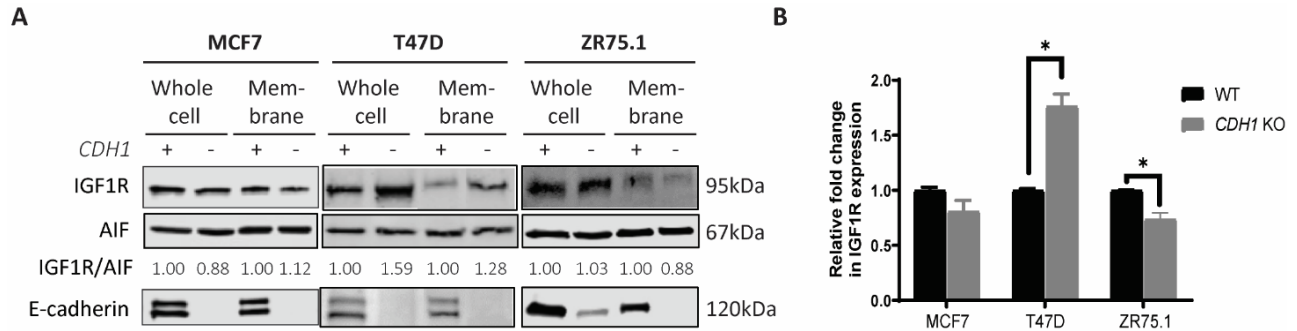


Figure 16: T47D *CDH1* KO cells express higher IGF1R levels

(A) Cell fractionation assay was performed on MCF7, T47D and ZR75.1 WT and *CDH1* KO cells to assess whole cell and membrane IGF1R expression levels. IGF1R bands were quantified and normalized to membrane control, AIF1. (B) qRT-PCR of IGF1R for the cell line models studied. Fold change in expression were calculated by normalizing delta Ct values to the respective WT values. Statistical differences were evaluated using unpaired t-test ($p=0.0105$ for T47D cell pair and $p=0.0246$ for ZR75.1 cell pair). Representative experiment shown, $n=2$ experiments with 2 biological and 3 technical repeats for each cell line.

5.3.2 *CDH1* KO cells exhibit higher IGF1 receptor availability for ligand binding

We next explored the possibility that IGF1 receptors are more available for ligand binding when E-cadherin is lost, thus allowing ligand hypersensitivity. Cells were serum-starved overnight and stimulated with 0, 5 or 10nM biotinylated IGF1 the next morning for 15 minutes at 4°C to decelerate receptor internalization. Cells were then treated with a crosslinker (BS3) to crosslink IGF1 to its receptor and immunoblotted for α -biotin and IGF1R. MCF7, T47D and ZR74.1 KO cells showed a 2.1-fold, 4-fold and 1.7-fold higher ligand-receptor complex respectively when compared to their corresponding WT cell line controls (Figure 17). This result

was stronger in the T47D *CDH1* KO cells, likely due to the higher baseline IGF1R expression in these cells. To corroborate these findings in our ILC *CDH1* OE cell lines, we performed similar experiments but observed unexpected results. While we expected to notice a decrease in ligand-receptor complex in the *CDH1* OE cells, we observed a higher fraction of the complex in them (Appendix B, Figure 33). We hypothesize that this might be due to a hyperactive adherens junction in the cells following E-cadherin overexpression which could have led to a larger E-cadherin-IGF1R complex being crosslinked and detected. Overall, this led us to conclude that although IGF1R levels were mostly unchanged in KO cells, the receptors were more available to bind ligands and elicit a signaling response. This hypothesis suggests a repressive nature of E-cadherin on IGF1R.

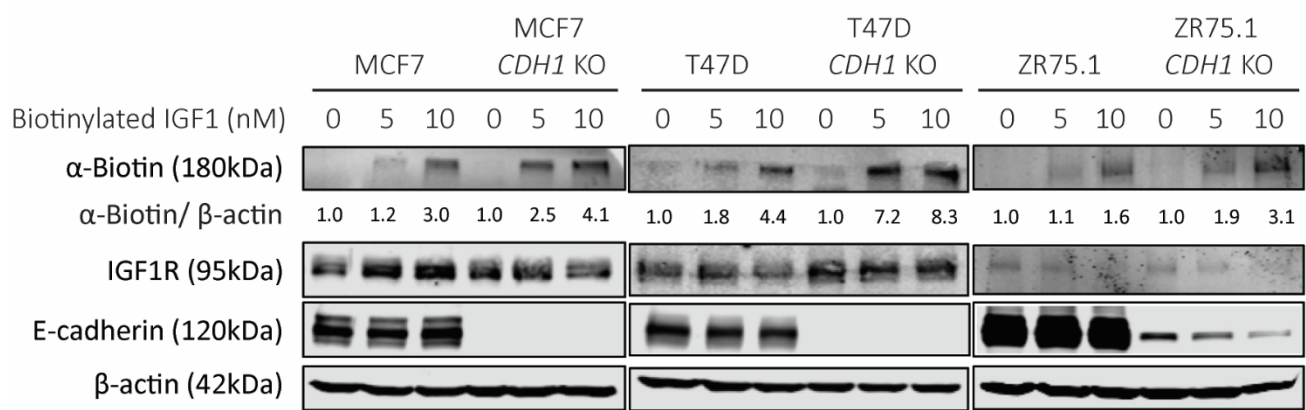


Figure 17: *CDH1* KO cells exhibit higher IGF1 receptor availability for ligand binding

MCF7, T47D and ZR75.1 WT and *CDH1* KO cells were stimulated with biotinylated IGF1 (0-10nM) for 15 minutes and crosslinked to assess ligand-receptor complex levels between WT and *CDH1* KO cells. α -biotin bands were quantified and normalized to loading control, β -actin. Representative experiment shown, n=3 for each experiment.

5.3.3 *CDH1* KO did not lead to changes in IGF1R re-localization on the membrane

We explored the potential for a physical interaction between IGF1R and E-cadherin on the cell membrane which could potentially physically and spatially prevent ligands from binding IGF1R. An immunoprecipitation performed for both IGF1R and E-cadherin in T47D cells did not reveal co-IP of either protein despite IP of the respective proteins and multiple attempts to optimize conditions (Figure 18A). Crosslinking attempts and lysis buffer optimizations with *n*-Octylglucoside were performed to stabilize any potential interaction between E-cadherin and IGF1R. However, no interactions were observed in any of these attempts. We next performed immunofluorescence to assess the localization of IGF1R and E-cadherin on the membrane and were able to observe colocalization of E-cadherin and IGF1R (Figure 18B). However, it is challenging to assess whether there is a physical interaction between E-cadherin and IGF1R based on the co-localization alone, given the difficulties faced with co-immunoprecipitation experiments. Importantly, our lab has previously shown co-localization between IGF1R and E-cadherin via Proximity Ligation Assay (PLA) (129), indicating the potential for their interaction, which could be repressive in nature based on the results presented here. Through these confocal images, we noticed a differential expression of IGF1R on the membrane of T47D WT versus KO cells which led us to probe whether KO cells have a re-localization of IGF1R on the membrane. To assess this, we stained for IGF1R and EpCAM and quantified the co-localization of IGF1R with EpCAM to compare levels of membrane localized IGF1R between WT and KO cells. However, no significant differences in membranous IGF1R localization were observed between the WT and KO cells (Figure 19). Our results suggest that although some IGF1R expression differences are noticed in the T47D KO cells, the overall lack of significant differences in Figure

19 suggests that increased receptor availability to bind ligand likely led to the observed elevated signaling induction upon ligand binding.

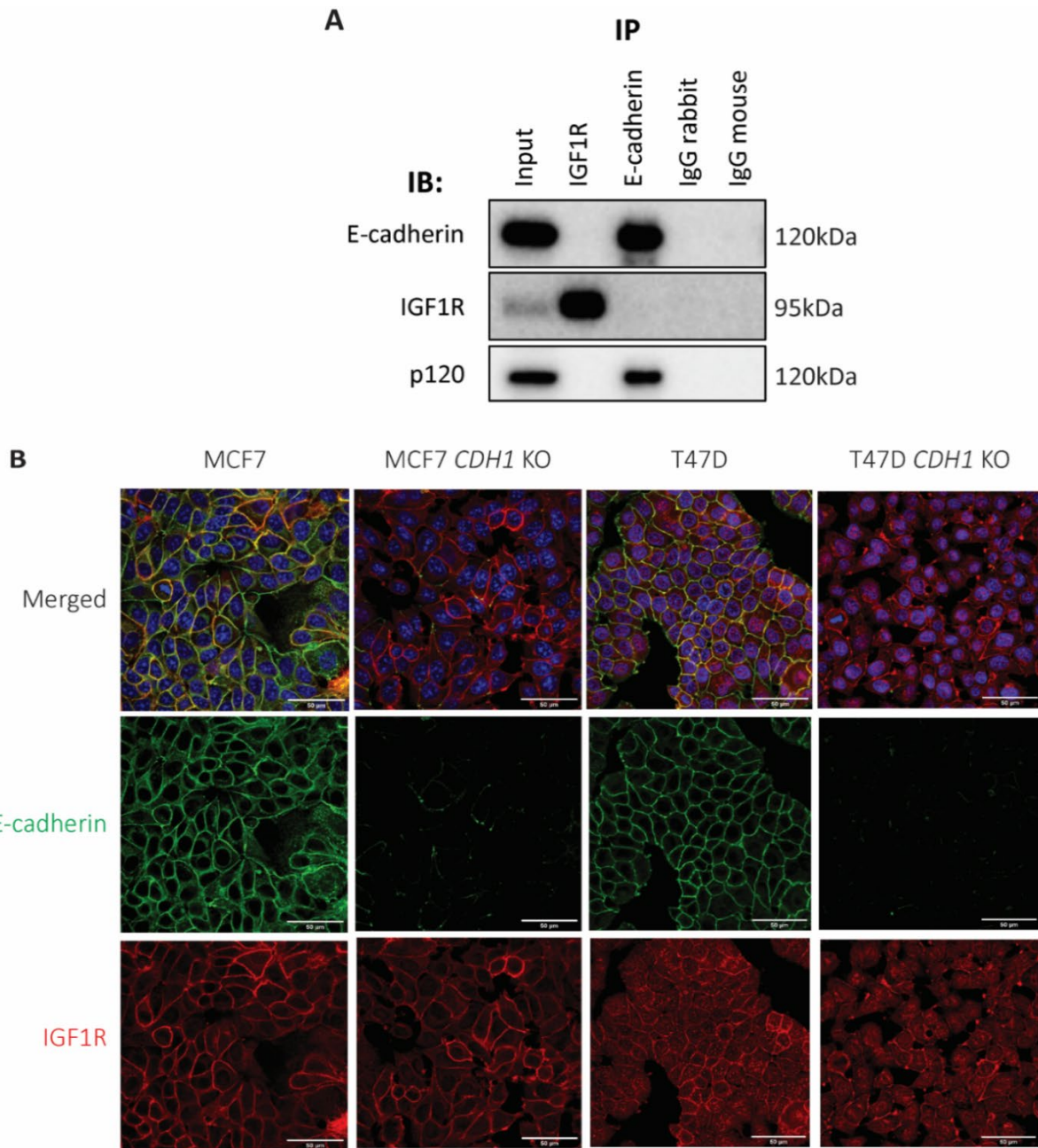


Figure 18: Co-localization of E-cadherin and IGF1R was observed although no interaction was detected via co-IP

(A) Immunoprecipitation of IGF1R and E-cadherin in T47D cells was assessed for a co-IP of the other protein, with p120 catenin assessed as a known interactor of E-cadherin. (B) Cell lines were dual stained for E-cadherin (green) and IGF1R (red) and imaged by confocal microscopy at a 60X objective. Scale bar: 50µm. Representative experiment shown for all, n=2-3 for each experiment.

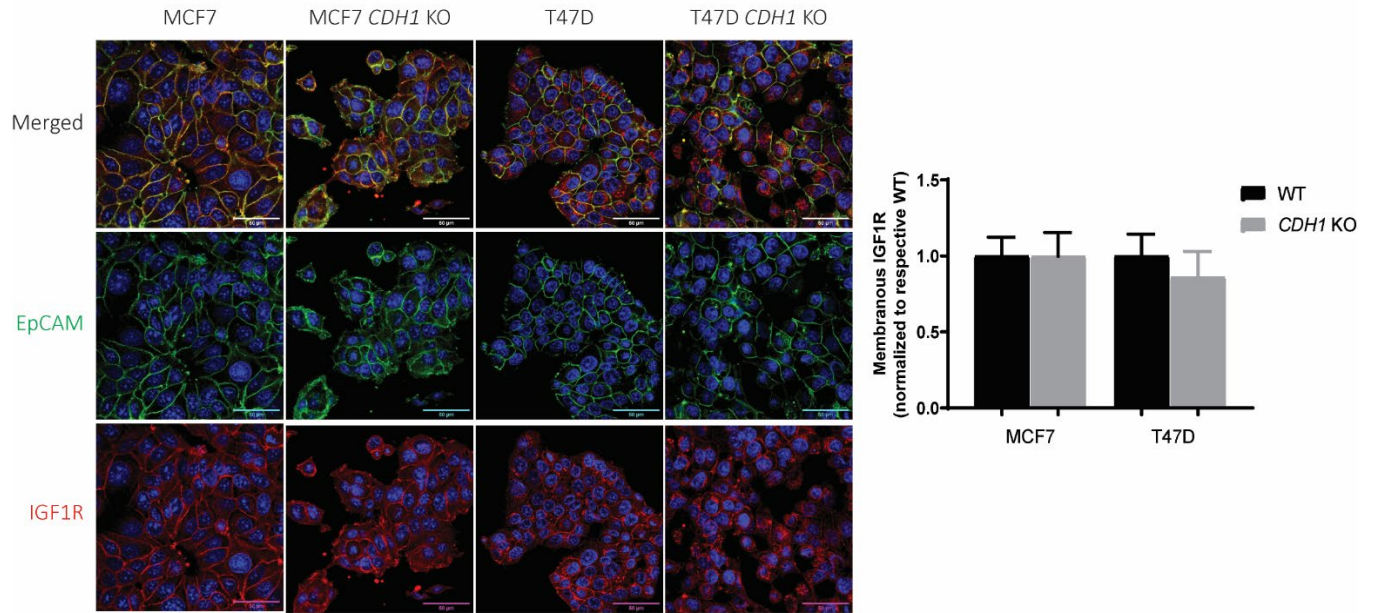


Figure 19: No re-localization of IGF1R observed following *CDH1* knockout

Cell lines were dual stained for EpCAM (green) and IGF1R (red) and imaged by confocal microscopy at a 60X objective. Scale bar: 50 μ m. 12 images for each cell line were quantified and graphed. Using EpCAM as a membrane control, the presence of IGF1R co-localization with EpCAM was quantified as membrane localization. Representative experiment shown for all, n=2 experiments.

5.3.4 IGF1R recycling is unchanged between WT and *CDH1* KO cells

In a final attempt to better understand the mechanism of IGF signaling regulation by E-cadherin, we hypothesized that the proximity of E-cadherin to IGF1R on the cell membrane might alter its endocytosis and thus affect the signaling response. To assess this, we subjected cells to surface biotinylation and tracked the levels of IGF1R on the membrane over a time course of 0 to 240 minutes post IGF1 stimulation. We observed a more rapid internalization, and slower return of IGF1R to the membrane, following IGF1 stimulation in the KO cells (Figure 20A, B). The slower return to the membrane over a 4-hour period also suggests the presence of endocytic signaling of IGF1R in the KO cells which further maintains the activity of signaling

(Chapter 4). This potentially indicates the internalization of a larger fraction of IGF1R in the KO cells given there are more of the ligand bound IGF1 receptors (previous experiment, Figure 17) than in WT cells. While the slower return to the membrane in KO cells was overall consistent, there were large variations between repeats, thus requiring final confirmations before a conclusion can be made. These are still preliminary experiments, and more work is needed to fully comprehend the role of E-cadherin in affecting receptor endocytosis and regulating IGF signaling.

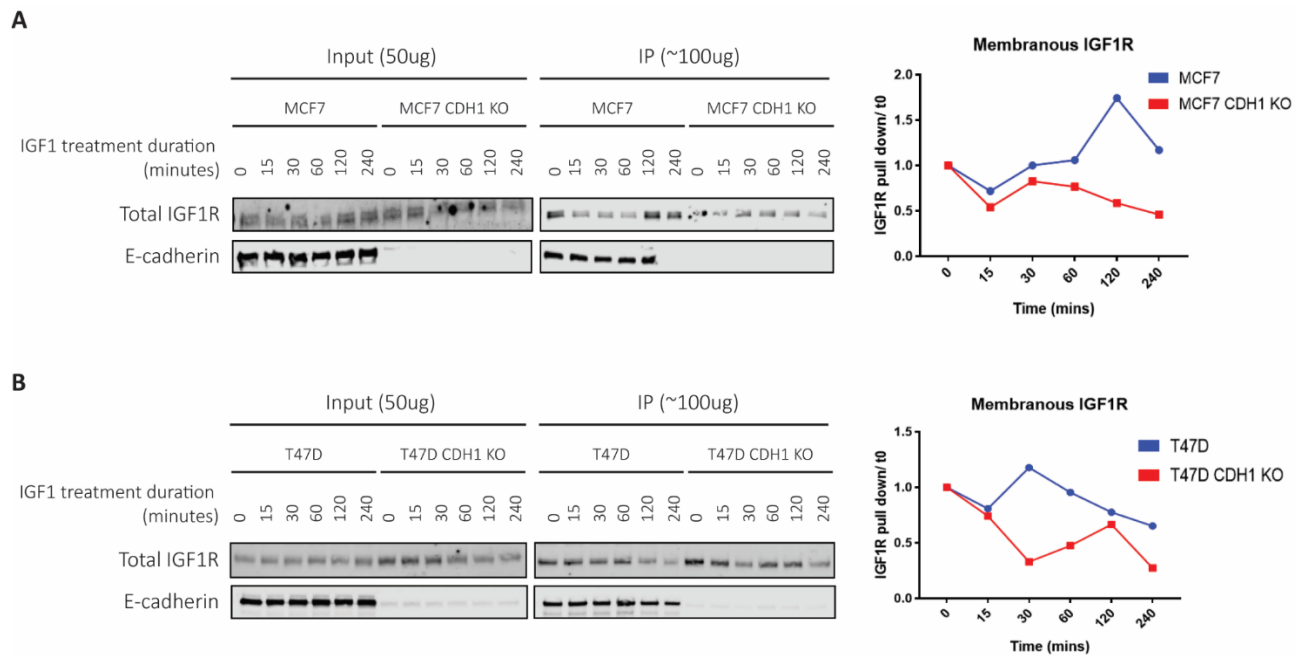


Figure 20: No clear differences in IGF1R recycling are observed between WT and *CDH1* KO cells

(A) MCF7 and (B) T47D WT and *CDH1* KO cells were serum starved overnight and treated with 10nM IGF1 over a time course assay. Cells were labeled with EZ-Link™ Sulfo-NHS-Biotin and pulled down with Pierce Streptavidin Agarose. Eluted protein was immunoblotted for IGF1R and E-cadherin. Graphs show representative bands quantified using the LiCOR system, representative experiment shown, n=2.

5.4 Discussion

In this chapter, we explored the potential for a physical interaction between E-cadherin and IGF1R which could lead to the signaling regulation observed thus far. Several studies have attributed spatial accessibility of IGF1R for ligand binding as a limiting factor in IGF1R signaling activation (158, 237). Consistent with these reports, we showed that loss of E-cadherin in our KO cells conferred increased IGF ligand binding by IGF1R, and subsequent pathway activation as shown in Chapter 4. Based on qRT-PCR and cell fractionation assays, we learned that this increased ligand-receptor binding is not solely due to IGF1R upregulation as two of the three cell lines show unchanged IGF1R expression. With the current findings, we can conclude that, when present, E-cadherin spatially represses IGF1R from being able to freely associate with and bind to IGF1 to elicit a signaling response. This agrees with the available literature on the topic where E-cadherin has been observed to form a large complex with IGF1R, IRS1 and SHC, which could thus affect the signaling activation levels due to spatial constrictions (237).

Despite previous reports on E-cadherin repressing growth factor receptors (129, 158, 237) and its co-localization with EGFR (158) and IGF1R (237), we were unable to find an association in our models by co-IP despite numerous attempts, suggesting that this might not be how E-cadherin affects IGF1R ligand binding. However, further experimentation with additional optimization could potentially be performed to confirm or refute a physical interaction between the proteins. Our inability to show direct interactions between E-cadherin and IGF1R does not sufficiently preclude their association via other substrates such as IRS1 as has been shown before (237) and hence does not refute our hypothesis. This indirect association might be sufficient to alter IGF1R's ability to bind its ligands efficiently and thus affect signaling levels as

seen in Chapter 4. It should be noted that we were previously able to note co-localization in a PLA assay (129). The formation of a ternary complex involving E-cadherin, growth factor receptors and integrins is an ongoing topic of investigation thought to affect cell mobility (241), which could additionally complicate immunoprecipitation by increasing the complex size and the proximity between E-cadherin and IGF1R. Similar interactions have been reported for E-cadherin and EGFR (158, 242), although we did not observe an increased sensitivity to the EGF ligand in our *CDHI* KO cell lines.

Evidence of downregulation of E-cadherin by growth factors promoting EMT has been reported previously (157, 237); while there is also evidence of growth factor signaling regulation by E-cadherin (158), suggesting that a bidirectional feedback loop may exist. These studies were initially almost exclusively performed in the context of EGFR where multiple groups have shown that E-cadherin inhibits ligand-dependent activation of EGFR signaling (140, 158, 160). However, a recent study by Teo and colleagues supports our findings by reporting on ILC cell lines generated from a p53-deficient metastatic mouse model exhibiting PI3K/AKT pathway activation and enhanced sensitivity to pathway inhibition (130). Critically, a compelling study also showed the upregulation of cell-cell adhesion in IGF1R overexpressing MCF7 cells, which was subsequently reduced using E-cadherin blocking antibodies (237). This suggests the importance of addressing the bidirectional regulation that we have not yet addressed as part of this study.

Our T47D *CDHI* KO cells' E-cadherin/IGF1R immunofluorescence results also brought about new questions regarding a potential IGF1R re-localization following E-cadherin knockout.

Further imaging using EpCAM as a control membrane marker and quantification for its co-localization with IGF1R did not show any differences between WT and KO cell lines although some significant results were obtained in our previous *CDH1* knockdown models (129), suggesting discrepant results between stable knockout and transient knockdown cell line models. Additional attempts to understand if IGF1R endocytosis is affected by E-cadherin presence/absence via surface biotinylation assays were inconclusive. Studies investigating IGF1R endocytosis and periods of sustained Akt signaling have been reported and are contradictory, with some studies supporting the requirement for IGF1R to be endocytosed for sustained signaling (229) and the opposite with other studies reporting on the need for IGF1R to remain on the membrane for continuous Akt activation (231). Critically, the role of E-cadherin in the process is still unknown. Overall, we have been able to delineate that E-cadherin loss allows IGF1R to be more available for ligand binding with the underlying mechanism yet to be discovered.

6.0 Targeting IGF Pathway Hyperactivity in *CDH1* Knockout Cells

6.1 Introduction

Given the well-known role of IGFs in mammary gland development and breast cancer progression, many pre-clinical studies and clinical trials have been conducted using IGF1R inhibitors. These inhibitors include humanized monoclonal antibodies that bind and subsequently downregulate the receptor and small molecule tyrosine kinase inhibitors to inhibit pathway activation and signaling (53, 104, 221, 243-245). Unfortunately, these trials ended with little to no response in the patient populations studied and there are currently no FDA approved agents directly targeting IGF1R (178-180). Several potential explanations for lack of efficacy of these agents include a compensatory mechanism of IR hyperactivation during IGF1R inhibition, and dual inhibition of IGF1R and IR causing hyperinsulinemia and other adverse effects (246-249). Although the inhibitors tested showed some response in small subsets of patients, the inability of a larger populations of patients to respond caused the trials to fail overall, often without in-depth analysis on those cases which did respond. Our studies were fueled by the desire to identify possible biomarkers of sensitivity and response to IGF1R-targeted agents. In this chapter we explore if loss of E-cadherin can be used to better select and stratify patients for IGF targeted therapies and enhance patient response. Further categorization of patients in clinical trials based on their tumors' specific histologic and molecular subtype may allow for a better targeting of the IGF1 pathway.

This chapter will address the potential of exploiting loss of E-cadherin in ILC as a biomarker to stratify patients for IGF1/IGF1R targeted therapies by comparing IDC parental and *CDHI* KO cell lines. Due to over 90% of ILC being ER+, Selective Estrogen Receptor Degraders (SERDs) are a common therapeutic option for patients with ILC. However, endocrine resistance develops in about 30% of patients who receive hormone therapy (250), thus highlighting the imperative need to develop alternative therapies. As shown in previous chapters, >90% of patients with ILC have a loss of E-cadherin in the tumors and enhanced IGF1 signaling suggesting that the IGF1 pathway may be a good therapeutic target. Our previous work with *CDHI* knockdown IDC cells line and an IGF1R small molecule tyrosine kinase inhibitor BMS-754807 showed that MCF7 si*CDHI* cells were more sensitive to BMS-754807 when grown in ultralow attachment conditions than parental control cells (129). These studies were performed in transient knock-down models, and the next challenge was to examine whether similar results could be obtained with our stable *CDHI* KO isogenic cell lines. We also performed preliminary studies with BMS-754807 and Fulvestrant in an ILC cell line, SUM44PE and showed significant synergism with the combination therapy (129), thus highlighting the need to investigate this further.

This chapter will explore the potential role of utilizing E-cadherin as a functional biomarker of response for IGF and Akt targeted therapies in patients whose tumors have a loss of E-cadherin. We specifically assess inhibitors targeting IGF1R and its downstream activators, PI3K, Akt and MEK to analyze the sensitivity of these models to the pathway inhibitors following loss of E-cadherin.

6.2 Materials and methods

6.2.1 Cell culture

Cell lines utilized in this study were obtained from ATCC: MCF7 (RRID: CVCL_0031), T47D (RRID: CVCL_0553) and ZR75.1 (RRID: CVCL_0588). Cell lines were maintained in 10% fetal bovine serum (FBS; Life Technologies) supplemented media (Thermo Fisher Scientific): MCF7 in DMEM; and T47D and ZR75.1 in RPMI. Cell lines were cultured for less than 6 months at a time, routinely tested to be Mycoplasma free and authenticated by the University of Arizona Genetics Core (Tucson, Arizona) by short tandem repeat DNA profiling.

6.2.2 Dose Response assays

Cells were plated in 50 μ L of media at 9,000 cells/well in 2D and ULA (Corning #3474) 96-well plates. Treatments were added 24 hours post seeding in an additional 50 μ L of respective media. IGF1R inhibitors BMS-754807 (Selleckchem #S1124) and OSI-906 (Selleckchem #S1091), PI3K inhibitor Alpelisib (Selleckchem #S2814), Akt inhibitor MK-2206 (Selleckchem #S1078), MEK inhibitor U0126 (Selleckchem #S1102) and Fulvestrant (Selleckchem #S1191) were dissolved in DMSO with a final \leq 0.5% DMSO concentration in treatments. Plates were collected at day 6 and measured by CellTiter-Glo (Promega #PR-G7573) following the manufacturer's protocol. Cell viability values were analyzed following blank cell deductions and normalization to vehicle readings. IC50 values for viability were calculated by nonlinear regression and statistical differences evaluated using sum-of-squares Global f-test ($p < 0.05$). Synergy was assessed using SynergyFinder (251).

6.2.3 Immunoblotting

Protein for immunoblotting experiments were harvested using RIPA buffer (50mM Tris pH 7.4, 150mM NaCl, 1mM EDTA, 0.5% Nonidet P-40, 0.5% NaDeoxycholate, 0.1% SDS) supplemented with 1x HALT protease and phosphatase cocktail (Thermo Fisher #78442), probe sonicated for 15 seconds (20% amplitude) and centrifuged at 14,000rpm at 4°C for 15 minutes. Protein concentration was assessed using BCA assay (Thermo Fisher #23225) and 50ug of protein per sample was run on 10% SDS-PAGE gel, then transferred to PVDF membrane. Membrane blocking was performed with Intercept PBS blocking buffer (LiCor #927-40000) for one hour at room temperature and probed with primary antibodies overnight at 4°C: pIGF1R/IR (Cell Signaling Technology #3024; RRID:AB_331253), IGF1R (Cell Signaling Technology #3027; RRID:AB_2122378), pAkt S473 (Cell Signaling Technology #4060; RRID:AB_2315049), Akt (Cell Signaling Technology #9272; RRID:AB_329827), InsR (Cell Signaling Technology #3025; RRID:AB_2280448), E-cadherin (BD Biosciences #610182; RRID:AB_397581) and β -actin (Millipore Sigma #A5441, RRID:AB_476744). This was followed by 1 hour room temperature incubation with secondary antibodies (1:10,000; anti-mouse 680LT: LiCor #925-68020; anti-rabbit 800CW: LiCor #925-32211). Membranes were subsequently imaged on the LiCor Odyssey CLx Imaging system, with band quantifications performed with built in software.

6.2.4 Patient derived breast organoid culture and dose response assays

IDC organoids (IPM-BO-56 and 102) and ILC organoids (IPM-BO-30, 41, 46, 77 and 114) were established by the Institute for Precision Medicine (Pittsburgh, PA) and maintained in media as detailed in (252) with 1nM β -estradiol (Sigma-Aldrich #E8875) supplementation. For dose

response assays, organoids were dissociated to single cell suspension with Trypsin and plated in 50 μ L of organoid media at 3,000 or 5,000 cells/well in 96-well round bottom plates (Falcon #353227) depending on the growth rate. Akt inhibitor MK2206 (Selleckchem #S1078; dissolved in DMSO) treatments were added 24 hours post seeding in an additional 50 μ L of organoid media. Organoids were monitored every day to ensure vehicle treated wells were growing well and remained at an appropriate density. Media was refreshed on day 6 and plates collected on day 12 with cell viability quantified by CellTiter-Glo 3D (Promega #G9681). Dose response assay analysis was performed as described above.

6.3 Results

6.3.1 T47D *CDHI* KO cells are sensitive to IGF1R, PI3K and Akt inhibitors

Motivated by the increased sensitivity of *CDHI* KO cells to IGF ligands and the potential for clinical translation, we sought to determine if these cells were also sensitive to IGF1R inhibitors. MCF7, T47D and ZR75.1 parental and *CDHI* KO cells were utilized for an 8-point dose response curve with IGF1R inhibitors BMS754807 and OSI906. Responses to the drug concentrations were normalized to vehicle treated wells with the IC50 values compared between parental and *CDHI* KO cells for statistical significance. To validate that the inhibitors were indeed effective in suppressing signaling, we exposed cells to a dose response of BMS754807 and MK2206 and performed immunoblotting by probing for IGF1R and Akt activation. Both MCF7 and ZR75.1 *CDHI* KO cells did not show any significant difference in sensitivity to IGF1R inhibitors when compared to their corresponding WT cells (Figure 21A-C). However,

BMS754807 treatment did inhibit IGF1R and Akt signaling in these cell lines, albeit at a lower efficacy in *CDHI* KO cells, potentially owing to their increased ligand sensitivity (Figure 21D). Only T47D *CDHI* KO cells were more sensitive to the tested IGF1R inhibitors, BMS-754807 ($p < 0.0001$) and OSI-906 ($p = 0.003$) compared to WT cells (Figure 21 D-G).

Given the higher incidence of *PIK3CA* hotspot mutations and occurrence of *PTEN* loss in ILC (31, 45, 253), we examined if the loss of E-cadherin in these IDC cell lines also sensitizes them to PI3K and Akt inhibitors, Alpelisib and MK-2206, respectively. As with the IGF1R inhibitors, only T47D *CDHI* KO cells showed increased sensitivity to MK2206 ($p < 0.0001$) and an overall increased sensitivity trend to Alpelisib upon averaging statistical analysis of repeated experiments (Figure 22A-D). No statistically significant differences in drug sensitivity were observed between MCF7 and ZR75.1 parental and their respective *CDHI* KO cell lines (Figure 22 D-G). All inhibitor testing were performed in 2D and ULA plates, with no significant differences observed between the conditions. Panels shown in the figures are from experiments done in 2D plates.

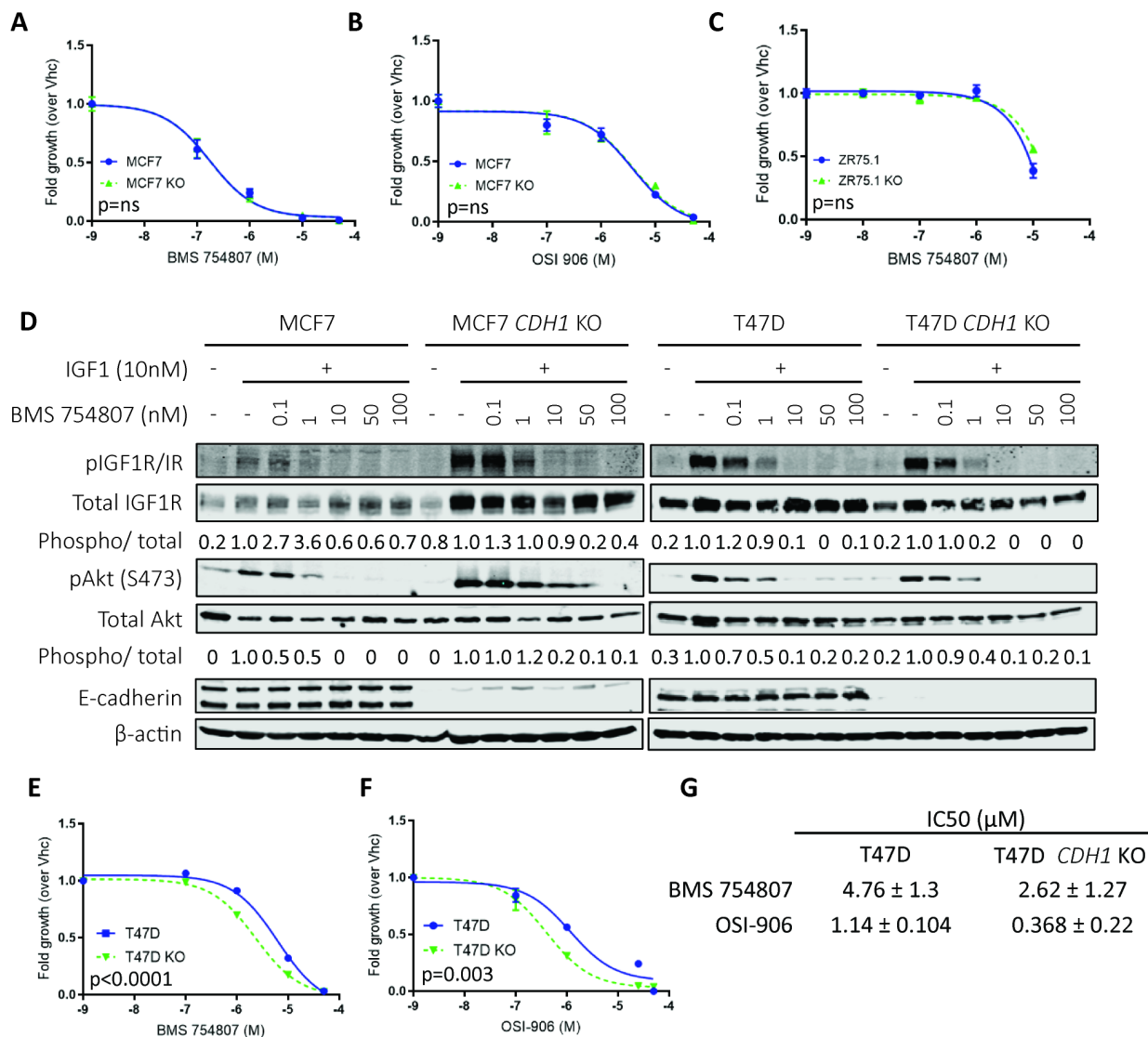


Figure 21: T47D *CDH1* KO cells express susceptibility to IGF1R Akt inhibitors

IDC parental and *CDH1* KO cells were seeded in 96-well 2D plates and treated with IGF1R inhibitors (OSI-906 or BMS-754807) for 6 days. MCF7 conditions in the panels as follows: (A) BMS-754807; (B) OSI-906 and (C) ZR75.1 with BMS754807. T47D conditions in the panels as follows: (D) BMS-754807; (E) OSI-906. CellTiter Glo assay was used to assess cell viability (relative luminescence) and data was normalized to vehicle treated control. (F) Summary of IC50 from 3 separate experiments, each with six biological replicates. Data was normalized to vehicle treated control. IC50 values for viability were calculated by nonlinear regression and statistical differences evaluated using sum-of-squares Global f-test (* $p \leq 0.05$; ** $p \leq 0.01$; *** $p \leq 0.001$; **** $p \leq 0.0001$; representative experiment shown; $n=3$ (each with six biological replicates)). (G) MCF7 and T47D WT and *CDH1* KO cells were treated with BMS754807 in increasing doses to assess signaling inhibition of the compounds used for cell viability assays. For quantification, phosphorylated protein levels were normalized to corresponding total protein levels and loading controls. Inhibitor treated sample values were further normalized to respective cell line vehicle treated samples. Representative experiment shown, $n=2$ for each experiment).

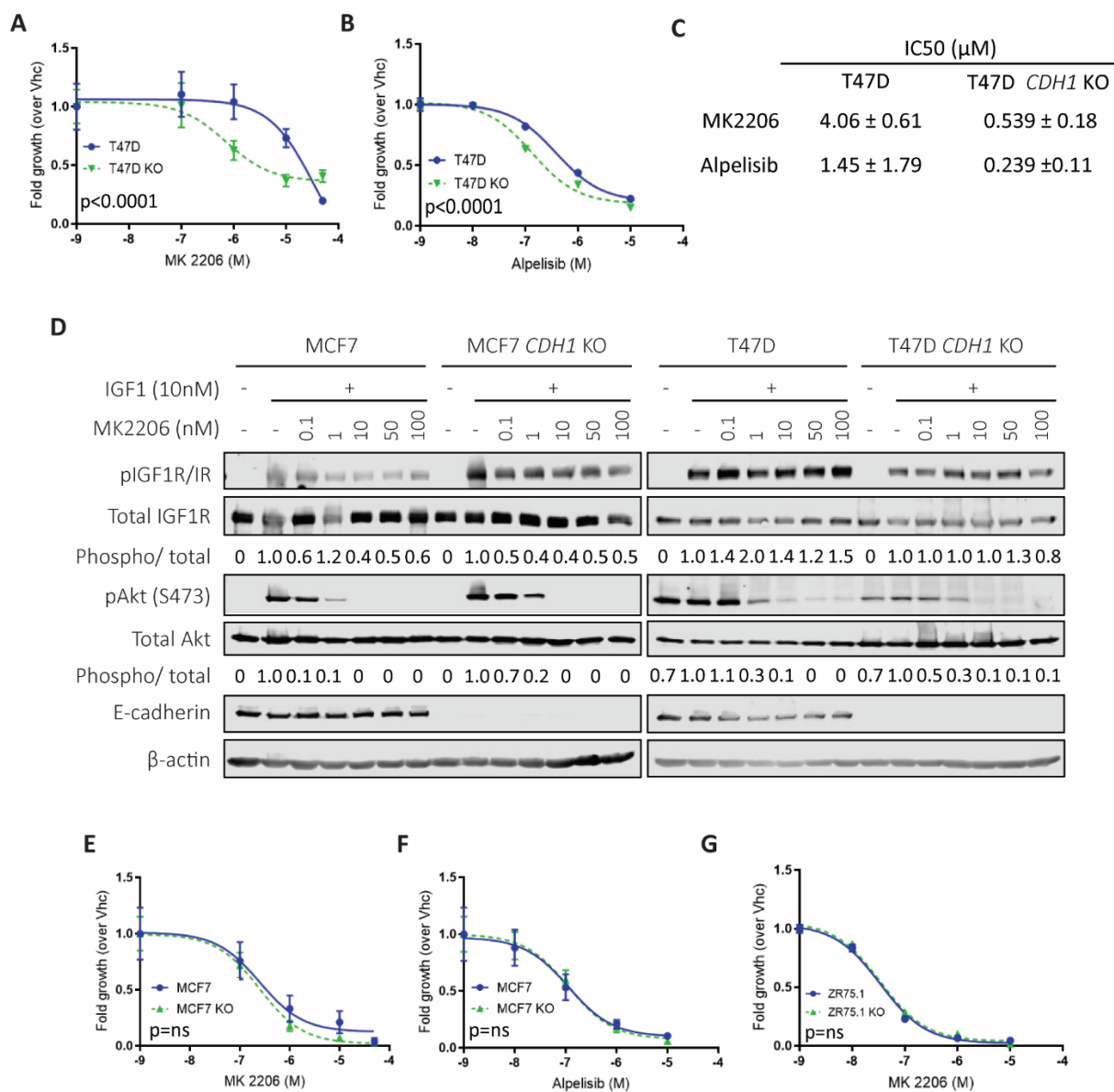


Figure 22: T47D *CDH1* KO cells express susceptibility to PI3K and Akt inhibitors

IDC parental and *CDH1* KO cells were seeded in 96-well 2D plates and treated with PI3K inhibitor (Alpelisib) or Akt inhibitor (MK2206) for 6 days. T47D conditions in the panels as follows: (A) MK2206; (B) Alpelisib. CellTiter Glo assay was used to assess cell viability (relative luminescence) and data was normalized to vehicle treated control. (C) Summary of IC50 from 3 separate experiments, each with six biological replicates. (D) MCF7 and T47D WT and *CDH1* KO cells were treated with MK2206 in increasing doses to assess signaling inhibition of the compounds used for cell viability assays. For quantification, phosphorylated protein levels were normalized to corresponding total protein levels and loading controls. Inhibitor treated sample values were further normalized to respective cell line vehicle treated samples. Representative experiment shown, $n=2$ for each experiment). MCF7 conditions in the panels as follows: (E) MK2206; (F) Alpelisib. ZR75.1 conditions in panel (G) for MK2206. CellTiter Glo assay was used to assess cell viability (relative luminescence) and data was normalized to vehicle treated control. Data was normalized to vehicle treated control. IC50 values for viability were calculated by nonlinear regression and statistical differences

evaluated using sum-of-squares Global f-test (* $p \leq 0.05$; ** $p \leq 0.01$; *** $p \leq 0.001$; **** $p \leq 0.0001$; representative experiment shown; $n=3$ (each with six biological replicates)).

6.3.2 MCF7 and T47D *CDHI* KO cells exhibit sensitivity to a combination of MEK and IGF1R inhibitors

Next, we assessed if the lack of change in sensitivity to IGF1R and Akt inhibitors in the MCF7 *CDHI* KO cells might be explained by activation of alternative pathways. A recent study in colon cancer showed that BMS754807 treatment led to a hyperactive MEK signaling (254), which led us to perform a combination treatment of BMS-754807 with a MEK inhibitor, U0126. We observed a strong additive effect where both MCF7 and T47D *CDHI* KO cells were more sensitive than their corresponding WT cells (Figure 23A, C). While this was an expected result in the T47D cells, it is interesting to note the additive effect in the MCF7 *CDHI* KO cells as this suggests the activation of alternative pathways following IGF1R, PI3K and Akt independent inhibitions. To understand if this was a synergistic relationship between IGF1R and MEK inhibitors, we utilized the SynergyFinder platform (251), with the ZIP method as an output (Figure 23B, D). Zip scores of less than -10 signifies that the interaction between two drugs is likely to be antagonistic, scores between -10 to 10 refers to an additive interaction while a ZIP score larger than 10 suggest the interaction is likely to be synergistic (251). In MCF7 and T47D WT and *CDHI* KO cells, synergy scores were between -9.717 to 10.995, which validates an additive but not a synergistic drug combination effect. Thus, this combination could be further studied as a potential therapeutic approach in tumors lacking E-cadherin. This is especially important given the high levels of resistance observed with single agent tyrosine kinase inhibitors and the need for combination therapies to offer higher therapeutic efficacy (255, 256).

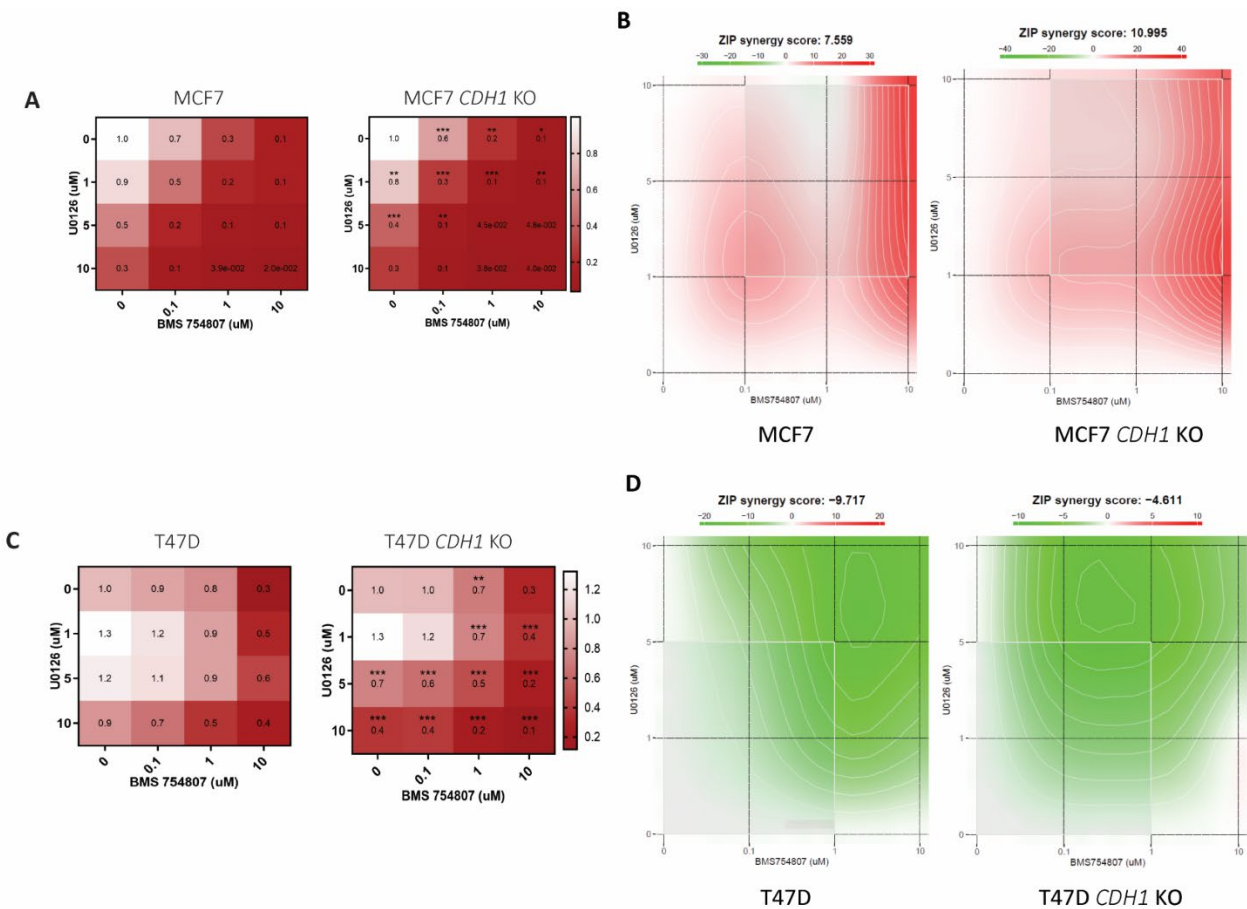


Figure 23: MCF7 and T47D *CDH1* KO cells exhibit sensitivity to a combination of MEK and IGF1R inhibitors

(A, B) MCF7 and (C, D) T47D WT and *CDH1* KO cells were seeded in 96-well 2D plates and treated a combination of MEK inhibitor (U0126) and BMS-754807 for 6 days. CellTiter Glo assay was used to assess cell viability (relative luminescence) and data was normalized to vehicle treated control. IC50 values for viability were calculated by nonlinear regression and statistical differences evaluated using sum-of-squares Global f-test (* $p \leq 0.05$; ** $p \leq 0.01$; *** $p \leq 0.001$; **** $p \leq 0.0001$; representative experiment shown; $n=3$ (each with three biological replicates)). ZIP synergy score output for (B) MCF7 and (D) T47D.

6.3.3 T47D *CDH1* KO cells exhibit sensitivity to a combination of Akt inhibitor and Fulvestrant

Over 90% of ILC are estrogen receptor (ER) positive (50). Results from multiple clinical trials have indicated that patients with ILC have a poorer prognosis than those with IDC, with

more frequent late recurrences (19,23,24). This finding highlights the need to improve treatment options available to patients with ILC based on the unique features of their disease, by introducing combination therapies that specifically target a patient's unique tumor characteristics for better therapeutic efficacy (257-259). Therefore, we evaluated the efficacy of combining MK2206, an Akt inhibitor with good activity in T47D KO cells, with endocrine therapy, the SERD Fulvestrant. We observed a higher susceptibility in the T47D *CDHI* KO cells (Figure 24A), supporting the notion of targeting the IGF pathway concurrently with targeting ER. The combination of these therapies also resulted in an additive effect (ZIP scores of 0.09 and 1.754 respectively), with the strongest additive effect seen in KO cells (Figure 24B). These results support the study of combinatory therapies in pre-clinical studies to better target the activation of the IGF pathway following E-cadherin loss.

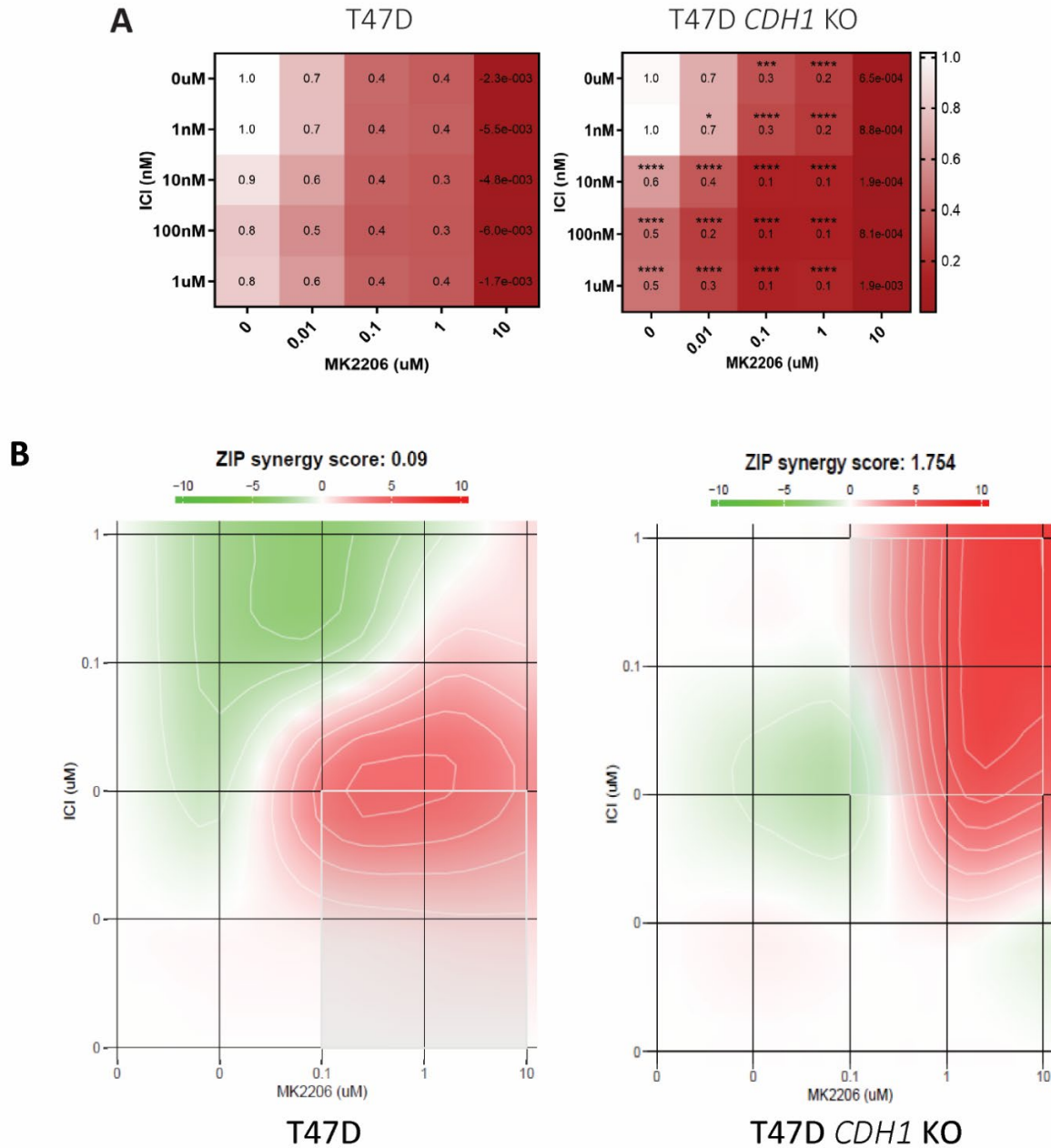


Figure 24: T47D *CDH1* KO cells exhibit sensitivity to a combination of Akt inhibitor and Fulvestrant

(A) T47D WT and *CDH1* KO cells were seeded in 96-well 2D plates and treated a combination of Akt inhibitor (MK2206) and Fulvestrant for 6 days. CellTiter Glo assay was used to assess cell viability (relative luminescence) and data was normalized to vehicle treated control. IC50 values for viability were calculated by nonlinear regression and statistical differences evaluated using sum-of-squares Global f-test (* $p \leq 0.05$; ** $p \leq 0.01$; *** $p \leq 0.001$; **** $p \leq 0.0001$; representative experiment shown; $n=3$ (each with three biological replicates)). (B) ZIP synergy score output for T47D.

6.3.4 ILC patient derived organoids exhibit patterns of higher susceptibility to the Akt inhibitor, MK2206

Finally, to analyze pathway inhibition in a more physiologically relevant model, we utilized ILC and IDC patient-derived organoids (PDO) to compare Akt inhibition sensitivity. Our close association with the Institute for Precision Medicine (University of Pittsburgh and UPMC) allowed access to a steadily growing bank of breast cancer PDOs using culture conditions adapted from the Clevers group (252). This initiative is successfully executed by Daniel D. Brown, PhD in association with a group of surgeons at the Magee Womens Hospital, led by Priscilla F. McAuliffe MD, PhD. This resource is extremely valuable in allowing for a direct hypothesis testing with patient derived samples. I treated 2 IDC and 5 ILC breast PDOs (imaged in Figure 25 A, B) with an 8-point dose response assay for MK2206 at 6 replicates per dose and refreshed media on day 6 with assay completion on day 12. Organoid viability was measured using CellTiter-Glo 3D and normalized to vehicle controls. As with our cell line results, no significant IDC versus ILC differences in sensitivity was observed, however, ILC organoids demonstrated a trend towards increased sensitivity to treatment (Figure 26 and Appendix C, Figure 34). We observed differences in growth kinetics and drug sensitivity of the individual PDO, likely reflecting inter-tumor heterogeneity seen in patients. Further work should include increasing the number of PDOs studied and assessing if there is a clinically meaningful difference between the ILC and IDC sensitivities to IGF1R inhibitors in vitro.

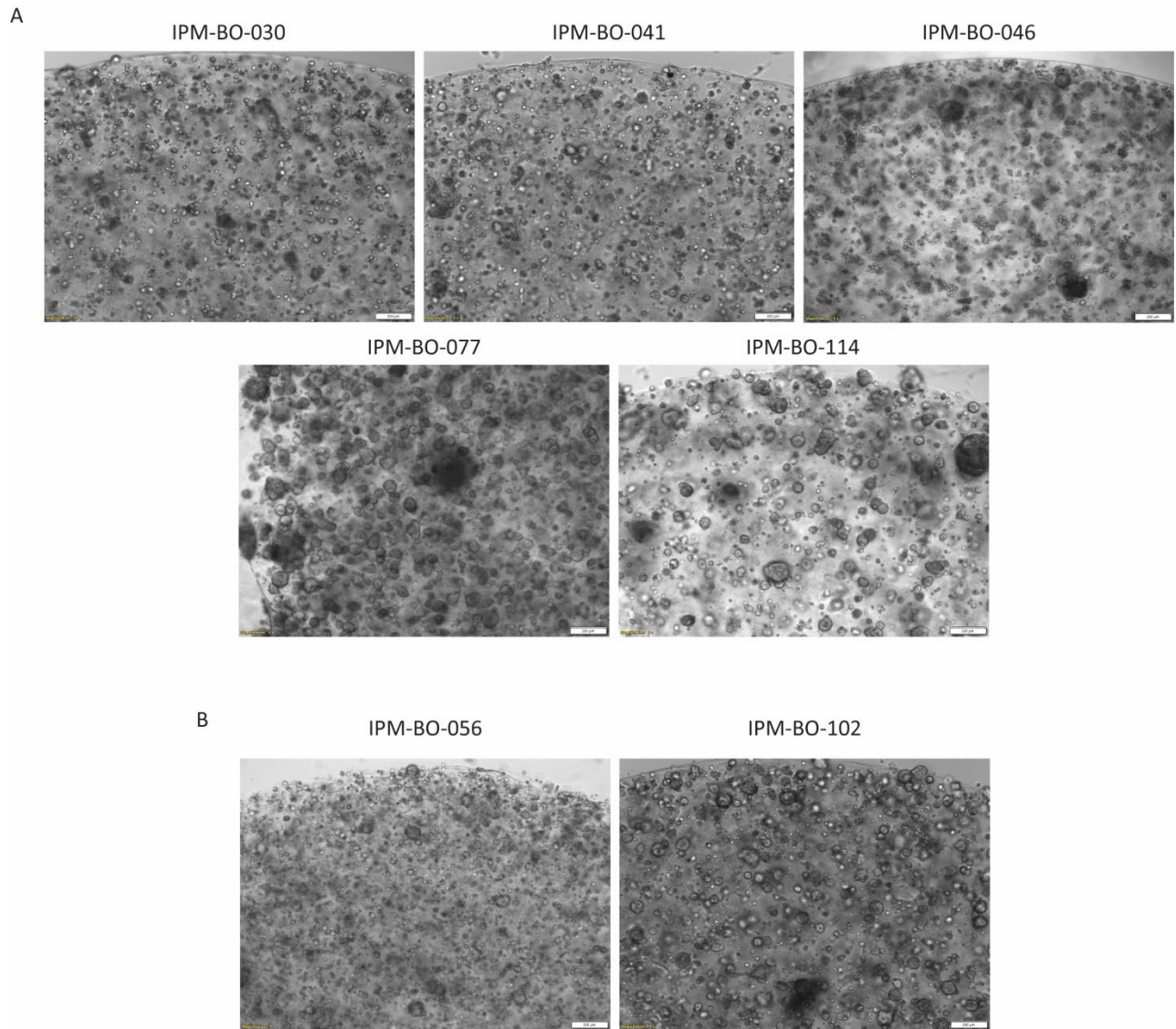


Figure 25: IDC and ILC Patient Derived Organoids exhibit altered morphology

Five ILC (A) and two IDC (B) patient derived breast organoids established by Dr Daniel D. Brown through the Institute for Precision Medicine were utilized in this drug response study. Grape-like morphology of ILC organoids can be observed in (A) while IDC organoids form tighter clusters (B). Images taken with brightfield microscope at 4X, scale bar: 200 μ m.

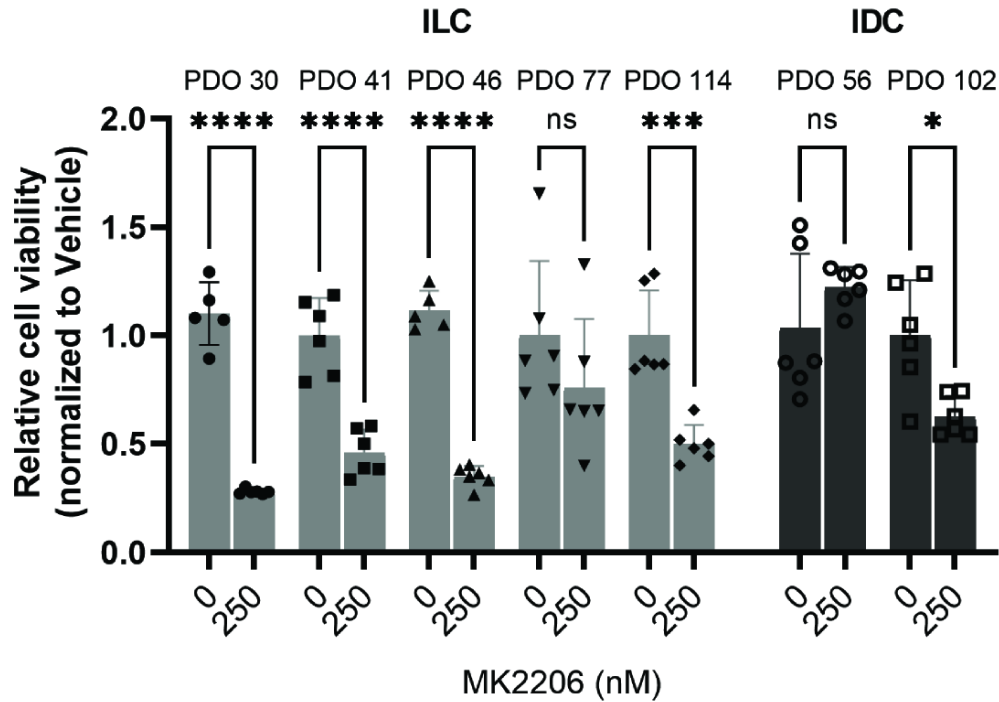


Figure 26: ILC organoids exhibit patterns of higher susceptibility to Akt inhibitor MK2206

Patient derived IDC and ILC organoids were treated with Akt inhibitor (MK2206) for 12 days and viability assessed with CellTiter Glo 3D (relative luminescence). Data from vehicle and wells treated with 250nM MK2206 are shown. Data was normalized to vehicle treated control. IC50 values for viability were calculated by nonlinear regression and statistical differences evaluated using sum-of-squares Global f-test (* $p \leq 0.05$; ** $p \leq 0.01$; *** $p \leq 0.001$; **** $p \leq 0.0001$; representative experiment shown; $n=1$ (each with six biological replicates)).

6.4 Discussion

In this chapter, we investigated the potential of utilizing E-cadherin as a functional biomarker of as a suitable population of breast cancers for IGF-targeted therapies. Although inhibitors of IGF1R have not been approved for clinic use, inhibitors of downstream activators such as PI3K, Akt and MEK have been successfully developed and clinically approved. With comprehensive studies, these compounds can be used in tumors with mutations leading to *PIK3CA* activation and *PTEN* loss such as in ILC (4), and maybe more so important given the

high IGF pathway activation found in the SCAN-B dataset (Chapter 2) and in *CDHI* knockout cells (Chapter 4).

We reported increased sensitivity to IGF1R/PI3K/Akt and MEK inhibitors in T47D *CDHI* KO cells and a trend towards increased sensitivity to an Akt inhibitor in ILC PDOs compared to IDC PDOs. Given the genetic landscape of MCF7, T47D and ZR75.1 cells, these models are primed for hyperactive Akt signaling, which we have observed to be further enhanced by loss of E-cadherin. The *PIK3CA* helical domain mutation in MCF7 cells (E545K) is reported to have a more aggressive phenotype over the kinase domain mutation in T47D (H1047R) (260), which may explain the absence of additional sensitivity in MCF7 *CDHI* KO cells to compounds tested since the *PIK3CA* mutation may effectively mask any potential effect of E-cadherin loss. With the possibility of IGF1R inhibitor efficacy being reduced by hyperactive downstream pathways such as MEK as seen in colon carcinoma (254) and the possibilities of downstream activation inhibition being overhauled by hyperactive receptor tyrosine kinases (261), we tested and observed an additive effect of treating cells with an IGF1R inhibitor in combination with a MEK inhibitor.

Although not robust, the increased sensitivity to IGF1R/PI3K/Akt inhibitors seen in *CDHI* KO cells is promising and supports our hypothesis. A 2018 study by Bajrami et al performed a synthetic lethality study on *CDHI* deficient cells by knocking out *CDHI* in MCF7 cells (132). They proceeded with two parallel synthetic lethality tests, a drug sensitivity screen targeting 80 small molecule inhibitors and a siRNA sensitivity screen targeting over 1000 genes where a shortlist of genes was obtained. A critical finding from this study was the discovery of *CDHI* synthetic lethality with ROS Proto-Oncogene 1 (ROS1), a receptor tyrosine kinase

implicated in multiple signaling pathways including MAPK and PI3K/Akt. Further experimentation revealed effective cell viability reduction with Foretinib and Crizotinib treatments *in vitro* and *in vivo* which led to two clinical trials currently underway (NCT03620643 with crizotinib and NCT04551495 with Entrectinib). The success of such discoveries being translated into the clinic is a promising precedent for our current studies. In addition, synthetic lethality targets of E-cadherin are an attractive topic with multiple studies having been reported recently with vesicle trafficking, plasma membrane organization and dynamics being among the new discoveries (133, 134, 262).

Additive effects of combining Akt inhibitors with Fulvestrant was also found to be beneficial in E-cadherin deficient cells, providing novel therapeutic benefits which require further exploration *in vivo*. With over 90% of ILC being ER+, SERDs and SERMs are a mainstay therapeutic option for patients with ILC. However, endocrine resistance eventually occurs in about 30% of cases (250) highlighting the need for combination treatments, such as the combination of hormone therapy with IGF-targeted therapy for patients with ILC. Our previous investigation with the ILC cell line SUM44PE showed a synergistic effect between BMS-754807 and Fulvestrant, further supporting the potential of this combination therapy (129). This is especially important given endocrine resistance and the need for additional therapies for combination treatments. Better understanding of a patient's unique disease features will allow us to inhibit multiple targets and prevent resistance, especially given that tumor heterogeneity has been associated with poor outcome and decreased response to treatments (263, 264). Short term adaptations to single agent therapies such as PI3K inhibitor in *PIK3CA*-mutant ER+ breast cancer has been seen via increased ER activity which can limit the antitumor activity of the

inhibitor and render it inefficient (265). Such situations can be prevented by comprehensively characterizing patient tumors and their drivers to map out a personalized and efficacious treatment plan. Acquired resistance to single agents such as TKI inhibitors are also well characterized where additional downstream inhibitors will be a great addition to therapies for a better clinical outcome (256, 265, 266).

Finally, the use of PDO to compare IDC and ILC provided a valuable model to test our hypothesis. This model allowed us to compare therapeutic benefit of Akt inhibitor MK2206 in IDC and ILC tumors in a primary patient-derived setting. Multiple studies are currently underway in PDO to examine response to therapy with the goal of identifying precision medicine approaches to maximize clinical outcomes (267-269). Although a clear conclusion could not be made from our PDO experiments given the limitations of the model such as limited PDO lines tested and their intrinsic variations, we did find a pattern of increased susceptibility to Akt inhibition in the ILC PDO. The growing collection of PDOs at the Institute for Precision Medicine will be extremely valuable in helping us validate our hypothesis in additional PDO lines.

Through our cell line and PDO models, we were able to show a context and background dependent response to IGF pathway inhibitors. Although not definitive, we have observed a strong trend of increased sensitivity in ILC and *CDHI* KO cells line towards these inhibitors tested. This is a very promising result supporting our hypothesis of utilizing *CDHI* loss as a functional biomarker of response for targeting the IGF pathway. The power of these studies could be increased by testing the efficacy of inhibitors targeting the IGF pathway in additional cell line models and organoids *in vitro* as well as *in vivo* to investigate the potential of efficiently

exploiting E-cadherin as a biomarker of therapeutic response. A valuable retrospective study could also be done by analyzing the subset of patients who have responded well to IGF therapies over the years of clinical trials to learn whether they have alterations in the *CDH1* gene.

7.0 Assessing E-Cadherin Regulation of IGF Signaling in Murine Model with Mammary Gland-Specific *CDH1* Deletion

7.1 Introduction

With IGF1 sensitivity and susceptibility to IGF and Akt inhibitors observed in cell lines and PDO models, we sought to validate our findings in a murine model to confirm that loss of E-cadherin can alter signaling response to IGF1. E-cadherin is a critical protein wherein its deletion at the organismal level is not feasible (270). Therefore, several systems for conditional deletion of E-cadherin in the mammary gland have been established as a means of studying the role of E-cadherin in mammary development and breast cancer. In hormone-inducible MMTV-Cre; *Cdh1* flox females, E-cadherin deletion was observed in the differentiating alveolar epithelial cells of the mammary gland. Although the *Cdh1* deleted mammary gland developed normally up to mid-pregnancy, it showed altered morphology around birth of offspring, reduced milk production and subsequently these females failed to nurse their litters (271). Analysis of these *Cdh1* deleted mammary glands also showed increased apoptosis levels, resembling that of involuted mammary glands (271), thus highlighting the importance of E-cadherin in mammary gland development. This study was initially performed to assess the possibility of obtaining mammary tumors through *Cdh1* deletion only, however, no tumors were observed. Although this would have been a good model for us to assess the role of E-cadherin in regulating IGF signaling, the MMTV-Cre model has been shown to also drive *Cdh1* deletion in other epithelial cells in other tissues such as salivary glands, kidneys, and lung (271).

Knowing the inability of MMTV-Cre; *Cdh1* flox mice model to generate mammary tumors, Patrick Derksen and Jos Jonkers developed a model where the Cre recombinase was driven by Keratin 14 (K14) promoter (272). The K14 promoter drives Cre expression in several epithelial tissues including the mammary epithelium and skin. Critically, this study did not observe any abnormal mammary glands in virgin, pregnant and parous mice with all females still being able to nurse their pups. However, with the addition of *Trp53* deletion to this model, the group was able to observe invasive and metastatic mammary tumors, with resemblance to human ILC (272). The same group further refined their mechanism of E-cadherin deletion and introduced the *WAP*-Cre system (273) to specifically delete E-cadherin only in the mammary gland and prevent skin tumors they had observed with the K14-Cre model (274). Whey acidic protein (*WAP*) is expressed in the luminal cells in the mammary gland and is critical in pregnant and lactating mammary epithelial cells. Although efficient Cre recombinase activity was detected in the mammary gland, they did not observe any morphological abnormalities in the mammary gland of virgin, pregnant or parous females (274). However, these females did show reduced milk production and were not able to nurse their litters as well as the WT females. Importantly, no tumors were detected until a *Trp53* deletion was introduced as in the previous study, where pleiomorphic ILC-like tumors were observed. This study hypothesized the high apoptotic process seen in the previous study as a potential explanation as to why no tumors were observed with *Cdh1* deletion alone (271).

This chapter will explore our work on utilizing the *WAP*-Cre; *Cdh1* flox system discussed above to conditionally delete *Cdh1* in the mammary gland to assess signaling sensitivity to IGF1. With the potential of apoptosis playing a major role following *Cdh1* deletion, we harvested

tissues at early lactation to avoid additional complexities. This work was done in collaboration with several lab colleagues: Dr Jagmohan Hooda, Dr Zheqi Li, Christy Smolak, Yang Wu, Beth Knapick and Jian Chen.

7.2 Materials and methods

7.2.1 Mouse colony

All animals in this cohort were housed at the animal facility in the Magee Womens Research Institute. All experiments were approved under protocols 20016647 and 20016546 by our local Institutional Animal Care and Use Committee (IACUC). The *WAP*Cre cohort were B6129-Tg (*WAP*-Cre)11738Mam/J, stock number 003552 from JAX. The *Cdh1* flox animals were B6.129-*Cdh1*tm2Kem/J, stock number 005319 from JAX. Weekly cage changes and daily food/ water checks were performed by animal facility staff. Cage and colony maintenance were performed as specified in the respective IACUC protocol. Breeding was done in monogamous pairs or in harem groups of 1 male with 2 females. Litters were weaned on day 21 as per our protocol and tail tipped for genotyping. Daily checks were performed to affirm health and monitor pregnancy status of study animals. Mice colony maintenance was performed by Christy Smolak and Dr Jagmohan Hooda.

7.2.2 PCR for genotyping

DNA extraction was performed using tail snips with Qiagen DNeasy Blood and Tissue kit (#69504). For genotyping, tail DNA were subjected to PCRs using GoTaq Master Mix (#M7122) and the following primers. *WAP* primers; F: TAGAGCTGTGCCAGCCTCTTC and R: GTGAAACAGCATTGCTGTCACTT. Internal control primer set; F: CAAATGTTGCTTGTCTGGTG and R: GTCAGTCGAGTGCACAGTTT. *IMR* primers for *Cdh1* flox detection; F: GGGTCTCACCGTAGTCCTCA and R: GATCTTTGGGAGAGCAGTCG. Genotyping efforts were done with Christy Smolak, Beth Knapick and Jian Chen.

7.2.3 LR3-IGF1 tail vein injections

Mice were restrained and their tail warmed with a heat lamp to get a clear view of the tail vein. The tail vein region was sterilized with alcohol swabs before being injected with 25µg LR3-IGF1 (GroPep # BU100) in 100uL PBS + 10mg/mL BSA, or 100uL PBS + 10mg/mL BSA, administered with a 26-gauge needle. Mice were placed in a cage for 9.5 minutes, then moved into an isoflurane induction chamber for 30 seconds and euthanized by cervical dislocation at 10 minutes post injection. Dissections were started immediately. All mammary glands, two liver lobes and kidneys were harvested and either flash frozen in cryovials, placed in FFPE cassette for fixation, or frozen in OCT compound. Mammary gland 4 from one side of each mouse was fixed on a slide for whole mount fixation and imaging with carmine alum staining. All tail vein injections were performed by Dr Jagmohan Hooda.

7.2.4 Immunohistochemistry for E-cadherin and H&E

Tissue samples in formalin fixed paraffin embedded (FFPE) cassettes were fixed in 10% neutral buffered formalin (Sigma Aldrich #F554-4L) overnight and switched into 70% ethanol until embedded by the Pitt Biospecimen Core (PBC) at Hillman Cancer Center. Embedded samples were cut at 4 μ m sections and used for H&E staining by PBC, and 5 unstained sections were obtained for IHC in the lab. Standard IHC protocol for E-cadherin was performed with the Cell Signaling antibody (CST #3195), 1:100 dilution. Slides were mounted with Permount (Fisher Scientific #SP15100), left to cure overnight at room temperature and imaged at 20X and 40X magnifications on a brightfield microscope.

7.2.5 Mammary gland whole mounts

Mammary gland whole mounts were performed as detailed here (275-278). Briefly, dissected mammary gland was spread on a glass slide and fixed in Carnoy's fixative at 4°C overnight. Tissues were rehydrated the following day and stained in carmine alum at 4°C for 2 nights. Slides were dehydrated and cleared in Xylene until fat is sufficiently cleared from the glands. Overnight incubation in methyl salicylate was performed before being mounted with Permount and imaged at 20X and 40X magnification. At the time of this preparation, the whole mounts were not sufficiently cleared and hence, we were not able to capture representative images.

7.2.6 Immunoblotting

Protein for immunoblotting experiments were harvested using RIPA buffer (Cell Signaling Technology #9806) supplemented with 1x HALT protease and phosphatase cocktail (Thermo Fisher #78442). Tissue samples were homogenized using a handheld homogenizer (Fisher Scientific) in RIPA buffer and probe sonicated for 15 seconds (20% amplitude). Samples were centrifuged at 14,000rpm at 4°C for 15 minutes. Protein concentration was assessed using BCA assay (Thermo Fisher #23225) and 100ug of protein per sample was run on 10% SDS-PAGE gel, then transferred to PVDF membrane. Membrane blocking was performed with Intercept PBS blocking buffer (LiCOR #927-40000) for one hour at room temperature and probed with primary antibodies overnight at 4°C: pIGF1R/IR (Cell Signaling Technology #3024; RRID:AB_331253), IGF1R (Cell Signaling Technology #3027; RRID:AB_2122378), pAkt S473 (Cell Signaling Technology #4060; RRID:AB_2315049), Akt (Cell Signaling Technology #9272; RRID:AB_329827), E-cadherin (BD Biosciences #610182; RRID:AB_397581) and β -actin (Millipore Sigma #A5441, RRID:AB_476744). This was followed by 1 hour room temperature incubation with secondary antibodies (1:10,000; anti-mouse 680LT: LiCor #925-68020; anti-rabbit 800CW: LiCor #925-32211). Membranes were subsequently imaged on the LiCOR Odyssey CLx Imaging system.

7.3 Results

7.3.1 Generation of *WAP*⁺; *Cdh1*^{fl/fl} mouse cohort

The objective of this section of the project was to establish a mouse model that has mammary gland specific deletion of *Cdh1* which will allow us to perform IGF1 injection and assess the differences in mammary gland IGF signaling between *Cdh1* WT and null females. To this end, we purchased a *WAP*-Cre mouse cohort and a *Cdh1* flox mice cohort from JAX. Upon receipt and mouse facility quarantine completion, these animals were genotyped for confirmation of *WAP*-Cre. The presence of the *WAP* driven recombinase returns a 497bp band and in the absence of the recombinase, no bands are present. This necessitated inclusion of an internal control primer set, with a 200bp PCR product that confirms PCR success. The binary results from these *WAP* set of primers also highlights the lack of a way to distinguish between a homozygous *WAP*-Cre positive versus a heterozygous *WAP*-Cre positive animal. For the *Cdh1* flox animals, a primer set from JAX (called IMR primers) were used to return a 310bp band for a flox allele and 243bp band for a WT allele, which allows the distinction between homozygous WT, heterozygous and homozygous flox animals.

Upon genotype confirmation, we backcrossed these animals from their C57BL/6 background to FVB/N background. Both cohorts were based on a C57BL/6 background, and we wanted to establish this cohort of animals in the FVB/N background given the known lower penetrance of mammary tumors in the C57BL/6 background (279, 280). As the *Cdh1* flox cohort in the lab had already gone through multiple backcrosses into the FVB/N background at this point, it was ready to be utilized for this new cohort establishment. The *WAP*-Cre cohort,

meanwhile, was new and had to be put through 2 rounds of backcrossing breeding with unedited FVB/N mice, also purchased from JAX. *WAPCre*⁺ animals were selected to then go through the third round of breeding with FVB/N *Cdh1* flox animals to begin establishing the *WAPCre*⁺; *Cdh1*^{fl/fl} cohort of animals (Fig 27). This round of breeding produced either *WAP*⁻; *Cdh1*^{wt/fl} animals or *WAP*⁺; *Cdh1*^{wt/fl} animals. By this stage, all offspring had white coats and we deemed the backcross as sufficient. The next rounds of breeding were performed to obtain offspring in the following genotypes: *WAP*⁺; *Cdh1*^{wt/wt}, *WAP*⁺; *Cdh1*^{wt/fl} and *WAP*⁺; *Cdh1*^{fl/fl}. Females of these genotypes were then utilized for the upcoming IGF1 injection experiments.

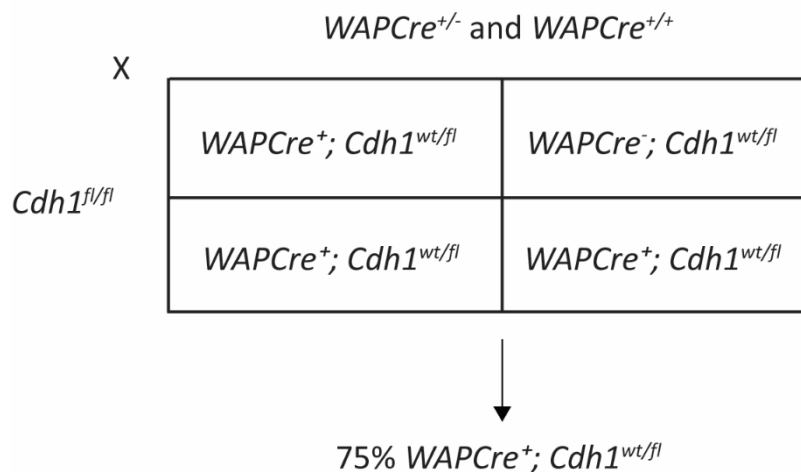


Figure 27: *WAPCre* and *Cdh1* flox breeding strategy

Hemizygous *WAPCre*⁺ animals after 2 rounds of backcrossing and *Cdh1*^{fl/fl} animals were bred as a final round of backcrossing into the FVB/N background and to obtain litters with both transgenes. With this strategy, we had a minimum of 50% success rate with getting *WAPCre*⁺; *Cdh1*^{wt/fl} animals to be used for the next round breeding.

The *WAP* promoter is highly active during pregnancy and lactation, with its activity declining post weaning (271, 273, 281-284). To activate *WAP* driven Cre recombinase, we took mice through pregnancy. To ensure *Cdh1* recombination and deletion, we performed 2 rounds of breeding of *WAP*⁺; *Cdh1*^{wt/wt} and *WAP*⁺; *Cdh1*^{fl/fl} females with males of any genotype as the

offspring were not necessary at this step of the experiment. The females were left with their respective male partners until they were confirmed to be pregnant with their second round of litters. The first set of offspring were weaned at 21 days which allowed the females to nurse them full term while with the second set of offspring, litters were sacrificed on day 7 and parent females injected with IGF1 and harvested shortly after. Of note, unexpectedly based on prior literature, our cohort of *WAP*⁺; *Cdh1*^{fl/fl} females were able to nurse their litters just as well as the *WAP*⁺; *Cdh1*^{wt/wt} females. The seven-day time point was chosen to ensure maximal *WAP*Cre expression while the female was still nursing and to avoid any potential complications of the apoptotic process during mammary gland involution in the late lactation period. Following IGF1 injection and tissue harvest, H&E staining, whole mount carmine staining, immunoblots and E-cadherin immunohistochemistry was performed. Unfortunately, at the time of this thesis writing, the whole mounts were not ready for imaging and were thus not included.

7.3.2 *WAP*Cre⁺; *Cdh1*^{wt/wt} and *WAP*Cre⁺; *Cdh1*^{fl/fl} mice mammary glands appeared similar by H&E

Following cohort establishment, we performed IGF1 injections in both *WAP*⁺; *Cdh1*^{wt/wt} and *WAP*⁺; *Cdh1*^{fl/fl} females. PBS or 25µg of LR3-IGF1 was injected in a 100uL volume via tail vein injection. Six animals for each genotype were injected, three with PBS and three with IGF1. Ten minutes after injections, animals were sacrificed and their mammary glands, kidneys and two lobes of liver harvested for downstream experimentation. The mammary gland tissues were either fixed for FFPE, fixed for whole mounting or flash frozen for protein/ DNA extraction. With the FFPE blocks, 4µm sections were cut and subjected to H&E staining to compare the

mammary gland structure of *WAP*⁺; *Cdh1*^{wt/wt} females to the *WAP*⁺; *Cdh1*^{fl/fl} females. As seen in Figure 28A-B, we were not able to detect any significant differences in mammary gland development between the two cohorts. We expected to see an effect of *Cdh1* loss in the mammary gland structure. With no differences observed, we proceeded to validate our model system and find out if there was indeed a *Cdh1* deletion as expected. To that end, we performed an E-cadherin IHC on the mammary gland FFPE sections from the same females.

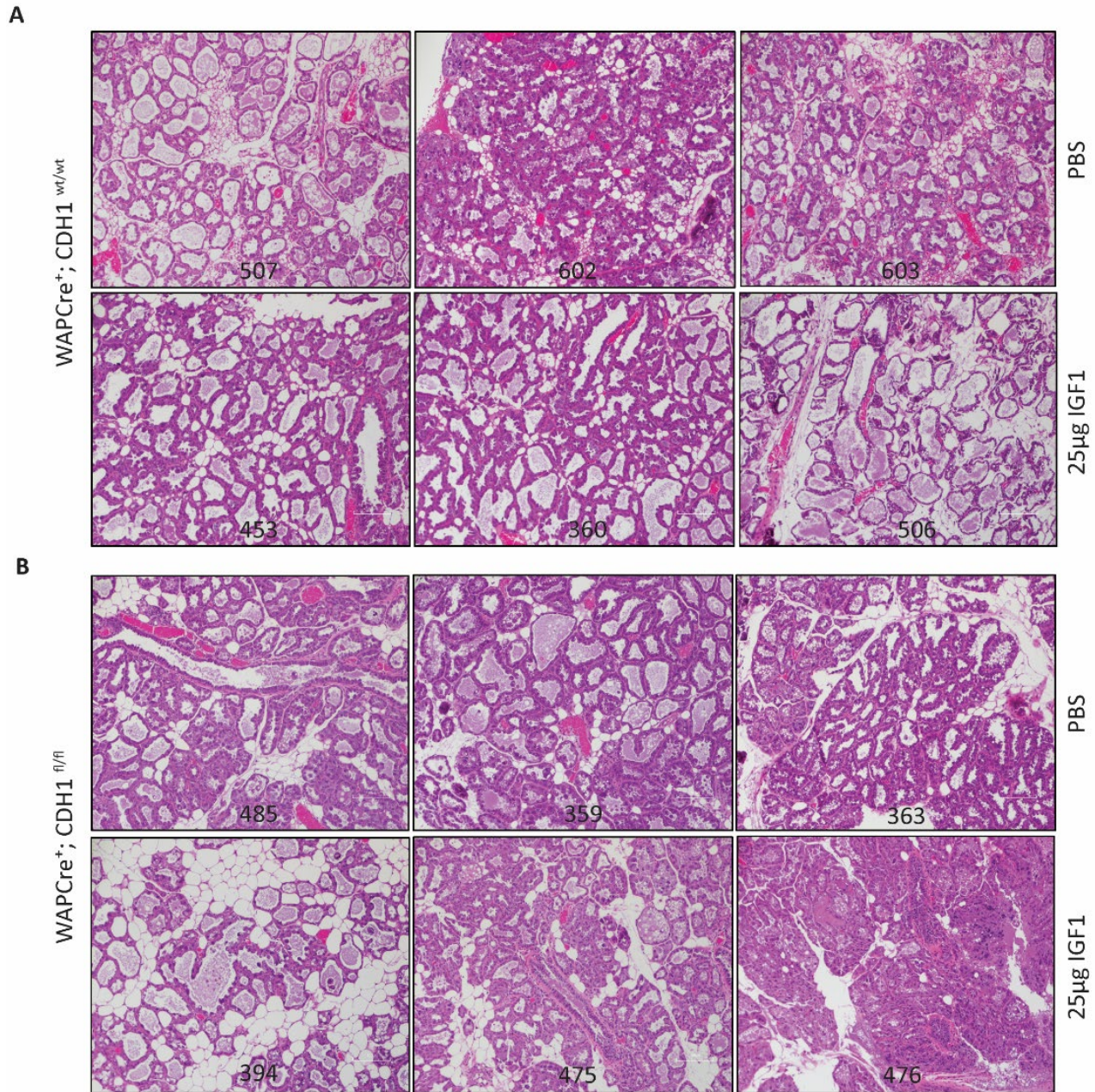


Figure 28: No significant differences observed between *WAPCre⁺; Cdh1^{wt/wt}* and *WAPCre⁺; Cdh1^{fl/fl}* mice mammary glands

WAPCre⁺; Cdh1^{wt/wt} and *WAPCre⁺; Cdh1^{fl/fl}* mice were injected with 100μL PBS or 100μL of 0.25μg/μL LR3-IGF1 and tissues harvested after 10 minutes for flash freezing or fixation. (A) *WAPCre⁺; Cdh1^{wt/wt}* mammary gland tissues and (B) *WAPCre⁺; Cdh1^{fl/fl}* mammary gland tissues were fixed in 10% formalin, sectioned and processed for H&E staining as shown. Images shown were taken at 10X; scale bar: 100μm. Mouse ear tag numbers for identification are indicated in black font in bottom middle corner.

7.3.3 E-cadherin expression was observed in *WAPCre⁺; Cdh1^{fl/fl}* animals

As seen in Figure 29A and B, E-cadherin IHC confirmed the presence of E-cadherin expression in both *WAP⁺; Cdh1^{wt/wt}* and *WAP⁺; Cdh1^{fl/fl}* cohorts. With these females having gone through 2 rounds of pregnancy - 1 full round of lactation for 21 days until weaning and the second litter weaned and sacrificed on day 7, we expected that we sacrificed the females at the height of their *WAPCre* expression which theoretically would elicit maximal *Cdh1* recombination, leading to its deletion. Unfortunately, we did not observe any loss of expression in the six *WAP⁺; Cdh1^{fl/fl}* females harvested. The lobular structures of the mammary glands can be clearly observed due to these harvests being done on day 7 post parturition as these females were still nursing. As the first step of this experiment was to delete *Cdh1* and to follow that up with an IGF1 stimulation step, the failure of the first step negated any subsequent step of understanding the role of E-cadherin in regulating IGF1 signaling in mice mammary glands. In addition to E-cadherin expression still being present in these *WAP⁺; Cdh1^{fl/fl}* animals, it is also crucial to appreciate its expression of the cell membrane; still localized at its usual position despite the attempt to delete it.

With these results, it became apparent that we were unable to obtain our mouse model of interest and will be looking into alternatives and potential interpretations of this result in the Discussion section. As a final step, we wanted to next perform a second confirmation of E-cadherin expression via immunoblotting and investigate whether the IGF1 injection was effective and whether a subsequent signaling activation occurred to validate our technique for future experiments.

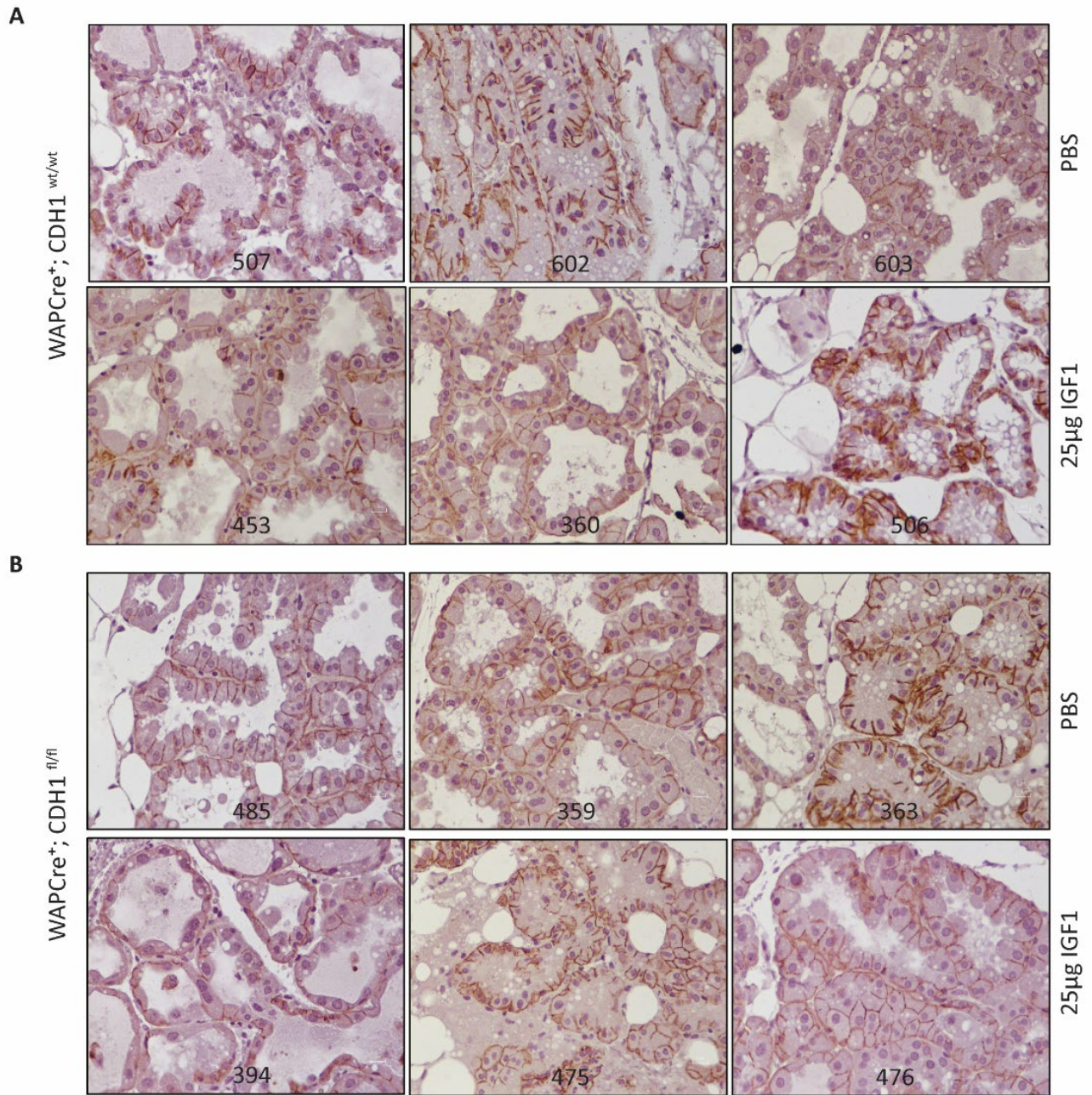


Figure 29: E-cadherin expression is present in WAPCre⁺; Cdh1^{fl/fl} animals

WAPCre⁺; Cdh1^{wt/wt} and WAPCre⁺; Cdh1^{fl/fl} mice were injected with 100µL PBS or 100µL of 0.25µg/µL LR3-IGF1 and tissues harvested after 10 minutes for flash freezing or fixation. (A) WAPCre⁺; Cdh1^{wt/wt} mammary gland tissues and (B) WAPCre⁺; Cdh1^{fl/fl} mammary gland tissues were fixed in 10% formalin and sectioned for an E-cadherin immunohistochemistry as shown. Images shown were taken at 40X; scale bar: 10µm. Mouse ear tag numbers for identification are indicated in black font in bottom middle corner.

7.3.4 Tail vein LR3-IGF1 injection activated IGF pathway in the mammary gland

We performed an immunoblot to assess E-cadherin expression as well as IGF1 signaling through IGF1R and Akt phosphorylation. Figure 30A shows a strong signaling in the mammary glands of mice injected with 25 μ g IGF1 compared to PBS-injected mice. As expected, based upon our staining data, E-cadherin expression was still present in the *WAP*⁺; *Cdh1*^{fl/fl} animals, and hence no conclusion can be made regarding the IGF signaling activation differences between the *WAP*⁺; *Cdh1*^{wt/wt} and *WAP*⁺; *Cdh1*^{fl/fl} animals. As negative controls, we blotted for the same proteins in the liver samples (Figure 30B) and noticed no IGF1R activation as expected. However, pAkt was present across samples, potentially exhibiting the background signaling levels in these animals.

Overall, the tail vein injection technique and tissue harvesting process proved to be successful and can be repeated for future experiments when we have the right mouse model. Our lab is currently considering the possibilities of establishing a new cohort of animals with validated success for *Cdh1* deletion (to be discussed in the discussion section), which can then be used for this assay.

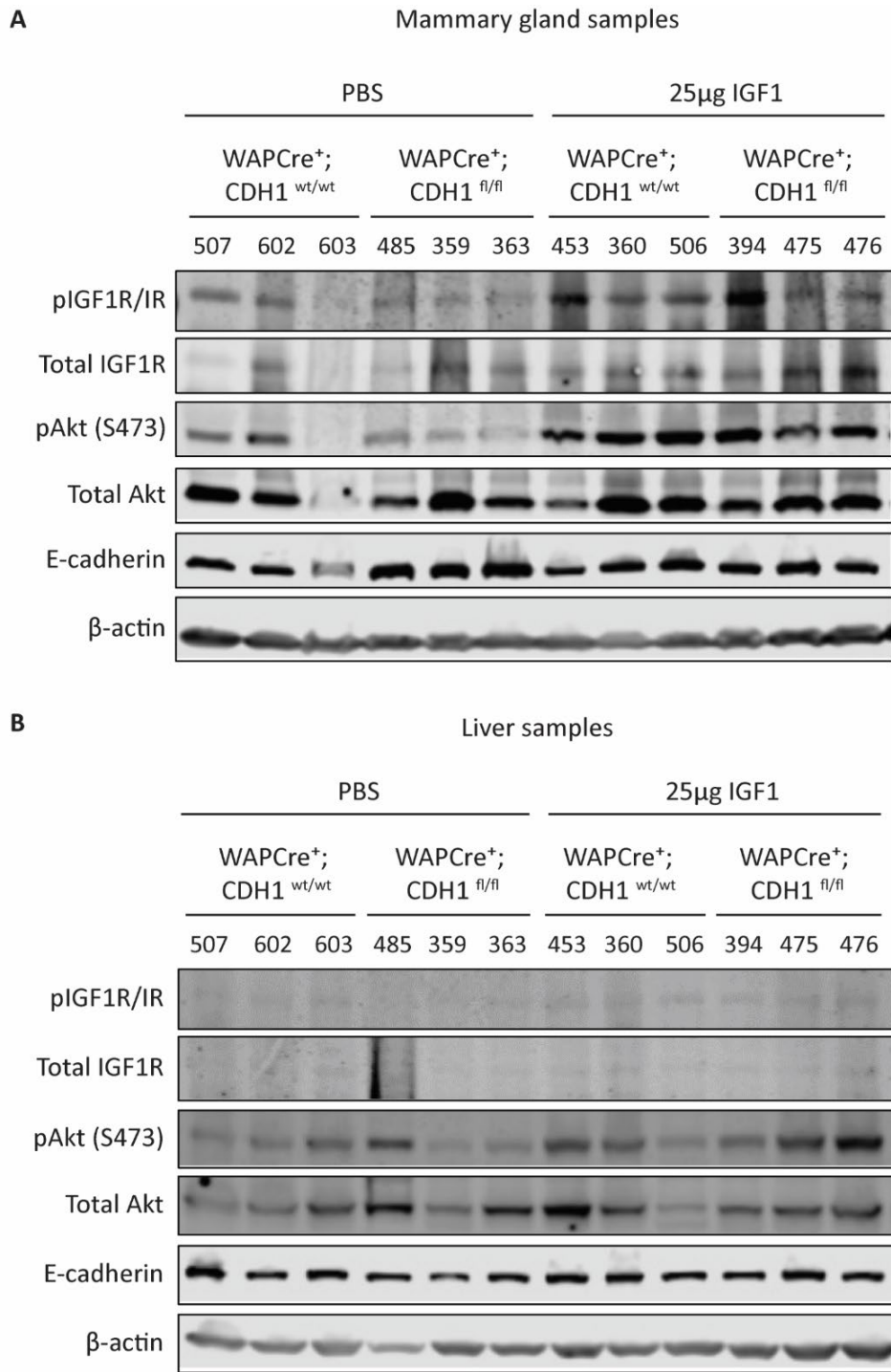


Figure 30: Tail vein IGF1 injection elicits IGF activation in the mammary gland

WAPCre⁺; Cdh1^{wt/wt} and *WAPCre⁺; Cdh1^{fl/fl}* mice were injected with 100µL PBS or 100µL of 0.25µg/µL LR3-IGF1 and tissues harvested after 10 minutes for flash freezing or fixation. (A) Mammary gland tissues and (B) liver were lysed in RIPA buffer and blotted for IGF signaling activation. Tail vein injections were performed by Dr Jagmohan Hooda.

7.3.5 Cre Reporter assay in mammary glands showed efficient RFP to GFP switch after pregnancy

Upon confirmation of no change in E-cadherin expression, we investigated whether the *WAP* promoter driven Cre recombinase was efficient. To this end, we utilized the Cre reporter strain from JAX, B6.129(Cg)-Gt (ROSA)26Sor^{tm4(ACTB-tdTomato,-EGFP)Luo/J}, stock number 007676. This mouse strain expresses membrane-Tomato fluorescence in all tissues which are switched to membrane-Green fluorescence upon Cre-driven recombination. This mouse model when bred with our *WAP*Cre mice allows us to assess whether our *WAP*Cre mouse model is efficient at driving Cre recombinase following *WAP* promoter activation to recombine the *Cdh1* loxP sites in the mammary glands. These mice were also backcrossed twice as our other mouse models, put through 1, 2 or 3 rounds of pregnancies with the animals sacrificed and tissues harvested on day 7 post parturition of the respective set of litters.

As seen in Figure 31A and B, mammary glands and livers from all animals were RFP positive. A patchy red to green fluorescence switch was seen specifically in the mammary glands with an increase in rounds of pregnancy. Thus, we can conclude that the *WAP* driven Cre in our mouse model is efficient at driving recombination. In addition, a tissue specificity to the mammary gland was also confirmed. Critically, when comparing between mammary glands from mice after 1, 2, and 3 pregnancy rounds, it is evident that one round of pregnancy did not activate sufficient Cre recombinase to drive the RFP to GFP switch. However, no significant differences were observed between 2 and 3 rounds of pregnancy, thus confirming that 2 rounds of pregnancy should have been sufficient to drive Cre activation in our *Cdh1*^{*fl/fl*} model. This shows that our previous experiment with 2 rounds of pregnancies should have been successful based on the Cre

activation, however, no *Cdh1* deletion was observed, thus suggesting that the challenge might lie within the *Cdh1* loxP sites or with an apoptotic induction following E-cadherin deletion as discussed in the introduction section of this chapter.

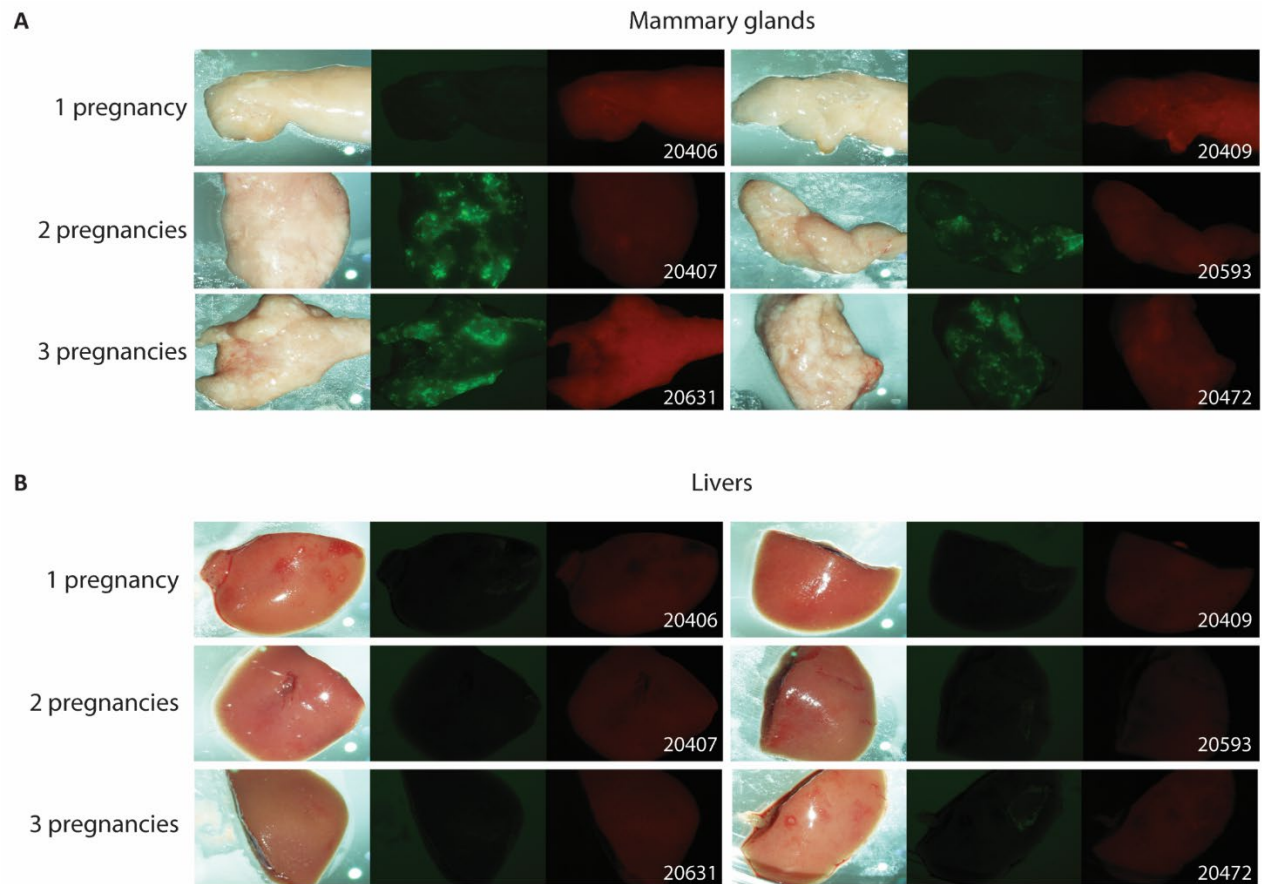


Figure 31: Cre Reporter assay in mammary glands shows efficient RFP to GFP switch with pregnancy

WAPCre⁺; *Cre Reporter*⁺ mice were sacrificed on day 7 post birth after their assigned rounds of pregnancies (A) Mammary gland tissues and (B) liver tissues were harvested and imaged for brightfield, GFP and RFP. Images shown were taken at 1X. Mouse ear tag numbers for identification are indicated in white font in the bottom right corner.

7.4 Discussion

Through this *WAP*⁺; *Cdh1*^{fl/fl} mouse cohort, we were unable to obtain animals with conditional mammary gland *Cdh1* deletion so that we could assess the impact of *Cdh1* on IGF1 signaling sensitivity. No abnormalities were detected in mammary gland development as shown by H&E staining and E-cadherin expression was still observed in the *WAP*⁺; *Cdh1*^{fl/fl} females even after 2 rounds of pregnancy. However, the IGF1 tail vein injection proved to be successful with strong pathway activation observed in the mammary gland tissues. To interpret these results, we probed the *WAP*Cre system to assess whether the Cre recombinase activity was efficient and noted that our cohort of *WAP*Cre animals were able to activate the RFP to GFP switch in Cre reporter animals by the second round of pregnancy with no appreciable increase observed after a third round of pregnancy. Thus, we are not yet able to clearly pinpoint the issue the model that led to the apparent failure of E-cadherin deletion.

We hypothesized that E-cadherin deletion may have caused apoptosis (271) resulting in a lack of detecting E-cadherin null cells by IHC and Western blotting. Further analysis of the literature support mass apoptosis during the involution process (282-285), however, the H&E images of our cohort of *WAP*⁺; *Cdh1*^{fl/fl} does not support the presence of regions of apoptotic cells. Further analysis and experiments will be needed to assess if the loss of E-cadherin does indeed cause loss of mammary epithelial cells. Another potential issue could have been the integrity of the loxP sites, which could be reassessed to confirm the potential of a successful recombination event. In addition, our *Cdh1* flox cohort was backcrossed into the FVB/N background over 6 years ago and has been in the colony since then where genomic or epigenomic drift in genotype could have occurred, thus potentially affecting the *Cdh1* flox site.

Finally, given the successful characterization of mammary tumors in mouse models with *WAP*⁺; *Cdh1*^{fl/fl} coupled with *Trp53* or *Pten* deletion (274, 286), one method of possibly circumventing the potential challenge of apoptosis of recombined cells would be to utilize these models since they may allow rescue of E-cadherin null cells and survival since they are now also expressing a tumor suppressor. The major challenge with this type of mouse model would be to eliminate the background of PI3K signaling being activated by PTEN deletion which could mask the effects brought about by E-cadherin deletion and IGF sensitivity, however, the *Trp53* deletion model may be beneficial for our purposes. Future work could assess the potential of utilizing these mouse models while also confirming the role of apoptosis in the cohort discussed here.

8.0 Conclusions

This study set out to understand the role of E-cadherin in regulating the IGF pathway in breast cancer. To understand this, we generated isogenic *CDHI* knockout models using three IDC cell lines where the deletion of E-cadherin caused reduced cell-cell attachment and morphology transformation into looser cell clusters in suspension. Furthermore, we found that E-cadherin loss was associated with enhanced anchorage independence and anoikis resistance, all of which are features observed in ILC. Interestingly, these KO cells also had higher survival in clonogenic assays compared to their parental cells, overall exhibiting enhanced tumorigenic properties compared to WT cells in part possibly due to the potential role of growth factor signaling pathways being more highly activated in the absence of E-cadherin (133, 233, 242). In addition, the *CDHI* KO cells also exhibited higher cell migration and invasion in the majority of our models, again highlighting the prominent role of E-cadherin in controlling metastatic phenotypes. Due to E-cadherin's role in maintaining cell-cell adhesion, its loss is often correlated with tumor invasion and metastasis (140, 287) although there have been contradicting studies with some groups reporting on the requirement for E-cadherin in metastasis (150). In Chapter 4 of this thesis, we showed that *CDHI* KO cells demonstrate increased migration towards Collagen I, a phenotype also observed in ILC cells (154). *CDHI* KO cells also showed an enhanced migration towards serum and IGF1, with T47D *CDHI* KO cells showing increased migration even in the absence of a chemoattractant. T47D *CDHI* KO also showed invasion through Collagen I, providing additional *in vitro* evidence supporting that the loss of E-cadherin may enhance metastatic phenotypes. While the *in vitro* nature of these findings is a limitation, these are encouraging data which should be validated with *in vivo* experimentation to delineate the role

of E-cadherin in metastasis and validate its effect on IGF signaling. Anoikis resistance phenotypes observed in Chapter 3 coupled with migratory phenotypes seen in Chapter 4 strongly supports metastatic progression upon E-cadherin loss (152). However, it will be critical to delineate the mechanism of how growth factor signaling enables *CDHI* KO cells to become more migratory. In the T47D *CDHI* KO cells, it was evident that they had increased chemotactic migration towards IGF1 and serum, however, additional experimentation is needed to assess the effect of IGF signaling on migration with evaluations such as wound-scratch assays.

A major finding from our study is the observation of *CDHI* KO cells' increased sensitivity to IGF1, IGF2 and insulin signaling. While this was apparent in short 15 minute-stimulations, longer time course assays with IGF1 also showed that the high activation levels persisted for the extent of signaling duration (as shown in Chapter 4). While we anticipated that this might be a pan-growth factor effect, it was evident that this was an IGF-specific phenotype, at least compared to the two other pathways probed (EGF and FGF). Although FGFR4 activation was higher in the *CDHI* KO cells, this was without significant downstream signaling activation. Through the studies performed in Chapter 5, we were able to attribute this increased signaling sensitivity to an increased receptor availability for ligand binding. Several studies have attributed spatial accessibility of IGF1R for ligand binding as a limiting factor in signaling activation (158, 237), and consistent with this notion, we found that loss of E-cadherin confers increased IGF ligand binding by IGF1R, and subsequent pathway activation. It will be important to confirm this finding with orthogonal approaches. Separate studies regarding IGF1R splice variants and receptor uncoupling during activation should also be performed to better understand the regulation of IGF signaling by E-cadherin. Although there have been reports on E-cadherin

repressing growth factor receptors (129, 158, 237) and co-localization (129, 237), we were unable to find a physical association between E-cadherin and IGF1R by co-IP despite numerous attempts. Ternary complexes involving E-cadherin, IGF1R and integrins are thought to affect cell mobility (241), and could possibly complicate co-immunoprecipitation. Interaction between E-cadherin and EGFR through co-IP has been reported, although we did not observe an increased sensitivity to the EGF ligand in our *CDHI* KO cell lines (158). Studies on E-cadherin and growth factor receptors were initially almost exclusively performed in the context of EGFR where multiple groups had shown that E-cadherin inhibits ligand-dependent activation of EGFR signaling (140, 158, 160), supporting our findings. A recent study by Teo and colleagues further supports our findings by reporting on ILC cell lines generated from a p53-deficient metastatic mouse model exhibiting enhanced PI3K/AKT pathway activation and sensitivity to pathway inhibition, which encourages future *in vivo* experimentation of these phenotypes (130).

Importantly, our study uncovered a context dependent increase in sensitivity to IGF1R, PI3K, Akt and MEK inhibitors in our *CDHI* KO models. This contributes to an increasing body of work delineating ILC as a unique breast cancer subtype, suggesting a potential for targeted therapeutic approaches towards the IGF1R/PI3K/Akt axis owing to the diagnostic loss of E-cadherin in this histological subtype. Of note, it is necessary to consider the inconsistencies observed in our models where the MCF7, T47D and ZR75.1 *CDHI* KO cells did not always agree on all assays performed. While ZR75.1 *CDHI* KO did not have a complete *CDHI* knockout which could affect the experimental results, the inconsistencies between MCF7 and T47D *CDHI* KO cells may be attributed to their genetic background differences. This highlights the importance of utilizing larger number of cell line models to obtain more robust conclusions.

Inhibitors of downstream activators such as PI3K, Akt and MEK have successfully been developed and are FDA approved. This is critical in malignancy with a high percentage of mutations leading to *PIK3CA* activation and *PTEN* loss such as in ILC (31), and even more important given the high IGF/Akt pathway activation found in the SCAN-B dataset (Chapter 2). Other studies with CRISPR MCF7 *CDHI* KO cells lines have shown that loss of E-cadherin leads to dependency upon ROS1 and enhanced sensitivity to crizotinib (288) for which a clinical trial is currently underway. We report increased sensitivity to IGF1R/PI3K/Akt and MEK inhibitors in T47D *CDHI* KO cells and an increased trend in sensitivity to an Akt inhibitor in ILC PDOs compared to IDC PDOs. Given the genetic landscape of MCF7, T47D and ZR75.1 cells, these models are primed for hyperactive Akt signaling, which we have shown to be further enhanced by loss of E-cadherin. The helical domain mutation in MCF7 cells (E545K) is reported to have a more aggressive phenotype over the kinase domain mutation in T47D (H1047R) (260), which may explain the absence of additional sensitivity in MCF7 *CDHI* KO cells to compounds tested since the *PIK3CA* mutation may effectively mask any potential effect from E-cadherin loss. With the possibility of IGF1R inhibitor efficacy being reduced by hyperactive downstream pathways such as MEK as seen in colon carcinoma (254) and by hyperactive receptor tyrosine kinases (261), we observed an additive effect of treating cells with an IGF1R inhibitor in combination with a MEK inhibitor. Due to over 90% of ILC being ER+ (39, 289-291) and endocrine therapy being an effective treatment option, it was important to assess the combination effects of MEK inhibition with endocrine therapy. This is especially important since about 30-40% of ILC tumors become endocrine resistant after years of endocrine therapy (250), thus needing additional therapeutic options. Additive effects of combining Akt inhibitors with Fulvestrant was found to be beneficial in E-cadherin deficient cells, supporting combination

therapies which require further exploration through patient derived organoids and animal experiments. Future studies will need to test the efficacy of inhibitors targeting the IGF pathway comparing cells +/- *CDH1* *in vivo* and investigate the potential of efficiently exploiting E-cadherin as a biomarker of therapeutic response.

Finally, we attempted to establish a mouse cohort of mammary gland specific *CDH1* deletion to better understand the role of E-cadherin in IGF signaling regulation, however, we were unsuccessful. While the WAP driven Cre recombinase was effective, no *CDH1* recombination and deletion was observed, and thus we were not able to study effects of E-cadherin expression on IGF signaling activation levels. We hypothesized that the apoptosis in E-cadherin null cells seen previously (281) could be a potential reason for why we were unable to detect any E-cadherin null cell in IHC, although further experimentation is necessary to detect apoptotic cells in the mammary glands. We propose the potential of utilizing the *WAP*⁺; *CDH1*^{fl/fl} *Trp53*^{-/-}, *WAP*⁺; *CDH1*^{fl/fl}; *Pten*^{-/-} or *WAP*⁺; *CDH1*^{fl/fl}; *Pik3ca*^{mut} mouse cohort as a method of overriding the possible E-cadherin deletion-driven apoptosis as *Trp53/Pten* deletion or *Pik3ca* mutation may allow E-cadherin null cells to survive, given the successful mammary tumor progression previously observed in this model (274, 286). The major challenge with this mouse model would be eliminating the background of PI3K signaling being activated by *Pten* deletion or *Pik3ca* mutation which could mask the effects brought about by E-cadherin deletion when we determine IGF sensitivity. However, the *Trp53* deletion model may not have such effects. It will also be crucial to confirm the role of apoptosis in the *WAP*⁺; *CDH1*^{fl/fl} cohort to validate our findings.

In summary, this project addressed the role of E-cadherin in regulating IGF signaling activation, controlling metastatic phenotypes, and identifying the use of specific inhibitors that can efficiently target elevated IGF1 signaling activation. We discussed novel findings of increased receptor availability for ligand binding due to loss of E-cadherin and increased susceptibility to IGF1R/PI3K/Akt and MEK inhibitors upon *CDH1* deletion. These results add to a growing body of evidence suggesting that loss of *CDH1* may represent a biomarker of response to IGF pathway inhibitors and further asserts the need for investigation into the clinical translation of these findings. While the *in vitro* nature of our studies in a small panel of cell lines is a limitation, we were able to strongly delineate the cellular- and context-dependent functions of E-cadherin in IGF driven tumor phenotypes. Our findings require translation into *in vivo* models with the goal of validating E-cadherin loss as a functional biomarker of response for IGF pathway inhibitors in breast cancer as well as the utilization of E-cadherin expression as a vital patient stratification tool in clinical trials.

Appendix A

Chapter 4 Supplementary Figures

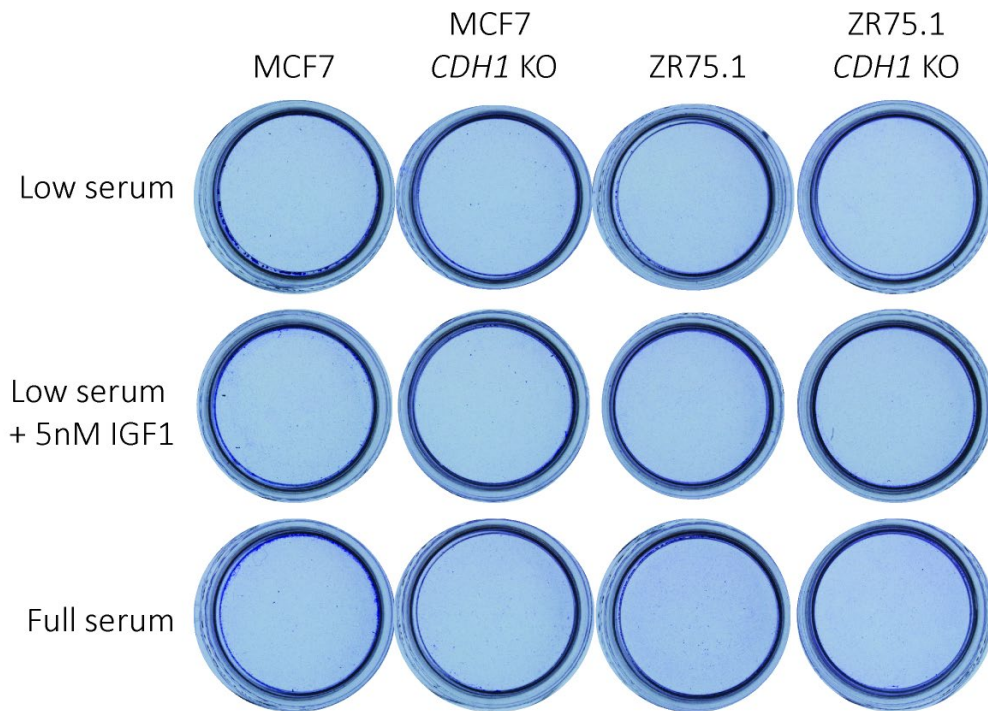


Figure 32: MCF7 and ZR75.1 WT and KO cells do not invade Collagen I

MCF7 and ZR75.1 WT and *CDH1* KO cells were plated at 300,000 cells/ well in collagen I inserts in 24-well plates. Representative images of crystal violet-stained collagen I inserts from invasion assays towards the indicated attractants after 72 hours are shown. Representative experiment shown, n=2.

Appendix B

Chapter 5 Supplementary Figures

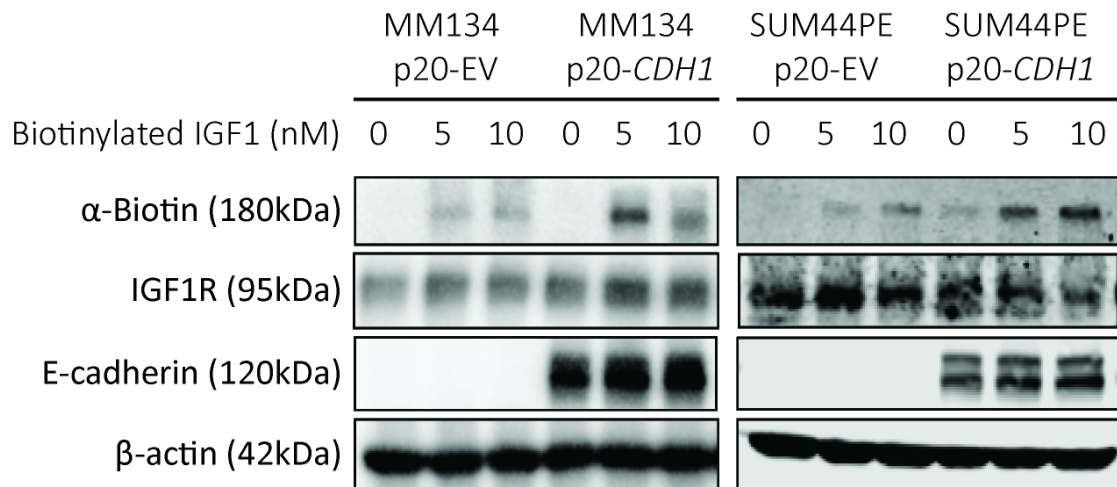


Figure 33: ILC *CDH1* OE cells demonstrate higher IGF1 receptor availability for ligand binding

MM134 and SUM44 p20-EV and p20-*CDH1* cells were stimulated with biotinylated IGF1 (0-10nM) for 15 minutes and crosslinked to assess ligand-receptor complex levels between WT and *CDH1* KO cells. α -biotin bands show the amount of IGF1 bound IGF1R expression levels in respective samples. Representative experiment shown, n=3 for each experiment.

Appendix C

Chapter 6 Supplementary Figures

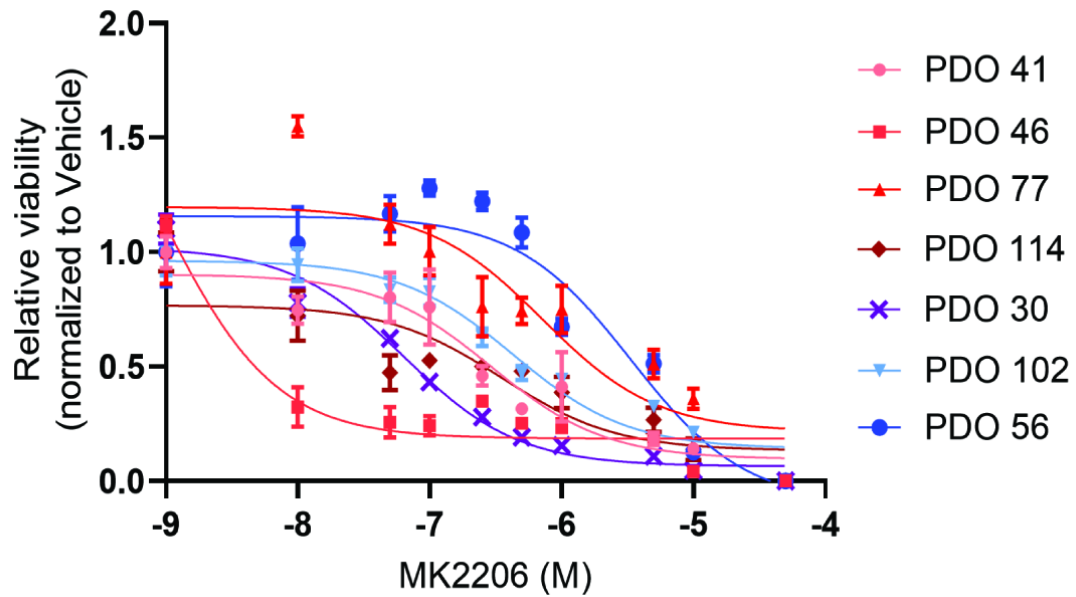


Figure 34: IDC and ILC breast PDOs exhibit variability in response to Akt inhibitor MK2206

Patient derived IDC and ILC organoids were treated with Akt inhibitor (MK2206) for 12 days and viability assessed with CellTiter Glo 3D (relative luminescence), and data was normalized to vehicle treated control. IC₅₀ values for viability were calculated by nonlinear regression and statistical differences evaluated using sum-of-squares Global f-test ($p < 0.05$; representative experiment shown; $n=3$ (each with six biological replicates)).

Appendix D

Table 1: Antibodies Used in IB, IF and IHC Experiments
 Compilation of all antibodies used in this thesis project.

Protein	Company	Catalog Number	Host Species	Dilution
β -Actin	Sigma	A5441	Mouse	1:10000
AKT	Cell Signaling	9272	Mouse	1:1000
pAKT ^{S473}	Cell Signaling	4060	Rabbit	1:1000
E-cadherin	BD Biosciences	610182	Mouse	1:1000
E-cadherin	Cell Signaling	3195	Rabbit	1:100
pIGF1R/ InsR	Cell Signaling	3024	Rabbit	1:500
pEGFR Tyr1068	Cell Signaling	2234	Rabbit	1:1000
IGFR	Cell Signaling	3027	Rabbit	1:1000
InsR	Cell Signaling	3025	Rabbit	1:1000
EGFR	Cell Signaling	4267	Rabbit	1:1000
IRS1	Cell Signaling	2390	Rabbit	1:1000
B-catenin	BD Biosciences	610154	Mouse	1:1000
p120	BD Biosciences	610134	Mouse	1:200
a-Biotin	Cell Signaling	5597S	Rabbit	1:1000
Non-phospho B-catenin (Ser45)	Cell Signaling	19807T	Rabbit	1:1000
pFGFR4 Y642	Signalway Antibody	11836	Rabbit	1:1000
FGFR4	Cell Signaling	8562	Rabbit	1:1000
pFRS2 Tyr196	Cell Signaling	3864	Rabbit	1:1000
pSTAT3 Tyr705	Cell Signaling	9131	Rabbit	1:1000
P-p44/42 MAPK	Cell Signaling	4377	Rabbit	1:1000
EpCAM	Cell Signaling	2929	Mouse	1:100
Anti-Mouse AlexaFluor488	Invitrogen	A11017	Mouse	1:200
Anti-Rabbit AlexaFluor488	Invitrogen	A21206	Rabbit	1:200
Anti-Rabbit AlexaFluor647	Invitrogen	A27040	Rabbit	1:200

Bibliography

- 1.Siegel RL, Miller KD, Fuchs HE, Jemal A. Cancer statistics, 2022. *CA: A Cancer Journal for Clinicians*. 2022;72(1):7-33.
- 2.Pfeiffer RM, Webb-Vargas Y, Wheeler W, Gail MH. Proportion of U.S. Trends in Breast Cancer Incidence Attributable to Long-term Changes in Risk Factor Distributions. *Cancer Epidemiology Biomarkers & Prevention*. 2018;27(10):1214-22.
- 3.Lebeau A. Precancerous Lesions of the Breast. *Breast Care*. 2010;5(4):204-6.
- 4.Van Seijen M, Lips EH, Thompson AM, Nik-Zainal S, Futreal A, Hwang ES, et al. Ductal carcinoma in situ: to treat or not to treat, that is the question. *British Journal of Cancer*. 2019;121(4):285-92.
- 5.Eroles P, Bosch A, Perez-Fidalgo JA, Lluch A. Molecular biology in breast cancer: intrinsic subtypes and signaling pathways. *Cancer Treat Rev*. 2012;38(6):698-707.
- 6.Johnson KS, Conant EF, Soo MS. Molecular Subtypes of Breast Cancer: A Review for Breast Radiologists. *Journal of Breast Imaging*. 2021;3(1):12-24.
- 7.Perou CM, Sorlie T, Eisen MB, van de Rijn M, Jeffrey SS, Rees CA, et al. Molecular portraits of human breast tumours. *Nature*. 2000;406(6797):747-52.
- 8.Sorlie T. Molecular portraits of breast cancer: tumour subtypes as distinct disease entities. *Eur J Cancer*. 2004;40(18):2667-75.
- 9.Sorlie T, Tibshirani R, Parker J, Hastie T, Marron JS, Nobel A, et al. Repeated observation of breast tumor subtypes in independent gene expression data sets. *Proc Natl Acad Sci U S A*. 2003;100(14):8418-23.
- 10.van 't Veer LJ, Dai H, van de Vijver MJ, He YD, Hart AA, Mao M, et al. Gene expression profiling predicts clinical outcome of breast cancer. *Nature*. 2002;415(6871):530-6.
- 11.Prat A, Pineda E, Adamo B, Galvan P, Fernandez A, Gaba L, et al. Clinical implications of the intrinsic molecular subtypes of breast cancer. *Breast*. 2015;24 Suppl 2:S26-35.
- 12.Tang P, Tse GM. Immunohistochemical Surrogates for Molecular Classification of Breast Carcinoma: A 2015 Update. *Arch Pathol Lab Med*. 2016;140(8):806-14.

13. Vuong D, Simpson PT, Green B, Cummings MC, Lakhani SR. Molecular classification of breast cancer. *Virchows Arch.* 2014;465(1):1-14.
14. Loi S. Molecular analysis of hormone receptor positive (luminal) breast cancers: what have we learnt? *Eur J Cancer.* 2008;44(18):2813-8.
15. Goldhirsch A, Wood WC, Coates AS, Gelber RD, Thurlimann B, Senn HJ, et al. Strategies for subtypes--dealing with the diversity of breast cancer: highlights of the St. Gallen International Expert Consensus on the Primary Therapy of Early Breast Cancer 2011. *Ann Oncol.* 2011;22(8):1736-47.
16. Fan W, Chang J, Fu P. Endocrine therapy resistance in breast cancer: current status, possible mechanisms and overcoming strategies. *Future Medicinal Chemistry.* 2015;7(12):1511-9.
17. Kennecke H, Yerushalmi R, Woods R, Cheang MC, Voduc D, Speers CH, et al. Metastatic behavior of breast cancer subtypes. *J Clin Oncol.* 2010;28(20):3271-7.
18. Wu Q, Li J, Zhu S, Wu J, Chen C, Liu Q, et al. Breast cancer subtypes predict the preferential site of distant metastases: a SEER based study. *Oncotarget.* 2017;8(17):27990-6.
19. Sorlie T, Perou CM, Tibshirani R, Aas T, Geisler S, Johnsen H, et al. Gene expression patterns of breast carcinomas distinguish tumor subclasses with clinical implications. *Proc Natl Acad Sci U S A.* 2001;98(19):10869-74.
20. Slamon DJ, Leyland-Jones B, Shak S, Fuchs H, Paton V, Bajamonde A, et al. Use of Chemotherapy plus a Monoclonal Antibody against HER2 for Metastatic Breast Cancer That Overexpresses HER2. *New England Journal of Medicine.* 2001;344(11):783-92.
21. Swain SM, Kim SB, Cortes J, Ro J, Semiglazov V, Campone M, et al. Pertuzumab, trastuzumab, and docetaxel for HER2-positive metastatic breast cancer (CLEOPATRA study): overall survival results from a randomised, double-blind, placebo-controlled, phase 3 study. *Lancet Oncol.* 2013;14(6):461-71.
22. Geyer CE, Forster J, Lindquist D, Chan S, Romieu CG, Pienkowski T, et al. Lapatinib plus capecitabine for HER2-positive advanced breast cancer. *N Engl J Med.* 2006;355(26):2733-43.
23. Verma S, Miles D, Gianni L, Krop IE, Welslau M, Baselga J, et al. Trastuzumab Emtansine for HER2-Positive Advanced Breast Cancer. *New England Journal of Medicine.* 2012;367(19):1783-91.
24. Wang Y, Ikeda DM, Narasimhan B, Longacre TA, Bleicher RJ, Pal S, et al. Estrogen Receptor–Negative Invasive Breast Cancer: Imaging Features of Tumors with and without Human Epidermal Growth Factor Receptor Type 2 Overexpression. *Radiology.* 2008;246(2):367-75.

25. Hammond MEH, Hayes DF, Dowsett M, Allred DC, Hagerty KL, Badve S, et al. American Society of Clinical Oncology/College of American Pathologists Guideline Recommendations for Immunohistochemical Testing of Estrogen and Progesterone Receptors in Breast Cancer (Unabridged Version). *Archives of Pathology & Laboratory Medicine*. 2010;134(7):e48-e72.
26. Wolff AC, Hammond ME, Hicks DG, Dowsett M, McShane LM, Allison KH, et al. Recommendations for human epidermal growth factor receptor 2 testing in breast cancer: American Society of Clinical Oncology/College of American Pathologists clinical practice guideline update. *J Clin Oncol*. 2013;31(31):3997-4013.
27. Wolff AC, Hammond MEH, Allison KH, Harvey BE, Mangu PB, Bartlett JMS, et al. Human Epidermal Growth Factor Receptor 2 Testing in Breast Cancer: American Society of Clinical Oncology/College of American Pathologists Clinical Practice Guideline Focused Update. *J Clin Oncol*. 2018;36(20):2105-22.
28. Carey LA, Dees EC, Sawyer L, Gatti L, Moore DT, Collichio F, et al. The Triple Negative Paradox: Primary Tumor Chemosensitivity of Breast Cancer Subtypes. *Clinical Cancer Research*. 2007;13(8):2329-34.
29. Li CI, Anderson BO, Daling JR, Moe RE. Trends in incidence rates of invasive lobular and ductal breast carcinoma. *JAMA*. 2003;289(11):1421-4.
30. Rakha EA, Ellis IO. Lobular breast carcinoma and its variants. *Semin Diagn Pathol*. 2010;27(1):49-61.
31. Ciriello G, Gatza ML, Beck AH, Wilkerson MD, Rhee SK, Pastore A, et al. Comprehensive Molecular Portraits of Invasive Lobular Breast Cancer. *Cell*. 2015;163(2):506-19.
32. Barroso-Sousa R, Metzger-Filho O. Differences between invasive lobular and invasive ductal carcinoma of the breast: results and therapeutic implications. *Therapeutic Advances in Medical Oncology*. 2016;8(4):261-6.
33. Antonella Ferro CE, Alessia Caldara, Renza Triolo, Mattia Barbareschi, Lucia Veronica Cuorvo, MariaChiara DiPasquale, Nicola L Decarli, Salvatore Mussari, and Enzo Galligioni, editor Invasive lobular (ILC) versus invasive ductal (IDC) breast cancer (BC): Clinical-pathologic features and clinical outcomes in monoinstitutional series. 2012 ASCO Annual Meeting I; 2012: *Journal of Clinical Oncology*.
34. Du T, Zhu L, Levine KM, Tasdemir N, Lee AV, Vignali DAA, et al. Invasive lobular and ductal breast carcinoma differ in immune response, protein translation efficiency and metabolism. *Sci Rep*. 2018;8(1):7205.

35. Chen Z, Yang J, Li S, Lv M, Shen Y, Wang B, et al. Invasive lobular carcinoma of the breast: A special histological type compared with invasive ductal carcinoma. *PLoS One*. 2017;12(9):e0182397.
36. Vos CB, Cleton-Jansen AM, Berx G, de Leeuw WJ, ter Haar NT, van Roy F, et al. E-cadherin inactivation in lobular carcinoma in situ of the breast: an early event in tumorigenesis. *Br J Cancer*. 1997;76(9):1131-3.
37. Yoshiura K, Kanai Y, Ochiai A, Shimoyama Y, Sugimura T, Hirohashi S. Silencing of the E-cadherin invasion-suppressor gene by CpG methylation in human carcinomas. *Proc Natl Acad Sci U S A*. 1995;92(16):7416-9.
38. J R Graff 1 JGH, R G Lapidus, H Chopra, R Xu, D F Jarrard, W B Isaacs, P M Pitha, N E Davidson, S B Baylin. E-cadherin expression is silenced by DNA hypermethylation in human breast and prostate carcinomas. *Cancer Research*. 1995.
39. Reed AEM, Kutasovic JR, Lakhani SR, Simpson PT. Invasive lobular carcinoma of the breast: morphology, biomarkers and 'omics. *Breast Cancer Research*. 2015;17(1):12.
40. Michael Grimm BR, Maryam B. Lustberg, Robert Wesolowski, Sagar D. Sardesai, Jeffrey Bryan VanDeusen, Mathew Amprayil Cherian, Daniel G. Stover, Margaret Elena Gatti-Mays, Ashley Pariser, Mahmoud Kassem, Julie Stephens, Marilly Palettas, Nicole Olivia Williams, editor Survival outcomes in patients with IDC and ILC breast cancer: A well matched single institution study. *Journal of Clinical Oncology* 2021.
41. Iorfida M, Maiorano E, Orvieto E, Maisonneuve P, Bottiglieri L, Rotmensz N, et al. Invasive lobular breast cancer: subtypes and outcome. *Breast Cancer Res Treat*. 2012;133(2):713-23.
42. Adachi Y, Ishiguro J, Kotani H, Hisada T, Ichikawa M, Gondo N, et al. Comparison of clinical outcomes between luminal invasive ductal carcinoma and luminal invasive lobular carcinoma. *BMC Cancer*. 2016;16(1).
43. Rakha EA, El-Sayed ME, Powe DG, Green AR, Habashy H, Grainge MJ, et al. Invasive lobular carcinoma of the breast: response to hormonal therapy and outcomes. *Eur J Cancer*. 2008;44(1):73-83.
44. Mathew A, Rajagopal PS, Villgran V, Sandhu GS, Jankowitz RC, Jacob M, et al. Distinct Pattern of Metastases in Patients with Invasive Lobular Carcinoma of the Breast. *Geburtshilfe Frauenheilkd*. 2017;77(6):660-6.
45. Desmedt C, Zoppoli G, Gundem G, Pruneri G, Larsimont D, Fornili M, et al. Genomic Characterization of Primary Invasive Lobular Breast Cancer. *J Clin Oncol*. 2016;34(16):1872-81.

46. Comprehensive molecular portraits of human breast tumours. *Nature*. 2012;490(7418):61-70.
47. Lien H-C, Chen Y-L, Juang Y-L, Jeng Y-M. Frequent alterations of HER2 through mutation, amplification, or overexpression in pleomorphic lobular carcinoma of the breast. *Breast Cancer Research and Treatment*. 2015;150(2):447-55.
48. McCart Reed AE, Kalinowski L, Simpson PT, Lakhani SR. Invasive lobular carcinoma of the breast: the increasing importance of this special subtype. *Breast Cancer Research*. 2021;23(1).
49. Metzger Filho O, Giobbie-Hurder A, Mallon E, Gusterson B, Viale G, Winer EP, et al. Relative Effectiveness of Letrozole Compared With Tamoxifen for Patients With Lobular Carcinoma in the BIG 1-98 Trial. *J Clin Oncol*. 2015;33(25):2772-9.
50. Sikora MJ, Cooper KL, Bahreini A, Luthra S, Wang G, Chandran UR, et al. Invasive lobular carcinoma cell lines are characterized by unique estrogen-mediated gene expression patterns and altered tamoxifen response. *Cancer Res*. 2014;74(5):1463-74.
51. Hakuno F, Takahashi S-I. 40 YEARS OF IGF1: IGF1 receptor signaling pathways. *Journal of Molecular Endocrinology*. 2018;61(1):T69-T86.
52. Kavran JM, McCabe JM, Byrne PO, Connacher MK, Wang Z, Ramek A, et al. How IGF-1 activates its receptor. *Elife*. 2014;3.
53. Boone DN, Lee AV. Targeting the Insulin-like Growth Factor Receptor: Developing Biomarkers from Gene Expression Profiling. *Critical Reviews™ in Oncogenesis*. 2012;17(2):161-73.
54. Pollak MN, Schernhammer ES, Hankinson SE. Insulin-like growth factors and neoplasia. *Nat Rev Cancer*. 2004;4(7):505-18.
55. Allard JB, Duan C. IGF-Binding Proteins: Why Do They Exist and Why Are There So Many? *Front Endocrinol (Lausanne)*. 2018;9:117.
56. Jones JI, Clemmons DR. Insulin-like growth factors and their binding proteins: biological actions. *Endocr Rev*. 1995;16(1):3-34.
57. Bergman D, Halje M, Nordin M, Engström W. Insulin-Like Growth Factor 2 in Development and Disease: A Mini-Review. *Gerontology*. 2013;59(3):240-9.
58. Brown J, Jones EY, Forbes BE. Interactions of IGF-II with the IGF2R/cation-independent mannose-6-phosphate receptor mechanism and biological outcomes. *Vitam Horm*. 2009;80:699-719.

- 59.Hassan AB. Keys to the hidden treasures of the mannose 6-phosphate/insulin-like growth factor 2 receptor. *Am J Pathol.* 2003;162(1):3-6.
- 60.Belfiore A, Malaguarnera R, Vella V, Lawrence MC, Sciacca L, Frasca F, et al. Insulin Receptor Isoforms in Physiology and Disease: An Updated View. *Endocrine Reviews.* 2017;38(5):379-431.
- 61.Kleinberg DL, Wood TL, Furth PA, Lee AV. Growth hormone and insulin-like growth factor-I in the transition from normal mammary development to preneoplastic mammary lesions. *Endocr Rev.* 2009;30(1):51-74.
- 62.Froesch ER, Schmid C, Schwander J, Zapf J. Actions of insulin-like growth factors. *Annu Rev Physiol.* 1985;47:443-67.
- 63.LeRoith D. Clinical relevance of systemic and local IGF-I: lessons from animal models. *Pediatr Endocrinol Rev.* 2008;5 Suppl 2:739-43.
- 64.Yakar S, Pennisi P, Wu Y, Zhao H, LeRoith D. Clinical relevance of systemic and local IGF-I. *Endocr Dev.* 2005;9:11-6.
- 65.Roberts CT, Owens JA, Sferruzzi-Perri AN. Distinct actions of insulin-like growth factors (IGFs) on placental development and fetal growth: lessons from mice and guinea pigs. *Placenta.* 2008;29 Suppl A:S42-7.
- 66.Rowzee AM, Lazzarino DA, Rota L, Sun Z, Wood TL. IGF Ligand and Receptor Regulation of Mammary Development. *Journal of Mammary Gland Biology and Neoplasia.* 2008;13(4):361-70.
- 67.Tatar M, Bartke A, Antebi A. The endocrine regulation of aging by insulin-like signals. *Science.* 2003;299(5611):1346-51.
- 68.Thissen JP, Ketelslegers JM, Underwood LE. Nutritional regulation of the insulin-like growth factors. *Endocr Rev.* 1994;15(1):80-101.
- 69.Butler AA, LeRoith D. Minireview: tissue-specific versus generalized gene targeting of the *igf1* and *igf1r* genes and their roles in insulin-like growth factor physiology. *Endocrinology.* 2001;142(5):1685-8.
- 70.Liu JL, Yakar S, LeRoith D. Conditional knockout of mouse insulin-like growth factor-1 gene using the Cre/loxP system. *Proc Soc Exp Biol Med.* 2000;223(4):344-51.

71. Richards RG, Klotz DM, Walker MP, Diaugustine RP. Mammary gland branching morphogenesis is diminished in mice with a deficiency of insulin-like growth factor-I (IGF-I), but not in mice with a liver-specific deletion of IGF-I. *Endocrinology*. 2004;145(7):3106-10.
72. Liu JP, Baker J, Perkins AS, Robertson EJ, Efstratiadis A. Mice carrying null mutations of the genes encoding insulin-like growth factor I (Igf-1) and type 1 IGF receptor (Igf1r). *Cell*. 1993;75(1):59-72.
73. Marshman E, Streuli CH. Insulin-like growth factors and insulin-like growth factor binding proteins in mammary gland function. *Breast Cancer Research*. 2002;4(6).
74. Bonnette SG, Hadsell DL. Targeted disruption of the IGF-I receptor gene decreases cellular proliferation in mammary terminal end buds. *Endocrinology*. 2001;142(11):4937-45.
75. Carboni JM, Lee AV, Hadsell DL, Rowley BR, Lee FY, Bol DK, et al. Tumor development by transgenic expression of a constitutively active insulin-like growth factor I receptor. *Cancer Res*. 2005;65(9):3781-7.
76. Jones RA, Campbell CI, Gunther EJ, Chodosh LA, Petrik JJ, Khokha R, et al. Transgenic overexpression of IGF-IR disrupts mammary ductal morphogenesis and induces tumor formation. *Oncogene*. 2007;26(11):1636-44.
77. Cannata D, Lann D, Wu Y, Elis S, Sun H, Yakar S, et al. Elevated Circulating IGF-I Promotes Mammary Gland Development and Proliferation. *Endocrinology*. 2010;151(12):5751-61.
78. Peyrat JP, Bonnetterre J, Hecquet B, Vennin P, Louchez MM, Fournier C, et al. Plasma insulin-like growth factor-1 (IGF-1) concentrations in human breast cancer. *Eur J Cancer*. 1993;29A(4):492-7.
79. Endogenous H, Breast Cancer Collaborative G, Key TJ, Appleby PN, Reeves GK, Roddam AW. Insulin-like growth factor 1 (IGF1), IGF binding protein 3 (IGFBP3), and breast cancer risk: pooled individual data analysis of 17 prospective studies. *Lancet Oncol*. 2010;11(6):530-42.
80. Kaaks R, Johnson T, Tikk K, Sookthai D, Tjonneland A, Roswall N, et al. Insulin-like growth factor I and risk of breast cancer by age and hormone receptor status-A prospective study within the EPIC cohort. *Int J Cancer*. 2014;134(11):2683-90.
81. Pasanisi P, Bruno E, Venturelli E, Manoukian S, Barile M, Peissel B, et al. Serum levels of IGF-I and BRCA penetrance: a case control study in breast cancer families. *Fam Cancer*. 2011;10(3):521-8.

- 82.Hartog H, Boezen HM, de Jong MM, Schaapveld M, Wesseling J, van der Graaf WT. Prognostic value of insulin-like growth factor 1 and insulin-like growth factor binding protein 3 blood levels in breast cancer. *Breast*. 2013;22(6):1155-60.
- 83.Duggan C, Wang CY, Neuhouser ML, Xiao L, Smith AW, Reding KW, et al. Associations of insulin-like growth factor and insulin-like growth factor binding protein-3 with mortality in women with breast cancer. *Int J Cancer*. 2013;132(5):1191-200.
- 84.Davison Z, de Blacquiére GE, Westley BR, May FE. Insulin-like growth factor-dependent proliferation and survival of triple-negative breast cancer cells: implications for therapy. *Neoplasia*. 2011;13(6):504-15.
- 85.D'Esposito V, Passaretti F, Hammarstedt A, Liguoro D, Terracciano D, Molea G, et al. Adipocyte-released insulin-like growth factor-1 is regulated by glucose and fatty acids and controls breast cancer cell growth in vitro. *Diabetologia*. 2012;55(10):2811-22.
- 86.Pacher M, Seewald MJ, Mikula M, Oehler S, Mogg M, Vinatzer U, et al. Impact of constitutive IGF1/IGF2 stimulation on the transcriptional program of human breast cancer cells. *Carcinogenesis*. 2007;28(1):49-59.
- 87.Dogan S, Johannsen AC, Grande JP, Cleary MP. Effects of intermittent and chronic calorie restriction on mammalian target of rapamycin (mTOR) and IGF-I signaling pathways in mammary fat pad tissues and mammary tumors. *Nutr Cancer*. 2011;63(3):389-401.
- 88.Christopoulos PF, Msaouel P, Koutsilieris M. The role of the insulin-like growth factor-1 system in breast cancer. *Molecular Cancer*. 2015;14(1):43.
- 89.Ford NA, Nunez NP, Holcomb VB, Hursting SD. IGF1 dependence of dietary energy balance effects on murine Met1 mammary tumor progression, epithelial-to-mesenchymal transition, and chemokine expression. *Endocr Relat Cancer*. 2013;20(1):39-51.
- 90.Pomatto-Watson LCD, Bodogai M, Bosomptra O, Kato J, Wong S, Carpenter M, et al. Daily caloric restriction limits tumor growth more effectively than caloric cycling regardless of dietary composition. *Nature Communications*. 2021;12(1).
- 91.Lope V, Martín M, Castelló A, Ruiz A, Casas AM, Baena-Cañada JM, et al. Overeating, caloric restriction and breast cancer risk by pathologic subtype: the EPIGEICAM study. *Scientific Reports*. 2019;9(1).
- 92.Guntur AR, Rosen CJ. IGF-1 regulation of key signaling pathways in bone. *BoneKEY Reports*. 2013;2.

93. Rieunier G, Wu X, Macaulay VM, Lee AV, Weyer-Czernilofsky U, Bogenrieder T. Bad to the Bone: The Role of the Insulin-Like Growth Factor Axis in Osseous Metastasis. *Clin Cancer Res.* 2019;25(12):3479-85.
94. Hiraga T, Myoui A, Hashimoto N, Sasaki A, Hata K, Morita Y, et al. Bone-derived IGF mediates crosstalk between bone and breast cancer cells in bony metastases. *Cancer Res.* 2012;72(16):4238-49.
95. Gee JM, Robertson JF, Gutteridge E, Ellis IO, Pinder SE, Rubini M, et al. Epidermal growth factor receptor/HER2/insulin-like growth factor receptor signalling and oestrogen receptor activity in clinical breast cancer. *Endocr Relat Cancer.* 2005;12 Suppl 1:S99-S111.
96. Karey KP, Sirbasku DA. Differential responsiveness of human breast cancer cell lines MCF-7 and T47D to growth factors and 17 beta-estradiol. *Cancer Res.* 1988;48(14):4083-92.
97. Lu Y, Zi X, Zhao Y, Mascarenhas D, Pollak M. Insulin-like growth factor-I receptor signaling and resistance to trastuzumab (Herceptin). *J Natl Cancer Inst.* 2001;93(24):1852-7.
98. Worthington J, Bertani M, Chan HL, Gerrits B, Timms JF. Transcriptional profiling of ErbB signalling in mammary luminal epithelial cells--interplay of ErbB and IGF1 signalling through IGFBP3 regulation. *BMC Cancer.* 2010;10:490.
99. Dearth RK, Kuitse I, Wang YF, Liao L, Hilsenbeck SG, Brown PH, et al. A moderate elevation of circulating levels of IGF-I does not alter ErbB2 induced mammary tumorigenesis. *BMC Cancer.* 2011;11:377.
100. Gualberto A, Pollak M. Emerging role of insulin-like growth factor receptor inhibitors in oncology: early clinical trial results and future directions. *Oncogene.* 2009;28(34):3009-21.
101. Burtrum D, Zhu Z, Lu D, Anderson DM, Prewett M, Pereira DS, et al. A fully human monoclonal antibody to the insulin-like growth factor I receptor blocks ligand-dependent signaling and inhibits human tumor growth in vivo. *Cancer Res.* 2003;63(24):8912-21.
102. Maloney EK, McLaughlin JL, Dagdigian NE, Garrett LM, Connors KM, Zhou XM, et al. An anti-insulin-like growth factor I receptor antibody that is a potent inhibitor of cancer cell proliferation. *Cancer Res.* 2003;63(16):5073-83.
103. Ianza A, Sirico M, Bernocchi O, Generali D. Role of the IGF-1 Axis in Overcoming Resistance in Breast Cancer. *Front Cell Dev Biol.* 2021;9:641449.
104. Ekyalongo RC, Yee D. Revisiting the IGF-1R as a breast cancer target. *npj Precision Oncology.* 2017;1(1).

- 105.Simpson A, Petnga W, Macaulay VM, Weyer-Czernilofsky U, Bogenrieder T. Insulin-Like Growth Factor (IGF) Pathway Targeting in Cancer: Role of the IGF Axis and Opportunities for Future Combination Studies. *Targeted Oncology*. 2017;12(5):571-97.
- 106.Gualberto A, Pollak M. Clinical development of inhibitors of the insulin-like growth factor receptor in oncology. *Curr Drug Targets*. 2009;10(10):923-36.
- 107.Gualberto A. Figitumumab (CP-751,871) for cancer therapy. *Expert Opin Biol Ther*. 2010;10(4):575-85.
- 108.Wang Y, Hailey J, Williams D, Wang Y, Lipari P, Malkowski M, et al. Inhibition of insulin-like growth factor-I receptor (IGF-IR) signaling and tumor cell growth by a fully human neutralizing anti-IGF-IR antibody. *Mol Cancer Ther*. 2005;4(8):1214-21.
- 109.Gao J, Chesebrough JW, Carlidge SA, Ricketts SA, Incognito L, Veldman-Jones M, et al. Dual IGF-I/II-neutralizing antibody MEDI-573 potently inhibits IGF signaling and tumor growth. *Cancer Res*. 2011;71(3):1029-40.
- 110.Friedbichler K, Hofmann MH, Kroeze M, Ostermann E, Lamche HR, Koessl C, et al. Pharmacodynamic and antineoplastic activity of BI 836845, a fully human IGF ligand-neutralizing antibody, and mechanistic rationale for combination with rapamycin. *Mol Cancer Ther*. 2014;13(2):399-409.
- 111.De Bono J, Lin C-C, Chen L-T, Corral J, Michalarea V, Rihawi K, et al. Two first-in-human studies of xentuzumab, a humanised insulin-like growth factor (IGF)-neutralising antibody, in patients with advanced solid tumours. *British Journal of Cancer*. 2020;122(9):1324-32.
- 112.Weyer-Czernilofsky U, Hofmann MH, Friedbichler K, Baumgartinger R, Adam PJ, Solca F, et al. Antitumor Activity of the IGF-1/IGF-2–Neutralizing Antibody Xentuzumab (BI 836845) in Combination with Enzalutamide in Prostate Cancer Models. *Molecular Cancer Therapeutics*. 2020;19(4):1059-69.
- 113.Schmid P, Sablin M-P, Bergh J, Im S-A, Lu Y-S, Martínez N, et al. A phase Ib/II study of xentuzumab, an IGF-neutralising antibody, combined with exemestane and everolimus in hormone receptor-positive, HER2-negative locally advanced/metastatic breast cancer. *Breast Cancer Research*. 2021;23(1).
- 114.Serra V, Markman B, Scaltriti M, Eichhorn PJ, Valero V, Guzman M, et al. NVP-BEZ235, a dual PI3K/mTOR inhibitor, prevents PI3K signaling and inhibits the growth of cancer cells with activating PI3K mutations. *Cancer Res*. 2008;68(19):8022-30.
- 115.Carboni JM, Wittman M, Yang Z, Lee F, Greer A, Hurlburt W, et al. BMS-754807, a small molecule inhibitor of insulin-like growth factor-1R/IR. *Mol Cancer Ther*. 2009;8(12):3341-9.

116. Haluska P, Carboni JM, Loegering DA, Lee FY, Wittman M, Saulnier MG, et al. In vitro and in vivo antitumor effects of the dual insulin-like growth factor-I/insulin receptor inhibitor, BMS-554417. *Cancer Res.* 2006;66(1):362-71.
117. Yee D, Lee AV. *Journal of Mammary Gland Biology and Neoplasia.* 2000;5(1):107-15.
118. Kaufman PA FJ, Bourgeois H, Kennecke H, De Boer R, Jacot W, et al, editor A Randomized, Double-Blind, Placebo-Controlled, Phase 2 Study of
AMG 479 With Exemestane (E) or Fulvestrant (F) in Postmenopausal Women
With Hormone-Receptor Positive (HR+) Metastatic (M) or Locally Advanced Breast Cancer 2010.
119. Cao L, Yu Y, Darko I, Currier D, Mayeenuddin LH, Wan X, et al. Addition to elevated insulin-like growth factor I receptor and initial modulation of the AKT pathway define the responsiveness of rhabdomyosarcoma to the targeting antibody. *Cancer Res.* 2008;68(19):8039-48.
120. Fox EM, Kuba MG, Miller TW, Davies BR, Arteaga CL. Autocrine IGF-I/insulin receptor axis compensates for inhibition of AKT in ER-positive breast cancer cells with resistance to estrogen deprivation. *Breast Cancer Res.* 2013;15(4):R55.
121. Clark AS, West K, Streicher S, Dennis PA. Constitutive and inducible Akt activity promotes resistance to chemotherapy, trastuzumab, or tamoxifen in breast cancer cells. *Mol Cancer Ther.* 2002;1(9):707-17.
122. Becker MA, Ibrahim YH, Cui X, Lee AV, Yee D. The IGF Pathway Regulates ER α through a S6K1-Dependent Mechanism in Breast Cancer Cells. *Molecular Endocrinology.* 2011;25(3):516-28.
123. Brachmann SM, Hofmann I, Schnell C, Fritsch C, Wee S, Lane H, et al. Specific apoptosis induction by the dual PI3K/mTor inhibitor NVP-BEZ235 in HER2 amplified and PIK3CA mutant breast cancer cells. *Proc Natl Acad Sci U S A.* 2009;106(52):22299-304.
124. Casa AJ, Potter AS, Malik S, Lazard Z, Kuitse I, Kim HT, et al. Estrogen and insulin-like growth factor-I (IGF-I) independently down-regulate critical repressors of breast cancer growth. *Breast Cancer Res Treat.* 2012;132(1):61-73.
125. Xing Y, Lin NU, Maurer MA, Chen H, Mahvash A, Sahin A, et al. Phase II trial of AKT inhibitor MK-2206 in patients with advanced breast cancer who have tumors with PIK3CA or AKT mutations, and/or PTEN loss/PTEN mutation. *Breast Cancer Research.* 2019;21(1).

- 126.Hirai H, Sootome H, Nakatsuru Y, Miyama K, Taguchi S, Tsujioka K, et al. MK-2206, an Allosteric Akt Inhibitor, Enhances Antitumor Efficacy by Standard Chemotherapeutic Agents or Molecular Targeted Drugs In vitro and In vivo. *Molecular Cancer Therapeutics*. 2010;9(7):1956-67.
- 127.Davies BR, Greenwood H, Dudley P, Crafter C, Yu D-H, Zhang J, et al. Preclinical Pharmacology of AZD5363, an Inhibitor of AKT: Pharmacodynamics, Antitumor Activity, and Correlation of Monotherapy Activity with Genetic Background. *Molecular Cancer Therapeutics*. 2012;11(4):873-87.
- 128.Erdem C, Nagle AM, Casa AJ, Litzenburger BC, Wang YF, Taylor DL, et al. Proteomic Screening and Lasso Regression Reveal Differential Signaling in Insulin and Insulin-like Growth Factor I (IGF1) Pathways. *Mol Cell Proteomics*. 2016;15(9):3045-57.
- 129.Nagle AM, Levine KM, Tasdemir N, Scott JA, Burlbaugh K, Kehm J, et al. Loss of E-cadherin Enhances IGF1–IGF1R Pathway Activation and Sensitizes Breast Cancers to Anti-IGF1R/InsR Inhibitors. *Clinical Cancer Research*. 2018;24(20):5165-77.
- 130.Teo K, Gomez-Cuadrado L, Tenhagen M, Byron A, Ratze M, van Amersfoort M, et al. E-cadherin loss induces targetable autocrine activation of growth factor signalling in lobular breast cancer. *Sci Rep*. 2018;8(1):15454.
- 131.Litzenburger BC, Creighton CJ, Tsimelzon A, Chan BT, Hilsenbeck SG, Wang T, et al. High IGF-IR Activity in Triple-Negative Breast Cancer Cell Lines and Tumorgrafts Correlates with Sensitivity to Anti-IGF-IR Therapy. *Clinical Cancer Research*. 2011;17(8):2314-27.
- 132.Bajrami I, Marlow R, Van De Ven M, Brough R, Pemberton HN, Frankum J, et al. E-Cadherin/ROS1 Inhibitor Synthetic Lethality in Breast Cancer. *Cancer Discovery*. 2018;8(4):498-515.
- 133.Godwin TD, Kelly ST, Brew TP, Bougen-Zhukov NM, Single AB, Chen A, et al. E-cadherin-deficient cells have synthetic lethal vulnerabilities in plasma membrane organisation, dynamics and function. *Gastric Cancer*. 2019;22(2):273-86.
- 134.Beetham H, Chen A, Telford BJ, Single A, Jarman KE, Lackovic K, et al. A high-throughput screen to identify novel synthetic lethal compounds for the treatment of E-cadherin-deficient cells. *Scientific Reports*. 2019;9(1).
- 135.van Roy F, Berx G. The cell-cell adhesion molecule E-cadherin. *Cell Mol Life Sci*. 2008;65(23):3756-88.

- 136.Rajeev Singhai VWP, Sanjog R Jaiswal, Shital D Patil, Mukund B Tayade, Amit V Patil. E-Cadherin as a diagnostic biomarker in breast cancer. *North American Journal of Medical Sciences* 2011.
- 137.Petrova YI, Schecterson L, Gumbiner BM. Roles for E-cadherin cell surface regulation in cancer. *Molecular Biology of the Cell*. 2016;27(21):3233-44.
- 138.Berx G, Roy FV. The E-cadherin/catenin complex: an important gatekeeper in breast cancer tumorigenesis and malignant progression. *Breast Cancer Research*. 2001;3(5).
- 139.Keller G, Vogelsang H, Becker I, Hutter J, Ott K, Candidus S, et al. Diffuse type gastric and lobular breast carcinoma in a familial gastric cancer patient with an E-cadherin germline mutation. *Am J Pathol*. 1999;155(2):337-42.
- 140.Jeanes A, Gottardi CJ, Yap AS. Cadherins and cancer: how does cadherin dysfunction promote tumor progression? *Oncogene*. 2008;27(55):6920-9.
- 141.Frixen UH, Behrens J, Sachs M, Eberle G, Voss B, Warda A, et al. E-cadherin-mediated cell-cell adhesion prevents invasiveness of human carcinoma cells. *J Cell Biol*. 1991;113(1):173-85.
- 142.Meiners S, Brinkmann V, Naundorf H, Birchmeier W. Role of morphogenetic factors in metastasis of mammary carcinoma cells. *Oncogene*. 1998;16(1):9-20.
- 143.Perl AK, Wilgenbus P, Dahl U, Semb H, Christofori G. A causal role for E-cadherin in the transition from adenoma to carcinoma. *Nature*. 1998;392(6672):190-3.
- 144.Vleminckx K, Vakaet L, Jr., Mareel M, Fiers W, van Roy F. Genetic manipulation of E-cadherin expression by epithelial tumor cells reveals an invasion suppressor role. *Cell*. 1991;66(1):107-19.
- 145.Heimann R, Lan F, McBride R, Hellman S. Separating favorable from unfavorable prognostic markers in breast cancer: the role of E-cadherin. *Cancer Res*. 2000;60(2):298-304.
- 146.Hunt NC, Douglas-Jones AG, Jasani B, Morgan JM, Pignatelli M. Loss of E-cadherin expression associated with lymph node metastases in small breast carcinomas. *Virchows Arch*. 1997;430(4):285-9.
- 147.Oka H, Shiozaki H, Kobayashi K, Inoue M, Tahara H, Kobayashi T, et al. Expression of E-cadherin cell adhesion molecules in human breast cancer tissues and its relationship to metastasis. *Cancer Res*. 1993;53(7):1696-701.

148. Siitonen SM, Kononen JT, Helin HJ, Rantala IS, Holli KA, Isola JJ. Reduced E-Cadherin Expression is Associated With Invasiveness and Unfavorable Prognosis in Breast Cancer. *American Journal of Clinical Pathology*. 1996;105(4):394-402.
149. St. Croix B, Sheehan C, Rak JW, Flørenes VA, Slingerland JM, Kerbel RS. E-Cadherin-dependent Growth Suppression is Mediated by the Cyclin-dependent Kinase Inhibitor p27KIP1. *Journal of Cell Biology*. 1998;142(2):557-71.
150. Padmanaban V, Krol I, Suhail Y, Szczerba BM, Aceto N, Bader JS, et al. E-cadherin is required for metastasis in multiple models of breast cancer. *Nature*. 2019;573(7774):439-44.
151. Na T-Y, Schecterson L, Mendonsa AM, Gumbiner BM. The functional activity of E-cadherin controls tumor cell metastasis at multiple steps. *Proceedings of the National Academy of Sciences*. 2020;117(11):5931-7.
152. Onder TT, Gupta PB, Mani SA, Yang J, Lander ES, Weinberg RA. Loss of E-Cadherin Promotes Metastasis via Multiple Downstream Transcriptional Pathways. *Cancer Research*. 2008;68(10):3645-54.
153. De Leeuw WJ, Berx G, Vos CB, Peterse JL, Van de Vijver MJ, Litvinov S, et al. Simultaneous loss of E-cadherin and catenins in invasive lobular breast cancer and lobular carcinoma in situ. *J Pathol*. 1997;183(4):404-11.
154. Tasdemir N, Bossart EA, Li Z, Zhu L, Sikora MJ, Levine KM, et al. Comprehensive Phenotypic Characterization of Human Invasive Lobular Carcinoma Cell Lines in 2D and 3D Cultures. *Cancer Res*. 2018;78(21):6209-22.
155. Schutte MvdWNBICHMvdHNJDAHJGMKHC. Mutant E-cadherin Breast Cancer Cells Do Not Display Constitutive Wnt Signaling. *Cancer Research*. 2001.
156. Sikora MJ, Jacobsen BM, Levine K, Chen J, Davidson NE, Lee AV, et al. WNT4 mediates estrogen receptor signaling and endocrine resistance in invasive lobular carcinoma cell lines. *Breast Cancer Research*. 2016;18(1).
157. St John MA. Inflammatory mediators drive metastasis and drug resistance in head and neck squamous cell carcinoma. *Laryngoscope*. 2015;125 Suppl 3:S1-11.
158. Qian X, Karpova T, Sheppard AM, McNally J, Lowy DR. E-cadherin-mediated adhesion inhibits ligand-dependent activation of diverse receptor tyrosine kinases. *EMBO J*. 2004;23(8):1739-48.

159. De-Freitas-Junior JCM, Carvalho S, Dias AM, Oliveira P, Cabral J, Seruca R, et al. Insulin/IGF-I Signaling Pathways Enhances Tumor Cell Invasion through Bisecting GlcNAc N-glycans Modulation. An Interplay with E-Cadherin. *PLoS ONE*. 2013;8(11):e81579.
160. Fedor-Chaiken M, Hein PW, Stewart JC, Brackenbury R, Kinch MS. E-Cadherin Binding Modulates EGF Receptor Activation. *Cell Communication & Adhesion*. 2003;10(2):105-18.
161. Brueffer C, Gladchuk S, Winter C, Vallon-Christersson J, Hegardt C, Hakkinen J, et al. The mutational landscape of the SCAN-B real-world primary breast cancer transcriptome. *EMBO Mol Med*. 2020;12(10):e12118.
162. Rahman M, Jackson LK, Johnson WE, Li DY, Bild AH, Piccolo SR. Alternative preprocessing of RNA-Sequencing data in The Cancer Genome Atlas leads to improved analysis results. *Bioinformatics*. 2015;31(22):3666-72.
163. Yoshihara K, Shahmoradgoli M, Martinez E, Vegesna R, Kim H, Torres-Garcia W, et al. Inferring tumour purity and stromal and immune cell admixture from expression data. *Nat Commun*. 2013;4:2612.
164. Hanzelmann S, Castelo R, Guinney J. GSEA: gene set variation analysis for microarray and RNA-seq data. *BMC Bioinformatics*. 2013;14:7.
165. Subramanian A, Tamayo P, Mootha VK, Mukherjee S, Ebert BL, Gillette MA, et al. Gene set enrichment analysis: a knowledge-based approach for interpreting genome-wide expression profiles. *Proc Natl Acad Sci U S A*. 2005;102(43):15545-50.
166. Ikediobi ON, Davies H, Bignell G, Edkins S, Stevens C, O'Meara S, et al. Mutation analysis of 24 known cancer genes in the NCI-60 cell line set. *Mol Cancer Ther*. 2006;5(11):2606-12.
167. Marcotte R, Sayad A, Brown KR, Sanchez-Garcia F, Reimand J, Haider M, et al. Functional Genomic Landscape of Human Breast Cancer Drivers, Vulnerabilities, and Resistance. *Cell*. 2016;164(1-2):293-309.
168. Hollestelle A, Nagel JHA, Smid M, Lam S, Elstrodt F, Wasielewski M, et al. Distinct gene mutation profiles among luminal-type and basal-type breast cancer cell lines. *Breast Cancer Research and Treatment*. 2010;121(1):53-64.
169. Andl CD, Rustgi AK. No one-way street: Cross-talk between E-cadherin and receptor tyrosine kinase (RTK) signaling—A mechanism to regulate RTK activity. *Cancer Biology & Therapy*. 2005;4(1):35-8.
170. Curto M, Cole BK, Lallemand D, Liu CH, McClatchey AI. Contact-dependent inhibition of EGFR signaling by Nf2/Merlin. *J Cell Biol*. 2007;177(5):893-903.

- 171.Niepel M, Hafner M, Pace EA, Chung M, Chai DH, Zhou L, et al. Analysis of growth factor signaling in genetically diverse breast cancer lines. *BMC Biology*. 2014;12(1):20.
- 172.Giuliano M, Trivedi MV, Schiff R. Bidirectional Crosstalk between the Estrogen Receptor and Human Epidermal Growth Factor Receptor 2 Signaling Pathways in Breast Cancer: Molecular Basis and Clinical Implications. *Breast Care*. 2013;8(4):256-62.
- 173.Du J, Yu Y, Zhan J, Zhang H. Targeted Therapies Against Growth Factor Signaling in Breast Cancer. *Advances in Experimental Medicine and Biology: Springer Singapore*; 2017. p. 125-46.
- 174.Jeibouei S, Akbari ME, Kalbasi A, Aref AR, Ajoudanian M, Rezvani A, et al. <p>Personalized medicine in breast cancer: pharmacogenomics approaches</p>. *Pharmacogenomics and Personalized Medicine*. 2019;Volume 12:59-73.
- 175.Sabatier R, Goncalves A, Bertucci F. Personalized medicine: present and future of breast cancer management. *Crit Rev Oncol Hematol*. 2014;91(3):223-33.
- 176.André F, Ciruelos E, Rubovszky G, Campone M, Loibl S, Rugo HS, et al. Alpelisib for PIK3CA-Mutated, Hormone Receptor–Positive Advanced Breast Cancer. *New England Journal of Medicine*. 2019;380(20):1929-40.
- 177.Armaghani AJ, Han HS. <p>Alpelisib in the Treatment of Breast Cancer: A Short Review on the Emerging Clinical Data</p>. *Breast Cancer: Targets and Therapy*. 2020;Volume 12:251-8.
- 178.Pappo AS, Patel SR, Crowley J, Reinke DK, Kuenkele K-P, Chawla SP, et al. R1507, a Monoclonal Antibody to the Insulin-Like Growth Factor 1 Receptor, in Patients With Recurrent or Refractory Ewing Sarcoma Family of Tumors: Results of a Phase II Sarcoma Alliance for Research Through Collaboration Study. *Journal of Clinical Oncology*. 2011;29(34):4541-7.
- 179.Pappo AS, Vassal G, Crowley JJ, Bolejack V, Hogendoorn PCW, Chugh R, et al. A phase 2 trial of R1507, a monoclonal antibody to the insulin-like growth factor-1 receptor (IGF-1R), in patients with recurrent or refractory rhabdomyosarcoma, osteosarcoma, synovial sarcoma, and other soft tissue sarcomas: Results of a Sarcoma Alliance. *Cancer*. 2014;120(16):2448-56.
- 180.Langer CJ, Novello S, Park K, Krzakowski M, Karp DD, Mok T, et al. Randomized, phase III trial of first-line figitumumab in combination with paclitaxel and carboplatin versus paclitaxel and carboplatin alone in patients with advanced non-small-cell lung cancer. *J Clin Oncol*. 2014;32(19):2059-66.
- 181.Barretina J, Caponigro G, Stransky N, Venkatesan K, Margolin AA, Kim S, et al. The Cancer Cell Line Encyclopedia enables predictive modelling of anticancer drug sensitivity. *Nature*. 2012;483(7391):603-7.

182. Adli M. The CRISPR tool kit for genome editing and beyond. *Nature Communications*. 2018;9(1).
183. Nidhi S, Anand U, Oleksak P, Tripathi P, Lal JA, Thomas G, et al. Novel CRISPR–Cas Systems: An Updated Review of the Current Achievements, Applications, and Future Research Perspectives. *International Journal of Molecular Sciences*. 2021;22(7):3327.
184. Tasdemir N, Ding K, Savariau L, Levine KM, Du T, Elangovan A, et al. Proteomic and transcriptomic profiling identifies mediators of anchorage-independent growth and roles of inhibitor of differentiation proteins in invasive lobular carcinoma. *Sci Rep*. 2020;10(1):11487.
185. Chen F, Ding K, Priedigkeit N, Elangovan A, Levine KM, Carleton N, et al. Single-Cell Transcriptomic Heterogeneity in Invasive Ductal and Lobular Breast Cancer Cells. *Cancer Res*. 2021;81(2):268-81.
186. Patro R, Duggal G, Love MI, Irizarry RA, Kingsford C. Salmon provides fast and bias-aware quantification of transcript expression. *Nat Methods*. 2017;14(4):417-9.
187. Sonesson C, Love MI, Robinson MD. Differential analyses for RNA-seq: transcript-level estimates improve gene-level inferences. *F1000Res*. 2015;4:1521.
188. Love MI, Huber W, Anders S. Moderated estimation of fold change and dispersion for RNA-seq data with DESeq2. *Genome Biol*. 2014;15(12):550.
189. Ghandi M, Huang FW, Jane-Valbuena J, Kryukov GV, Lo CC, McDonald ER, 3rd, et al. Next-generation characterization of the Cancer Cell Line Encyclopedia. *Nature*. 2019;569(7757):503-8.
190. Valenta T, Hausmann G, Basler K. The many faces and functions of beta-catenin. *EMBO J*. 2012;31(12):2714-36.
191. Kagawa S, Gu J, Honda T, McDonnell TJ, Swisher SG, Roth JA, et al. Deficiency of caspase-3 in MCF7 cells blocks Bax-mediated nuclear fragmentation but not cell death. *Clin Cancer Res*. 2001;7(5):1474-80.
192. Turner C, Devitt A, Parker K, MacFarlane M, Giuliano M, Cohen GM, et al. Macrophage-mediated clearance of cells undergoing caspase-3-independent death. *Cell Death Differ*. 2003;10(3):302-12.
193. Perks CM, Bowen S, Gill ZP, Newcomb PV, Holly JM. Differential IGF-independent effects of insulin-like growth factor binding proteins (1-6) on apoptosis of breast epithelial cells. *J Cell Biochem*. 1999;75(4):652-64.

- 194.Lang DS, Marwitz S, Heilenkotter U, Schumm W, Behrens O, Simon R, et al. Transforming growth factor-beta signaling leads to uPA/PAI-1 activation and metastasis: a study on human breast cancer tissues. *Pathol Oncol Res.* 2014;20(3):727-32.
- 195.Dabanaka K, Chung S, Nakagawa H, Nakamura Y, Okabayashi T, Sugimoto T, et al. PKIB expression strongly correlated with phosphorylated Akt expression in breast cancers and also with triple-negative breast cancer subtype. *Medical Molecular Morphology.* 2012;45(4):229-33.
- 196.Matthew EM, Yang Z, Peri S, Andrade M, Dunbrack R, Ross E, et al. Plk2 Loss Commonly Occurs in Colorectal Carcinomas but not Adenomas: Relationship to mTOR Signaling. *Neoplasia.* 2018;20(3):244-55.
- 197.Busby M, Hallett M, Plante I. The Complex Subtype-Dependent Role of Connexin 43 (GJA1) in Breast Cancer. *International Journal of Molecular Sciences.* 2018;19(3):693.
- 198.Phillips SL, Williams CB, Zambrano JN, Williams CJ, Yeh ES. Connexin 43 in the development and progression of breast cancer: What's the connection? (Review). *Int J Oncol.* 2017;51(4):1005-13.
- 199.Lombaerts M, Van Wezel T, Philippo K, Dierssen JWF, Zimmerman RME, Oosting J, et al. E-cadherin transcriptional downregulation by promoter methylation but not mutation is related to epithelial-to-mesenchymal transition in breast cancer cell lines. *British Journal of Cancer.* 2006;94(5):661-71.
- 200.Christgen M, Cserni G, Floris G, Marchio C, Djerroudi L, Kreipe H, et al. Lobular Breast Cancer: Histomorphology and Different Concepts of a Special Spectrum of Tumors. *Cancers.* 2021;13(15):3695.
- 201.Menet E, Becette V, Briffod M. Cytologic diagnosis of lobular carcinoma of the breast. *Cancer.* 2008;114(2):111-7.
- 202.Khalil AA, Ilina O, Gritsenko PG, Bult P, Span PN, Friedl P. Collective invasion in ductal and lobular breast cancer associates with distant metastasis. *Clinical & Experimental Metastasis.* 2017;34(6-7):421-9.
- 203.Sarrió D, Pérez-Mies B, Hardisson D, Moreno-Bueno G, Suárez A, Cano A, et al. Cytoplasmic localization of p120^{ctn} and E-cadherin loss characterize lobular breast carcinoma from preinvasive to metastatic lesions. *Oncogene.* 2004;23(19):3272-83.
- 204.Schackmann RCJ, Van Amersfoort M, Haarhuis JHI, Vlug EJ, Halim VA, Roodhart JML, et al. Cytosolic p120-catenin regulates growth of metastatic lobular carcinoma through Rock1-mediated anoikis resistance. *Journal of Clinical Investigation.* 2011;121(8):3176-88.

205. Guadamillas MC, Cerezo A, Del Pozo MA. Overcoming anoikis – pathways to anchorage-independent growth in cancer. *Journal of Cell Science*. 2011;124(19):3189-97.
206. Deng Z, Wang H, Liu J, Deng Y, Zhang N. Comprehensive understanding of anchorage-independent survival and its implication in cancer metastasis. *Cell Death & Disease*. 2021;12(7).
207. Mori S, Chang JT, Andrechek ER, Matsumura N, Baba T, Yao G, et al. Anchorage-independent cell growth signature identifies tumors with metastatic potential. *Oncogene*. 2009;28(31):2796-805.
208. Chen JC, Shao ZM, Sheikh MS, Hussain A, LeRoith D, Roberts CT, Jr., et al. Insulin-like growth factor-binding protein enhancement of insulin-like growth factor-I (IGF-I)-mediated DNA synthesis and IGF-I binding in a human breast carcinoma cell line. *J Cell Physiol*. 1994;158(1):69-78.
209. Butt AJ, Dickson KA, Jambazov S, Baxter RC. Enhancement of tumor necrosis factor-alpha-induced growth inhibition by insulin-like growth factor-binding protein-5 (IGFBP-5), but not IGFBP-3 in human breast cancer cells. *Endocrinology*. 2005;146(7):3113-22.
210. Sekiya T, Adachi S, Kohu K, Yamada T, Higuchi O, Furukawa Y, et al. Identification of BMP and activin membrane-bound inhibitor (BAMBI), an inhibitor of transforming growth factor-beta signaling, as a target of the beta-catenin pathway in colorectal tumor cells. *J Biol Chem*. 2004;279(8):6840-6.
211. Xie Y, Liu Y, Li Q, Chen J. Polo-like kinase 2 promotes chemoresistance and predicts limited survival benefit from adjuvant chemotherapy in colorectal cancer. *International Journal of Oncology*. 2018.
212. Alafate W, Xu D, Wu W, Xiang J, Ma X, Xie W, et al. Loss of PLK2 induces acquired resistance to temozolomide in GBM via activation of notch signaling. *Journal of Experimental & Clinical Cancer Research*. 2020;39(1).
213. Harrell JC, Shroka TM, Jacobsen BM. Estrogen induces c-Kit and an aggressive phenotype in a model of invasive lobular breast cancer. *Oncogenesis*. 2017;6(11).
214. Yao Q, Xu C, Zhao H, Chen H. CXCR4 in breast cancer: oncogenic role and therapeutic targeting. *Drug Design, Development and Therapy*. 2015:4953.
215. Susek KH, Karvouni M, Alici E, Lundqvist A. The Role of CXC Chemokine Receptors 1-4 on Immune Cells in the Tumor Microenvironment. *Front Immunol*. 2018;9:2159.
216. Kim H-J, Litzenburger BC, Cui X, Delgado DA, Grabiner BC, Lin X, et al. Constitutively Active Type I Insulin-Like Growth Factor Receptor Causes Transformation and Xenograft Growth

of Immortalized Mammary Epithelial Cells and Is Accompanied by an Epithelial-to-Mesenchymal Transition Mediated by NF- κ B and Snail. *Molecular and Cellular Biology*. 2007;27(8):3165-75.

217.Hawsawi Y, El-Gendy R, Twelves C, Speirs V, Beattie J. Insulin-like growth factor — Oestradiol crosstalk and mammary gland tumourigenesis. *Biochimica et Biophysica Acta (BBA) - Reviews on Cancer*. 2013;1836(2):345-53.

218.Baserga R, Peruzzi F, Reiss K. The IGF-1 receptor in cancer biology. *Int J Cancer*. 2003;107(6):873-7.

219.Kleinberg DL. Role of IGF-I in normal mammary development. *Breast Cancer Research and Treatment*. 1998;47(3):201-8.

220.Litzenburger BC, Kim HJ, Kuitse I, Carboni JM, Attar RM, Gottardis MM, et al. BMS-536924 reverses IGF-IR-induced transformation of mammary epithelial cells and causes growth inhibition and polarization of MCF7 cells. *Clin Cancer Res*. 2009;15(1):226-37.

221.Iams WT, Lovly CM. Molecular Pathways: Clinical Applications and Future Direction of Insulin-like Growth Factor-1 Receptor Pathway Blockade. *Clinical Cancer Research*. 2015;21(19):4270-7.

222.Morgillo F, De Vita F, Antonioli G, Orditura M, Auremma PP, Diadema MR, et al. Serum insulin-like growth factor 1 correlates with the risk of nodal metastasis in endocrine-positive breast cancer. *Curr Oncol*. 2013;20(4):e283-8.

223.Mezi S, Todi L, Orsi E, Angeloni A, Mancini P. Involvement of the Src-cortactin pathway in migration induced by IGF-1 and EGF in human breast cancer cells. *International Journal of Oncology*. 2012;41(6):2128-38.

224.De Blaquièrre GE, May FEB, Westley BR. Increased expression of both insulin receptor substrates 1 and 2 confers increased sensitivity to IGF-1 stimulated cell migration. *Endocrine-Related Cancer*. 2009;16(2):635-47.

225.Jambal P, Badtke MM, Harrell JC, Borges VF, Post MD, Sollender GE, et al. Estrogen switches pure mucinous breast cancer to invasive lobular carcinoma with mucinous features. *Breast Cancer Research and Treatment*. 2013;137(2):431-48.

226.Garcia-Recio S, Thennavan A, East MP, Parker JS, Cejalvo JM, Garay JP, et al. FGFR4 regulates tumor subtype differentiation in luminal breast cancer and metastatic disease. *J Clin Invest*. 2020;130(9):4871-87.

227. Levine KM, Friedigkeit N, Basudan A, Tasdemir N, Sikora MJ, Sokol ES, et al. FGFR4 overexpression and hotspot mutations in metastatic ER+ breast cancer are enriched in the lobular subtype. *NPJ Breast Cancer*. 2019;5:19.
228. Valastyan S, Weinberg RA. Tumor metastasis: molecular insights and evolving paradigms. *Cell*. 2011;147(2):275-92.
229. Romanelli RJ, Lebeau AP, Fulmer CG, Lazzarino DA, Hochberg A, Wood TL. Insulin-like Growth Factor Type-I Receptor Internalization and Recycling Mediate the Sustained Phosphorylation of Akt. *Journal of Biological Chemistry*. 2007;282(31):22513-24.
230. Baserga R. The insulin-like growth factor-I receptor as a target for cancer therapy. *Expert Opin Ther Targets*. 2005;9(4):753-68.
231. Yoneyama Y, Lanzerstorfer P, Niwa H, Umehara T, Shibano T, Yokoyama S, et al. IRS-1 acts as an endocytic regulator of IGF-I receptor to facilitate sustained IGF signaling. *eLife*. 2018;7.
232. Murphy JE, Padilla BE, Hasdemir B, Cottrell GS, Bunnett NW. Endosomes: a legitimate platform for the signaling train. *Proc Natl Acad Sci U S A*. 2009;106(42):17615-22.
233. Bruner HC, Derksen PWB. Loss of E-Cadherin-Dependent Cell–Cell Adhesion and the Development and Progression of Cancer. *Cold Spring Harbor Perspectives in Biology*. 2018;10(3):a029330.
234. Le TL, Yap AS, Stow JL. Recycling of E-cadherin: a potential mechanism for regulating cadherin dynamics. *J Cell Biol*. 1999;146(1):219-32.
235. Dean JL, McClendon AK, Hickey TE, Butler LM, Tilley WD, Witkiewicz AK, et al. Therapeutic response to CDK4/6 inhibition in breast cancer defined by ex vivo analyses of human tumors. *Cell Cycle*. 2012;11(14):2756-61.
236. Xu R, Zhang Y, Gu L, Zheng J, Cui J, Dong J, et al. Arf6 regulates EGF-induced internalization of E-cadherin in breast cancer cells. *Cancer Cell Int*. 2015;15(1):11.
237. Guvakova MA, Surmacz E. Overexpressed IGF-I receptors reduce estrogen growth requirements, enhance survival, and promote E-cadherin-mediated cell-cell adhesion in human breast cancer cells. *Exp Cell Res*. 1997;231(1):149-62.
238. Morcavallo A, Stefanello M, Iozzo RV, Belfiore A, Morrione A. Ligand-mediated endocytosis and trafficking of the insulin-like growth factor receptor I and insulin receptor modulate receptor function. *Front Endocrinol (Lausanne)*. 2014;5:220.

239. Martins AS, Ordóñez JL, Amaral AT, Prins F, Floris G, Debiec-Rychter M, et al. IGF1R Signaling in Ewing Sarcoma Is Shaped by Clathrin-/Caveolin-Dependent Endocytosis. *PLoS ONE*. 2011;6(5):e19846.
240. Goh LK, Sorkin A. Endocytosis of Receptor Tyrosine Kinases. *Cold Spring Harbor Perspectives in Biology*. 2013;5(5):a017459-a.
241. Canonici A, Steelant W, Rigot V, Khomitch-Baud A, Boutaghou-Cherid H, Bruyneel E, et al. Insulin-like growth factor-I receptor, E-cadherin and alpha v integrin form a dynamic complex under the control of alpha-catenin. *Int J Cancer*. 2008;122(3):572-82.
242. Bae G-Y, Choi S-J, Lee J-S, Jo J, Lee J, Kim J, et al. Loss of E-cadherin activates EGFR-MEK/ERK signaling, which promotes invasion via the ZEB1/MMP2 axis in non-small cell lung cancer. *Oncotarget*. 2013;4(12):2512-22.
243. Crudden C, Girnita A, Girnita L. Targeting the IGF-1R: The Tale of the Tortoise and the Hare. *Front Endocrinol (Lausanne)*. 2015;6:64.
244. Singh P, Alex JM, Bast F. Insulin receptor (IR) and insulin-like growth factor receptor 1 (IGF-1R) signaling systems: novel treatment strategies for cancer. *Med Oncol*. 2014;31(1):805.
245. Yang Y, Yee D. Targeting insulin and insulin-like growth factor signaling in breast cancer. *J Mammary Gland Biol Neoplasia*. 2012;17(3-4):251-61.
246. Dinchuk JE, Cao C, Huang F, Reeves KA, Wang J, Myers F, et al. Insulin Receptor (IR) Pathway Hyperactivity in IGF-IR Null Cells and Suppression of Downstream Growth Signaling Using the Dual IGF-IR/IR Inhibitor, BMS-754807. *Endocrinology*. 2010;151(9):4123-32.
247. Zhang H, Pelzer AM, Kiang DT, Yee D. Down-regulation of type I insulin-like growth factor receptor increases sensitivity of breast cancer cells to insulin. *Cancer Res*. 2007;67(1):391-7.
248. Buck E, Gokhale PC, Koujak S, Brown E, Eyzaguirre A, Tao N, et al. Compensatory insulin receptor (IR) activation on inhibition of insulin-like growth factor-1 receptor (IGF-1R): rationale for cotargeting IGF-1R and IR in cancer. *Mol Cancer Ther*. 2010;9(10):2652-64.
249. Ulanet DB, Ludwig DL, Kahn CR, Hanahan D. Insulin receptor functionally enhances multistage tumor progression and conveys intrinsic resistance to IGF-1R targeted therapy. *Proc Natl Acad Sci U S A*. 2010;107(24):10791-8.
250. Lei JT, Anurag M, Haricharan S, Gou X, Ellis MJ. Endocrine therapy resistance: new insights. *The Breast*. 2019;48:S26-S30.

251. Ianevski A, He L, Aittokallio T, Tang J. SynergyFinder: a web application for analyzing drug combination dose-response matrix data. *Bioinformatics*. 2020;36(8):2645.
252. Sachs N, de Ligt J, Kopper O, Gogola E, Bounova G, Weeber F, et al. A Living Biobank of Breast Cancer Organoids Captures Disease Heterogeneity. *Cell*. 2018;172(1-2):373-86 e10.
253. Michaut M, Chin SF, Majewski I, Severson TM, Bismeyjer T, de Koning L, et al. Integration of genomic, transcriptomic and proteomic data identifies two biologically distinct subtypes of invasive lobular breast cancer. *Sci Rep*. 2016;6:18517.
254. Wang Q, Zhang Y, Zhu J, Zheng H, Chen S, Chen L, et al. IGF-1R inhibition induces MEK phosphorylation to promote survival in colon carcinomas. *Signal Transduction and Targeted Therapy*. 2020;5(1).
255. Bonanno L, Jirillo A, Favaretto A. Mechanisms of acquired resistance to epidermal growth factor receptor tyrosine kinase inhibitors and new therapeutic perspectives in non small cell lung cancer. *Curr Drug Targets*. 2011;12(6):922-33.
256. Aldea M, Andre F, Marabelle A, Dogan S, Barlesi F, Soria JC. Overcoming Resistance to Tumor-Targeted and Immune-Targeted Therapies. *Cancer Discov*. 2021;11(4):874-99.
257. Montagna E, Colleoni M. Hormonal treatment combined with targeted therapies in endocrine-responsive and HER2-positive metastatic breast cancer. *Therapeutic Advances in Medical Oncology*. 2019;11:175883591989410.
258. Leary A, Dowsett M. Combination therapy with aromatase inhibitors: the next era of breast cancer treatment? *British Journal of Cancer*. 2006;95(6):661-6.
259. Bian L, Xu FR, Jiang ZF. Endocrine therapy combined with targeted therapy in hormone receptor-positive metastatic breast cancer. *Chin Med J (Engl)*. 2020;133(19):2338-45.
260. Zardavas D, Phillips WA, Loi S. PIK3CA mutations in breast cancer: reconciling findings from preclinical and clinical data. *Breast Cancer Research*. 2014;16(1):201.
261. Chandralapaty S, Sawai A, Scaltriti M, Rodrik-Outmezguine V, Grbovic-Huezo O, Serra V, et al. AKT Inhibition Relieves Feedback Suppression of Receptor Tyrosine Kinase Expression and Activity. *Cancer Cell*. 2011;19(1):58-71.
262. Brew T, Bougen-Zhukov N, Mitchell W, Decourtye L, Schulpen E, Nouri Y, et al. Loss of E-Cadherin Leads to Druggable Vulnerabilities in Sphingolipid Metabolism and Vesicle Trafficking. *Cancers (Basel)*. 2021;14(1).

263. Almendro V, Cheng YK, Randles A, Itzkovitz S, Marusyk A, Ametller E, et al. Inference of tumor evolution during chemotherapy by computational modeling and in situ analysis of genetic and phenotypic cellular diversity. *Cell Rep.* 2014;6(3):514-27.
264. Morris LGT, Riaz N, Desrichard A, Şenbabaoglu Y, Hakimi AA, Makarov V, et al. Pan-cancer analysis of intratumor heterogeneity as a prognostic determinant of survival. *Oncotarget.* 2016;7(9):10051-63.
265. Bosch A, Li Z, Bergamaschi A, Ellis H, Toska E, Prat A, et al. PI3K inhibition results in enhanced estrogen receptor function and dependence in hormone receptor-positive breast cancer. *Science Translational Medicine.* 2015;7(283):283ra51-ra51.
266. Engelman JA, Jänne PA. Mechanisms of Acquired Resistance to Epidermal Growth Factor Receptor Tyrosine Kinase Inhibitors in Non-Small Cell Lung Cancer: Fig. 1. *Clinical Cancer Research.* 2008;14(10):2895-9.
267. Liu L, Yu L, Li Z, Li W, Huang W. Patient-derived organoid (PDO) platforms to facilitate clinical decision making. *Journal of Translational Medicine.* 2021;19(1).
268. Bose S, Clevers H, Shen X. Promises and challenges of organoid-guided precision medicine. *Med.* 2021;2(9):1011-26.
269. Takahashi T. Organoids for Drug Discovery and Personalized Medicine. *Annual Review of Pharmacology and Toxicology.* 2019;59(1):447-62.
270. Larue L, Ohsugi M, Hirchenhain J, Kemler R. E-cadherin null mutant embryos fail to form a trophoderm epithelium. *Proceedings of the National Academy of Sciences.* 1994;91(17):8263-7.
271. Boussadia O, Kutsch S, Hierholzer A, Delmas V, Kemler R. E-cadherin is a survival factor for the lactating mouse mammary gland. *Mech Dev.* 2002;115(1-2):53-62.
272. Derksen PWB, Liu X, Saridin F, Van Der Gulden H, Zevenhoven J, Evers B, et al. Somatic inactivation of E-cadherin and p53 in mice leads to metastatic lobular mammary carcinoma through induction of anoikis resistance and angiogenesis. *Cancer Cell.* 2006;10(5):437-49.
273. Wagner K-U, Boulanger CA, Henry MD, Sgagias M, Hennighausen L, Smith GH. An adjunct mammary epithelial cell population in parous females: its role in functional adaptation and tissue renewal. *Development.* 2002;129(6):1377-86.
274. Derksen PWB, Braumuller TM, Van Der Burg E, Hornsveld M, Mesman E, Wesseling J, et al. Mammary-specific inactivation of E-cadherin and p53 impairs functional gland development

and leads to pleomorphic invasive lobular carcinoma in mice. *Disease Models & Mechanisms*. 2011;4(3):347-58.

275.Tolg C, Cowman M, Turley EA. Mouse Mammary Gland Whole Mount Preparation and Analysis. *Bio Protoc*. 2018;8(13):e2915.

276.Tolg C, Yuan H, Flynn SM, Basu K, Ma J, Tse KCK, et al. Hyaluronan modulates growth factor induced mammary gland branching in a size dependent manner. *Matrix Biol*. 2017;63:117-32.

277.Medina D. Preneoplastic lesions in murine mammary cancer. *Cancer Res*. 1976;36(7 PT 2):2589-95.

278.Sympson CJ. Targeted expression of stromelysin-1 in mammary gland provides evidence for a role of proteinases in branching morphogenesis and the requirement for an intact basement membrane for tissue-specific gene expression [published erratum appears in *J Cell Biol*. *The Journal of Cell Biology*. 1994;125(3):681-93.

279.Rose-Hellekant TA, Gilchrist K, Sandgren EP. Strain background alters mammary gland lesion phenotype in transforming growth factor-alpha transgenic mice. *Am J Pathol*. 2002;161(4):1439-47.

280.Rowse GJ, Ritland SR, Gendler SJ. Genetic modulation of neu proto-oncogene-induced mammary tumorigenesis. *Cancer Res*. 1998;58(12):2675-9.

281.Wagner K-U, Wall RJ, St-Onge L, Gruss P, Wynshaw-Boris A, Garrett L, et al. Cre-mediated gene deletion in the mammary gland. *Nucleic Acids Research*. 1997;25(21):4323-30.

282.Stein T, Morris JS, Davies CR, Weber-Hall SJ, Duffy M-A, Heath VJ, et al. *Breast Cancer Research*. 2004;6(2):R75.

283.Stein T, Salomonis N, Gusterson BA. Mammary Gland Involution as a Multi-step Process. *Journal of Mammary Gland Biology and Neoplasia*. 2007;12(1):25-35.

284.Strange R, Li F, Saurer S, Burkhardt A, Friis RR. Apoptotic cell death and tissue remodelling during mouse mammary gland involution. *Development*. 1992;115(1):49-58.

285.Lund LR, Romer J, Thomasset N, Solberg H, Pyke C, Bissell MJ, et al. Two distinct phases of apoptosis in mammary gland involution: proteinase-independent and -dependent pathways. *Development*. 1996;122(1):181-93.

286. Boelens MC, Nethe M, Klarenbeek S, de Ruiter JR, Schut E, Bonzanni N, et al. PTEN Loss in E-Cadherin-Deficient Mouse Mammary Epithelial Cells Rescues Apoptosis and Results in Development of Classical Invasive Lobular Carcinoma. *Cell Rep.* 2016;16(8):2087-101.
287. Petrova YI, Schecterson L, Gumbiner BM. Roles for E-cadherin cell surface regulation in cancer. *Mol Biol Cell.* 2016;27(21):3233-44.
288. Bajrami I, Marlow R, van de Ven M, Brough R, Pemberton HN, Frankum J, et al. E-Cadherin/ROS1 Inhibitor Synthetic Lethality in Breast Cancer. *Cancer Discov.* 2018;8(4):498-515.
289. Sastre-Garau X, Jouve M, Asselain B, Vincent-Salomon A, Beuzeboc P, Dorval T, et al. Infiltrating lobular carcinoma of the breast. Clinicopathologic analysis of 975 cases with reference to data on conservative therapy and metastatic patterns. *Cancer.* 1996;77(1):113-20.
290. Rakha EA, Gill MS, El-Sayed ME, Khan MM, Hodi Z, Blamey RW, et al. The biological and clinical characteristics of breast carcinoma with mixed ductal and lobular morphology. *Breast Cancer Res Treat.* 2009;114(2):243-50.
291. Dixon JM, Anderson TJ, Page DL, Lee D, Duffy SW. Infiltrating lobular carcinoma of the breast. *Histopathology.* 1982;6(2):149-61.